

1

New, Light Weakly-Coupled Particles

1 [authors to be added]

2 1.1 Overview

3 The Standard Model (SM) of particle physics has achieved remarkable success as a result of several decades
4 of *exploration*, of constantly pushing the boundaries of our knowledge of theory, experiment, and technology.
5 However, while the SM provides a theoretically consistent description of all known particles and their
6 interactions (ignoring gravity) up to the Planck scale, it is clearly incomplete as it does not address several
7 pieces of evidence for new physics beyond the SM.

8 One particularly powerful piece of evidence for new physics comes from the existence of dark matter (DM).
9 DM dominates the matter density in our Universe, but very little is known about it. Its existence provides a
10 strong hint that there may be a *dark sector*, consisting of particles that do not interact with the known strong,
11 weak, or electromagnetic forces. Given the intricate structure of the SM, which describes only a subdominant
12 component of the Universe, it would not be too surprising if the dark sector contains a rich structure itself,
13 with dark matter making up only a part of it. Indeed, many dark sectors could exist, each with its own
14 beautiful structure, distinct particles, and forces. These dark sectors may contain *new light weakly-coupled*
15 *particles* (NLWCPs), particles well below the Weak-scale that interact only feebly with ordinary matter.
16 Such particles could easily have escaped past experimental searches, but a rich experimental program has
17 now been devised to look for several well-motivated possibilities.

18 Dark sectors are motivated also by bottom-up and top-down theoretical considerations. They arise in many
19 theoretical extensions to the SM, such as moduli that are present in string theory or new (pseudo)-scalars
20 that appear naturally when symmetries are broken at high energy scales. Other powerful motivations include
21 the strong CP problem, and various experimental findings, including the discrepancy between the calculated
22 and measured anomalous magnetic moment of the muon and puzzling results from astrophysics. Besides
23 gravity, there are a few well-motivated interactions allowed by SM symmetries that provide a “portal” from
24 the SM sector into the dark sector. These portals include,

25 “Vector” portal:	Dark photons	$-\frac{\epsilon}{2\cos\theta_W}B_{\mu\nu}F'^{\mu\nu}$
“Axion” portal:	Pseudoscalars	$\frac{\partial_\mu a}{f_a}\bar{\psi}\gamma^\mu\gamma^5\psi$
“Higgs” portal:	Dark scalars	$(\mu S + \lambda S^2)H^\dagger H$
“Neutrino” portal:	Sterile neutrinos	$y_N LHN$

26 The Higgs and neutrino portal are best explored at high-energy colliders and neutrino facilities, respectively.
27 Our focus here will be on the vector and axion portals, which are particularly well-motivated possibilities
28 and can be explored with low-cost, high-impact experiments.

29 This paper is a summary of the physics motivation and experimental opportunities of the Intensity Frontier
 30 subgroup “New, Light Weakly-coupled Particles” of the Community Summer Study 2013 (“Snowmass on the
 31 Mississippi”). The outline of the remainder of this summary is as follows. §1.2 discusses the (QCD) axion
 32 and more general “axion-like” particles (ALPs). §1.3 reviews dark photons, focusing on sub-MeV and MeV-
 33 GeV masses. §1.4 describes sub-GeV dark matter, milli-charged particles and other hidden-sector particles.
 34 §1.5 focuses on chameleons. In all cases, we describe the theoretical motivation, the phenomenological
 35 motivation, the current constraints, and the current and future experimental opportunities. §1.6 contains
 36 our conclusions.

37 1.2 Axions and Axion-Like Particles

38 1.2.1 Theory & Theory Motivation

39 One of the unresolved puzzles in the Standard Model is the lack of any observed CP violation in the strong
 40 interactions described by Quantum Chromodynamics (QCD). While the weak interactions are known to
 41 violate CP , the strong interactions also contain a CP -violating term in the Lagrangian, $\frac{\Theta}{32\pi^2} G_{\mu\nu} \tilde{G}^{\mu\nu}$, where
 42 $G^{\mu\nu}$ is the gluon field strength. For non-zero quark masses, this term leads to (unobserved) CP -violating
 43 effects of the strong interactions. This so-called “strong CP problem” is often exemplified by the lack of
 44 observation of a neutron dipole moment down to a present experimental upper limit 10 orders of magnitude
 45 smaller than what is expected from a CP -violating QCD.

46 Solutions to this problem are scarce. Perhaps the most popular suggestion is the so-called Peccei-Quinn (PQ)
 47 $U(1)$ approximate global symmetry, which is spontaneously broken at a scale f_a . The axion is a hypothetical
 48 particle that arises as the pseudo-Nambu-Goldstone boson (PNGB) of this symmetry [1, 2, 3].

49 The axion mass is $m_a \sim 6 \text{ meV} (10^9 \text{ GeV}/f_a)$. Its coupling to ordinary matter is proportional to $1/f_a$
 50 and can be calculated in specific models. It couples to leptons and to photons, the latter being of the form
 51 $\mathcal{L} \supset -\frac{1}{4} g_{a\gamma} a F_{\mu\nu} \tilde{F}^{\mu\nu}$, where $g_{a\gamma} \sim 10^{-13} \text{ GeV} (10^{10} \text{ GeV}/f_a)$ [4] is a coupling that is model-dependent
 52 up to an $\mathcal{O}(1)$ factor. Moreover, since $m_a \ll \Lambda_{QCD}$, the axion’s coupling to quarks should be described
 53 through its coupling to hadrons, which occurs through small mixing with the π^0 and η mesons. All of these
 54 interactions can play a role in searches for the axion, and allow the axion to be produced or detected in the
 55 laboratory and emitted by the sun or other stars.

56 The basic physical mechanism that leads to the axion — the spontaneous breaking at a high energy scale of
 57 a $U(1)$ approximate global symmetry, generating a light PNGB — also allows for other axion-like particles
 58 (ALPs). Unlike axions, which are linked to the strong interactions and whose masses and couplings are
 59 determined by a single new parameter f_a , ALPs are much less constrained, and their masses and couplings
 60 to photons are independent parameters. Searches for ALPs should not therefore be limited to the parameter
 61 space of the axion itself. Both ALPs and axions are generic in string theory [6, 5, 7, 8, 9, 10, 11], with the
 62 natural size of their decay constant f_a being the string scale, varying typically between 10^9 and 10^{17} GeV.

63 1.2.2 Phenomenological Motivation and Current Constraints

64 Fig. 1-1 (top) shows the allowed axion parameter space as a function of f_a or, equivalently, m_a . Direct
 65 searches for such particles and calculations of their effect on the cooling of stars and on the supernova
 66 SN1987A exclude most values of $f_a < 10^9$ GeV. Some of these constrain only the axion coupling to photons

67 ($g_{a\gamma}$), while others constrain the axion coupling to electrons (g_{ae}). Recent and future laboratory tests (the
68 latter shown in light green) can probe $f_a \sim 10^9 - 10^{12}$ GeV, or even higher f_a .

69 The parameter space for ALPs is shown in Fig. 1-1 (bottom). The axion parameter space lies within an
70 order of magnitude from the line labelled “KSVZ axion,” which represents a particular QCD axion model.
71 Experimentally excluded regions (dark green), constraints from astronomical observations (gray) or from
72 astrophysical, or cosmological arguments (blue) are shown. Sensitivity of a few planned experiments are
73 shown in light green.

74 1.2.2.1 Dark Matter

75 Axions and ALPs can naturally serve as the universe’s dark matter, meaning that the galactic halo may
76 be formed partly or entirely from these particles. They can be produced thermally or non-thermally in
77 the early universe. Thermally produced axions are disfavored by observations of the universe’s large scale
78 structure [12], but thermally produced ALP dark matter is still allowed in large parts of the parameter
79 space. Non-thermal production can occur through the “vacuum misalignment mechanism” or the decay of
80 axionic strings and domain walls. Axions with large f_a do not thermalize in the early universe and their
81 abundance today is set by the initial state set during the Peccei-Quinn phase transition. There are two
82 scenarios depending on whether the PQ transition took place after or before inflation. In the first case, the
83 dominant contribution arises from the decay of cosmic strings and domain walls into axions. This scenario
84 suggests values of $m_a \sim 80 - 400 \mu\text{eV}$ with large uncertainties arising from extrapolating the numerical result
85 for the string and domain wall decays [13, 14]. In the second scenario, inflation homogenizes the initial axion
86 field value in our observable universe and the dark matter density depends on this value. For natural values
87 $a_{\text{initial}} \sim f_a$ the observed DM density arises for $m_a \sim 12 \mu\text{eV}$. Accepting fine-tuning, smaller values of the
88 mass are possible when $a_{\text{initial}} \ll f_a$ and somewhat larger masses (perhaps up to meV [15]) can be achieved
89 by tuning towards $a_{\text{initial}} = \pi f_a$.

90 All in all, the natural values $m_a \sim 10^{-5} - 10^{-4}$ eV present a clear experimental target. The Axion Dark
91 Matter eXperiment (ADMX) will soon probe part of this preferred parameter space.

92 Extending these arguments to ALPs, a much larger parameter space needs to be explored as indicated in
93 Fig. 1-1; see also *e.g.*, [16].

94 One important constraint on axion (or ALP) dark matter is the generation of isocurvature temperature
95 fluctuations in the cosmic microwave background if the axion/ALP exists during inflation. CMB probes like
96 the Planck satellite constrain these fluctuations, setting very strong constraints on the Hubble scale during
97 inflation, $H_I \lesssim O(10^6)$ GeV. Observing tensor modes in the CMB allows to determine H_I , providing a
98 crucial test of axion/ALP dark matter.

99 It is noteworthy that axion or ALP dark matter may also form a Bose-Einstein condensate [17], which may
100 lead to caustic rings in spiral galaxies, which may already have been observed. This also has detectable
101 consequences in terrestrial direct detection experiments like ADMX.

102 1.2.2.2 Hints from astrophysics

103 In the last few years some astrophysical anomalies have found plausible explanations in terms of axion/ALPs
104 suggesting target areas in parameter space reachable by near-future experiments. We refer here to the
105 apparent non-standard energy loss of white dwarf stars, *e.g.*, [18, 19, 20, 21, 22] (see however [23]) and the
106 anomalous transparency of the universe for TeV gamma rays, *e.g.*, [24, 25, 26, 27, 28, 29]. The required

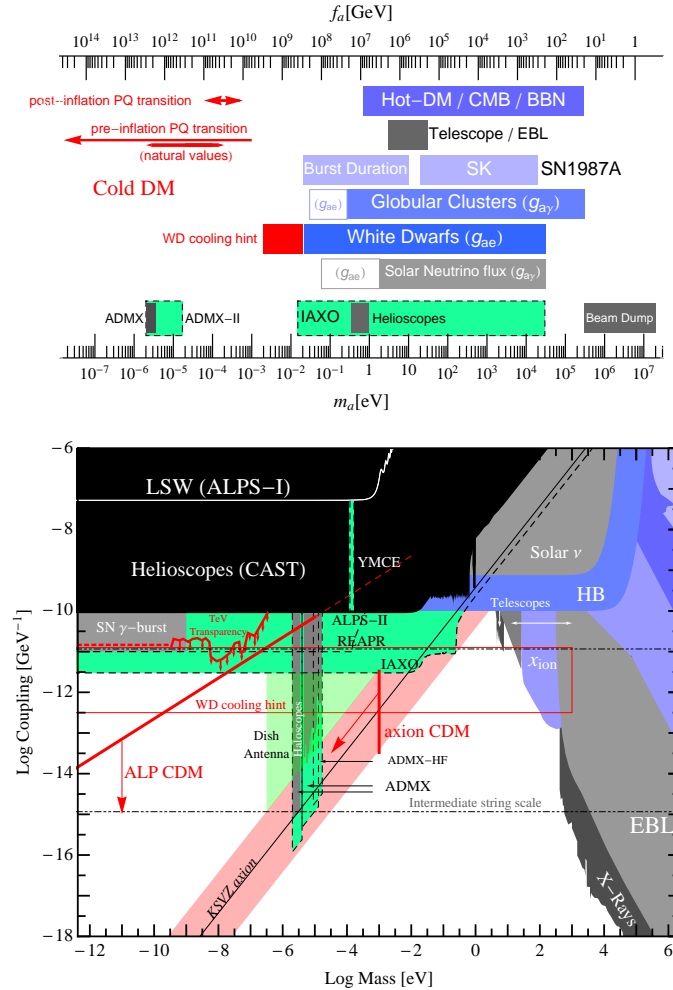


Figure 1-1. Parameter space for axions (top) and axion-like particles (ALPs) (bottom). In the bottom plot, the QCD axion models lie within an order of magnitude from the explicitly shown “KSVZ” axion line (red band). Colored regions are: experimentally excluded regions (dark green), constraints from astronomical observations (gray) or from astrophysical or cosmological arguments (blue), and sensitivity of planned and suggested experiments (light green) [ADMX [30], ALPS-II [31], IAXO [32, 33], Dish antenna [34]]. Shown in red are boundaries where ALPs can account for all the dark matter produced either thermally in the big bang or non-thermally by the misalignment mechanism.

107 coupling strengths seem within reach in controlled laboratory experiments at the intensity frontier, and can
 108 serve as useful benchmarks, c.f. Fig. 1-1.

109 Ultra-light axion-like particles can contribute to the dark matter in the universe, but affect structure
 110 formation in a manner distinct from cold dark matter (CDM). The distinction arises due to a scale dependent
 111 sound speed in the ultra-light ALPs fluid [35, 36, 37]. Large scale structure and the CMB thus allow one
 112 to constrain the fraction of dark matter that can be made up of such ALPs across a wide range of masses
 113 $10^{-33}eV < m_a < 10^{-18}eV$. Constraints were last made in 2006 using a simple grid-based likelihood and
 114 constrain axion density contributions at the 1-10% level in masses intermediate in this range. Constraints
 115 are limited on large scales by lack of data on the matter power spectrum at large scales, and on small scales
 116 by lack of non-linear models and the use of older (and possibly unreliable) Lyman-alpha constraints.

117 These constraints can be updated to include recent data and using a more sophisticated nested sampling
 118 technique to account for all degeneracies. Future surveys such as Euclid stand to improve constraints down
 119 to the sub-percent level, with specific improvements at the lowest masses and with discerning differences
 120 between ultra-light ALPs and thermal neutrinos of eV mass [38, 39]. The effect of these ALPs on the CMB
 121 and weak lensing tomography has been explored in detail in [38, 40]. Euclid weak lensing tomography will, if
 122 systematics can be properly understood, be the most powerful future probe of ultra-light ALPs, tightening
 123 constraints to the sub-percent level [38].

124 Furthermore, if these ALPs are fundamental fields present during inflation then they carry isocurvature
 125 perturbations. These are distinct from QCD axion isocurvature perturbations in two ways. Firstly, the
 126 effect on clustering that constrains the density fraction allows one to give marginalised constraints to the
 127 energy scale of inflation that are data driven, rather than relying on untestable priors about the fine-tuning
 128 of the QCD axion. Secondly, the lower mass allows these isocurvature perturbations to co-exist with tensor
 129 CMB modes of observable amplitude, which may allow cross-checks and consistency checks on theories of
 130 inflation, if detected [40]. The marginalized constraints probe low-scale inflation models. Assuming the
 131 existence of a ultra-light ALPs they rule out many simple inflationary models more strongly than tensor
 132 constraints in Planck, but are consistent with, for example, string theory models discussed in [41].

133 Finally, in the mass range $10^{-24}eV \leq m_a \lesssim 10^{-20}eV$, large scale structure formation with ultra-light ALPs
 134 is analogous to warm dark matter (WDM), and is thus relevant to problems with CDM structure formation,
 135 such as the cusp-core, missing-satellites, and too-big-to-fail problems [36]. The virtue of ultra-light ALPs is
 136 that they avoid the so-called ‘Catch 22’ of WDM [42]. Work on these large scale structure problems with
 137 axions is also work in preparation.

138 1.2.3 Status and Plans for Terrestrial experiments

139 1.2.3.1 Laser Experiments

140 The simplest and most unambiguous purely laboratory experiment to look for axions (or light scalars or
 141 pseudoscalars more generally) is photon regeneration[43] (“shining light through the wall”). A laser beam
 142 traverses a magnetic field, and the field stimulates a small fraction of photons to convert to axions of the
 143 same energy. A material barrier easily blocks the primary laser beam; in contrast, the axion component
 144 of the beam travels through the wall unimpeded and enters a second magnet. There, with the same
 145 probability, the axions are converted back to photons. Because the photon-regeneration rate goes as $g_{a\gamma\gamma}^4$,
 146 the sensitivity of the experiment is poor in its basic form, improved only by increasing the laser intensity,
 147 the magnetic field strength, or the length of the interaction regions. As initially suggested by Hoogeveen
 148 and Ziegenhagen[44] and recently discussed in detail,[45, 46, 47] very large gains may be realized in both
 149 the photon-regeneration rate and in the resulting limits on $g_{a\gamma\gamma}$ by introducing matched optical resonators
 150 in both the axion production and the photon regeneration regions.

151 Detailed designs for such an experiment exist, including the scheme for locking two matched high-finesse
 152 optical resonators, the signal detection method, and the ultimate noise limits.[46, 47, 48] Such experiments
 153 would improve on present limits on $g_{a\gamma\gamma}$ by at least a factor of 10. We note also that these experiments,
 154 although challenging, are feasible using well-established technologies developed for example for laser interfer-
 155 ometer gravitational-wave detectors.[49, 50] No new technology is needed. Two developed designs exist: the
 156 Resonantly Enhanced Axion-Photon Regeneration (REAPR) experiment, a Florida-Fermilab collaboration,
 157 and the Any Light Particle Search II (ALPS II) being mounted at DESY.

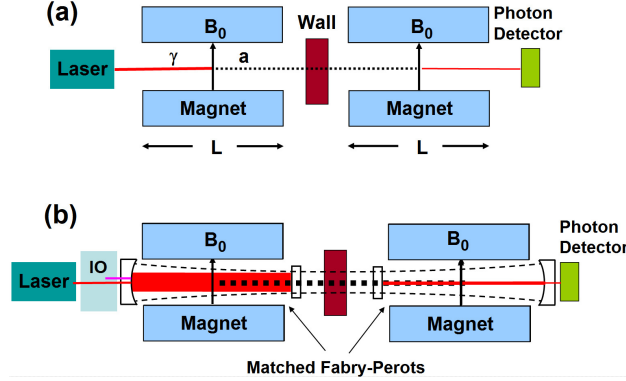


Figure 1-2. (a) Simple photon regeneration. (b) Resonant photon regeneration, employing matched Fabry-Perot cavities. The overall envelope schematically shown by the thin dashed lines indicates the important condition that the axion wave, and thus the Fabry-Perot mode, in the photon regeneration cavity must follow that of the hypothetically unimpeded photon wave from the Fabry-Perot mode in the axion generation magnet. Between the laser and the cavity are optics (IO) which manage mode matching of the laser to the cavity, imposes RF sidebands for reflection locking of the laser to the cavity, and provides isolation for the laser. The detection system is also fed by matching and beam-steering optics. Not shown is the second laser for locking the regeneration cavity and for heterodyne readout.

158 Figure 1-2(a) shows the photon regeneration experiment as usually conceived. If E_0 is the amplitude of the
 159 laser field propagating to the right, the amplitude of the axion field traversing the wall is $E_0\sqrt{P}$ where P is
 160 the conversion probability in the magnet on the LHS of Fig. 1-2a. Let P' be the conversion probability in the
 161 magnet on the RHS. The field generated on that side is then $E_S = E_0\sqrt{P'P}$ and the number of regenerated
 162 photons is $N_S = P'PN_0$ where N_0 is the number of photons in the initial laser beam.

163 It can be shown[51, 43, 52] that the photon to axion conversion probability P in a region of length L permeated
 164 by a constant magnetic field B_0 transverse to the direction of propagation, is given by ($\hbar = c = 1$)

$$P = \frac{1}{4}(g_{a\gamma\gamma}B_0L)^2. \quad (1.1)$$

165 This equation is written for the effect in vacuum and for the case where the where the difference between
 166 the axion and photon momenta $q = m_a^2/2\omega$ is small compared to $1/L$. The axion to photon conversion
 167 probability in this same region is also equal to P .

168 A number of photon regeneration experiments have been reported,[53, 54, 55, 56, 57, 58, 59] with the best
 169 limits[56, 59] being $g_{a\gamma\gamma} < 3.5 \times 10^{-7} \text{ GeV}^{-1}$. None of these experiments used cavities on the photon
 170 regeneration side of the optical barrier; recycling on the production side has been used in two.[53, 59]

171 Photon regeneration is enhanced by employing matched Fabry-Perot optical cavities, Fig. 1-2(b), one within
 172 the axion generation magnet and the second within the photon regeneration magnet.[44, 45, 46] The first
 173 cavity, the axion generation cavity, serves to build up the electric field on the input (left) side of the
 174 experiment. It is easy to see that when the cavity is resonant to the laser wavelength, the laser power
 175 in the high-field region is increased by a factor of \mathcal{F}_a/π where $\mathcal{F}_a = 4\pi T_{1a}/(T_{1a} + V_a)^2$ is the finesse of
 176 the cavity, T_{1a} is the transmittance of the input mirror, and V_a is the roundtrip loss of the cavity due to
 177 absorption of the coatings, scattering from defects, diffraction from the finite mirror size, and transmission
 178 through the end mirror. The increase in the laser power increases the number of created axions by a factor
 179 of \mathcal{F}_a/π . These axions propagate through the “wall” and reconvert into photons in the regeneration cavity
 180 at right. The intra-cavity photon field builds up under the conditions that the second cavity is resonant at
 181 the laser wavelength and that the spatial overlap integral η between the axion mode and the electric field

mode is good. This overlap condition requires that the spatial eigenmodes of the two cavities are extensions of each other, e.g., when the Gaussian eigenmode in one cavity propagated to the other cavity is identical to the Gaussian eigenmode of that cavity.

To detect the regenerated field, a small part is allowed to transmit through one of the cavity mirrors. The number of detected photons behind the regeneration cavity is [44, 45, 46]

$$N_S = \eta^2 \frac{\mathcal{F}_\gamma}{\pi} \frac{\mathcal{F}_a}{\pi} P^2 N_{in} \quad (1.2)$$

Note that resonant regeneration gives an enhancement factor of $\sim (\mathcal{F}/\pi)^2$ over simple photon regeneration. This factor may feasibly be 10^{10} , corresponding to an improvement in sensitivity to $g_{a\gamma\gamma}$ of ≈ 300 .

The resonantly-enhanced photon regeneration experiment, involving the design and active locking of high-finesse Fabry-Perot resonators and the heterodyne detection of weak signals at the shot-noise limit, is well supported by the laser and optics technology developed for LIGO. [49] We mention briefly the technical challenges and the means to address them planned by two realistic designs (REAPR and ALPS-II) and then discuss the expected sensitivities of these experiments.

The REAPR design utilizes a total of 12 Tevatron superconducting dipoles (each 5 T field, 6 m length, and 48 mm diameter bore), 6 for the axion generation cavity (total magnetic length of 36 m) and 6 for the photon regeneration cavity. ALPS-II plans to use 20 straightened HERA dipoles, with fields of 5.2 T and total magnetic length of 88 m. These magnets all exist and the magnet group at DESY has demonstrated that a dipole may be made almost straight and still function.

The layout requires that the optical cavities support mirror-image fundamental spatial modes, have a common or near common waist location, and should suppress all higher-order spatial modes. In addition, losses due to aperture effects should be kept very low, requiring not too big a divergence of the light away from the waist. These considerations, together with the dimensions of the available magnets, drive the design of the cavity parameters. [60]

The gain of the cavity and the circulating power stored in it is set by the input power, the transmission of the input mirror, absorption in both mirrors, scattering, clipping by finite apertures, and the residual transmission of the nominally 100% reflecting second mirror. Absorption values at 1064 nm of less than 1 ppm/bounce are commercially available. [61] Both REAPR and ALPS-II have designed cavities where clipping is not a limiting factor. The chosen parameters would allow a cavity finesse of comfortably above the anticipated value of 300,000 (REAPR) or 5000–40,000 (ALPS-II).

The efficiency of photon regeneration will also depend on alignment mismatches between the cavities. Angular or lateral misalignment of the optical axes would significantly reduce the spatial overlap between the two modes. Losses caused by a lateral shift δx scale with the beam size, those caused by an angular shift scale with the divergence angle, so that the overall efficiency is:

$$\eta \approx 1 - \frac{1}{2} \frac{\delta x^2}{w_1^2} - \frac{1}{2} \frac{\delta \alpha^2}{\Theta^2} \quad \text{with :} \quad \Theta = \frac{\lambda}{\pi w_1} \quad (1.3)$$

Requiring an efficiency $\eta > 0.95$, we obtain the following requirements on lateral and angular offsets for ~ 50 m scale experiments:

$$\delta x < 1 \text{ mm} \quad \delta \alpha < 10 \mu\text{rad} \quad (1.4)$$

One of the main challenges of the experiment is to align correctly the two cavities and maintain the alignment throughout the experiment. Recall that it is the axion field which couples the two cavities and that axions, in contrast to light, do not experience any refraction in wedged mirror substrates. In addition, we have to

219 avoid any leakage of photons from the production cavity into the photon generation cavity. Both conditions
 220 limit the number of possibilities for alignment sensing and control between the two cavities. Developing and
 221 testing the length and alignment sensing and control scheme is a key reason why both REAPR and ALPS-II
 222 have planned preliminary hidden-sector-photon searches prior to using magnets and full-length cavities.

223 The approach to alignment planned by REAPR has been described in some detail.[46, 47] The basic idea is
 224 first to align the two curved end mirrors as a single cavity and then to align the flat central mirrors of the two
 225 cavities to the axis defined by this initial step. The central mirrors, alignment sensing (quad) photodiodes,
 226 and other components are all mounted on a rigid, low-thermal-expansion optical bench. The central bench
 227 can be removed and reinserted during the construction process to verify the overall co-alignment of the two
 228 cavities. ALPS-II plans a similar approach.

229 Intrinsic to resonantly enhanced photon regeneration is the requirement that the axion generation and photon
 230 regeneration cavities are both on resonance at the same wavelength as that of the axion generating laser.
 231 The basic idea of REAPR is to use two lasers, with the second “offset locked” to the first one. The offset,
 232 set by a RF oscillator, is a multiple of the free spectral range of the cavities. This offset locking ensures that
 233 both cavities have common resonances while at the same time having the light used to lock the detection
 234 cavity be at a different frequency than the regenerated photons.[46, 47] ALPS-II will double the frequency
 235 of the generation laser into the a green, and use this $2\times$ light to lock the regeneration cavity.

236 Error signals for controlling the cavity lengths and angular misalignments are obtained by using phase
 237 modulated light, giving sidebands that monitor the phase change in the carrier caused by mismatches
 238 between the laser and the cavity eigenmode. The length sensing method is known as the Pound-Drever-
 239 Hall technique[62] while the angular sensing technique is based on wavefront sensing and is standard in all
 240 interferometric gravitational wave detectors.[63]

241 The two experiments plan quite different means to detect the (very weak) regenerated light. ALPS-II
 242 will employ a superconducting transition-edge sensor, which has nearly single-photon sensitivity at the
 243 1064 nm wavelength of these photons. REAPR will use heterodyne detection, with the regeneration cavity
 244 locking laser used as the local oscillator for the coherently regenerated optical field E_S , which occurs at the
 245 frequency of the axion-generation laser. When mixed at a photodetector with the laser field used for locking
 246 the regeneration-cavity, the beats between the two fields give a signal (written in terms of the number of
 247 photons N in both fields) of

$$S = N_{LO} + 2\sqrt{N_{LO}N_S} \cos \phi \cos \Omega t + 2\sqrt{N_{LO}N_S} \sin \phi \sin \Omega t \quad (1.5)$$

248 where Ω is the difference in laser frequencies, N_{LO} is the number of local oscillator photons, N_S is the
 249 number of signal (regenerated) photons. There are two quadrature components of the signal on account of
 250 the unknown phase ϕ from the distance between the two cavities.

251 The shot noise or variance in each quadrature can be calculated from the number of photons detected
 252 $\sigma_I = \sqrt{2N} = \sqrt{2N_{LO}} = \sigma_Q$. These in-phase and quadrature components are added, making the signal-to-
 253 noise ratio be

$$\frac{S_\Sigma}{\sigma_\Sigma} = \sqrt{N_S}, \quad (1.6)$$

254 where N_S is the number of regenerated photons in the signal field. As expected, to obtain a signal to noise
 255 ratio of one requires one detected photon.

256 For a baseline of 36-m, 5 T, magnets, an input power of 10 W, a cavity finesse of $\mathcal{F} \sim \pi \times 10^5$ ($T = 10 \text{ ppm} =$
 257 V) for both cavities, and 10 days of operation, we find at signal-to-noise ratio of unity,

$$g_{a\gamma\gamma}^{min} = \frac{2 \times 10^{-11}}{\text{GeV}} \left[\frac{0.95}{\eta} \right] \left[\frac{180 \text{ Tm}}{BL} \right] \left[\frac{3 \times 10^5}{\mathcal{F}} \right]^{1/2} \left[\frac{10 \text{ W}}{P_{in}} \right]^{1/4} \left[\frac{10 \text{ days}}{\tau} \right]^{1/4}. \quad (1.7)$$

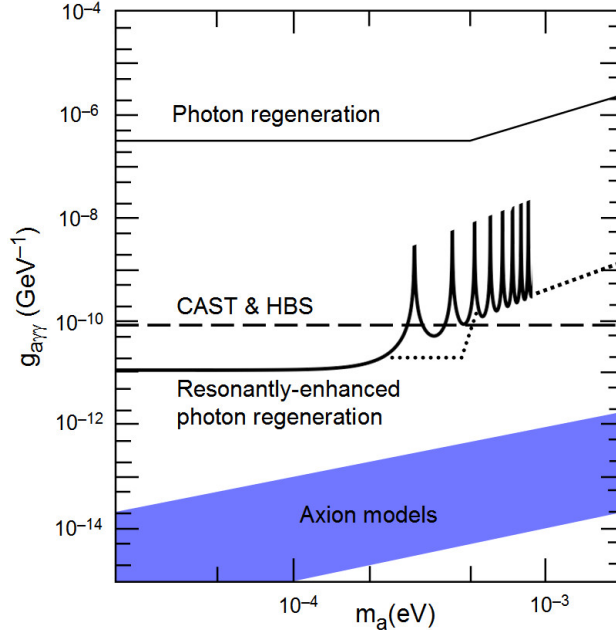


Figure 1-3. Exclusion plot of mass and photon coupling $(m_a, g_{a\gamma\gamma})$ for the axion, and the 95% CL exclusion limit for the resonantly enhanced photon regeneration (REPR) experiment. The existing exclusion limits indicated on the plot include the best direct solar axion search (CAST collaboration),[64] the Horizontal Branch Star limit,[65] and previous laser experiments.[56, 59]

258 The experiment yields a 95% exclusion limit (3σ) for axions or generalized pseudoscalars with $g_{a\gamma\gamma}^{min} <$
 259 $2.0 \times 10^{-11} \text{GeV}^{-1}$ after 90 days cumulative running, well into territory unexplored by stellar evolution
 260 bounds or direct solar searches. Note that the exclusion sensitivity follows the inverse of $\text{sinc}(qL/2)$; for
 261 REAPR the first null sensitivity occurs at $2.8 \times 10^{-4} \text{eV}$ and for ALPS-II at about half this value. The
 262 momentum mismatch between a massless photon and a massive axion defines the oscillation length of the
 263 process to be $L_{osc} = 2\pi/q$. (As pointed out in Ref. [43] however, there is a practical strategy to extend the
 264 mass range upwards if the total magnetic length L is comprised of a string of N individual identical dipoles
 265 of length l . In this case, one may configure the magnet string as a “wiggler” to cover higher regions of mass,
 266 up to values corresponding to the oscillation length determined by a single dipole.) The sensitivity of both
 267 nonresonant and resonant regeneration experiments, as well as other relevant limits, are shown in Fig. 1-3.

268 The optical prototypes being developed for the resonant regeneration experiment will also have sensitivity
 269 to photon-paraphoton oscillations.[66] Paraphotons are new weakly-interacting U(1) gauge bosons predicted
 270 to exist in generic models of beyond-the-standard-model physics including string theory.[67] They undergo
 271 kinetic mixing with the ordinary photon resulting in oscillations of photons to paraphotons and the possibility
 272 of performing a photon regeneration experiment. Unlike the case of photon-axion oscillations, photon-
 273 paraphoton oscillations do not require the presence of an external magnetic field, and so can be performed
 274 with just the prototype optics and data acquisition system. On account of the gain from the resonant cavities,
 275 a search with a REAPR or ALPS-II prototype with meter-length cavities supersedes the LIPSS limit[68] in
 276 less than 1 second of running. With a 10-day run, the sensitivity will be improved by a factor of 300,
 277 reaching mixing angles $\chi \approx 10^{-9}$, sufficient to determine whether paraphotons generated from the cosmic
 278 microwave background play an important role in cosmology. [69] While not the primary goal of the project,
 279 a physics result on paraphotons will come for free during the development phase of a resonantly-enhanced
 280 axion-photon regeneration experiment.

281 1.2.3.2 Microwave Cavities (Haloscopes)

282 Soon after the axion was realized to be a natural dark matter candidate, a detection concept was proposed
 283 that relies on the resonant conversion of dark matter axions into photons via the Primakoff effect [70].
 284 Though the axion mass is unknown, various production mechanisms in the early universe point to a mass
 285 scale of a few to tens of μeV if the axion is the dominant form of dark matter. The detection concept relies
 286 on dark matter axions passing through a microwave cavity in the presence of a strong magnetic field where
 287 they can resonantly convert into photons when the cavity frequency matches the axion mass. A $4.13 \mu\text{eV}$
 288 axion would convert into a 1 GHz photon, which can be detected with an ultra-sensitive receiver. Axions in
 289 the dark matter halo are predicted to have virial velocities of $10^{-3}c$, leading to a spread in axion energies of
 290 $\Delta E_a/E_a \sim 10^{-6}$ (or 1 kHz for our 1 GHz axion example).

291 Initial experiments run at Brookhaven National Laboratory [71] and the University of Florida [72] came
 292 within an order of magnitude of the sensitivity needed to reach plausible axion couplings. ADMX [73] was
 293 assembled at Lawrence Livermore National Laboratory and consists of a large, 8 T superconducting solenoid
 294 magnet with a 0.5 m diameter, 1 m long, open bore. Copper-plated stainless steel microwave cavities are
 295 used and have $Q_C \sim 10^5$, low enough to be insensitive to the expected spread in axion energies. The TM_{010}
 296 mode has the largest cavity form factor and is moved to scan axion masses by translating vertical copper or
 297 dielectric tuning rods inside the cavity from the edge to the center. TE and TEM modes do not couple to
 298 the pseudoscalar axion.

299 Using the ADMX setup and an estimated local dark matter density of $\rho_{DM} = 0.45 \text{ GeV}/\text{cm}^3$ [74], an axion
 300 conversion power $P_a \sim 10^{-24} \text{ W}$ is expected for plausible dark matter axions, with the possibility of scanning
 301 an appreciable frequency space (hundreds of MHz) in just a few years. Initial data runs were cooled with
 302 pumped LHe to achieve physical temperatures of $< 2 \text{ K}$ and used SQUID amplifiers to reach plausible
 303 dark matter axion couplings [75]. Recently the ADMX experiment has been moved to the University of
 304 Washington where it will be outfitted with a dilution refrigerator that will increase sensitivity and scan
 305 rate. A second ADMX site, dubbed ADMX-HF, is being constructed at Yale and will allow access to > 2
 306 GHz while ADMX scans from 0.4 - 2 GHz. To achieve a greater mass reach, near-quantum limited X-band
 307 amplifiers and large volume resonant cavities will have to be developed.

308 As shown in Fig. 1-1, ADMX and ADMX-HF are uniquely sensitive to axion and ALP dark matter in the
 309 range of a few to tens of μeV . The experiments also have exceptional sensitivity to hidden-photons in the
 310 same mass region, as shown in Fig. 1-7.

311 1.2.3.3 Helioscopes

312 Axions could be produced from blackbody photons in the solar core via the Primakoff effect [76] in the
 313 presence of strong electromagnetic fields in the plasma. Since the interaction of these axions with ordinary
 314 matter is extraordinarily weak, they can escape the solar interior, stream undisturbed to Earth and reconvert
 315 in a strong laboratory transverse magnetic field via the inverse Primakoff effect [77, 78, 79]. The minimum
 316 requirements for such a helioscope experiment of high sensitivity are a powerful magnet of large volume
 317 and an appropriate x-ray sensor covering the exit of the magnet bore. Ideally, the magnet is equipped with
 318 a mechanical system enabling it to follow the Sun and thus increasing exposure time. Sensitivity can be
 319 further enhanced by the use of x-ray optics to focus the putative signal and therefore reducing detector size
 320 and background levels.

321 The first axion helioscope search was carried out at Brookhaven National Lab in 1992 with a static dipole
 322 magnet [80]. A second-generation experiment, the Tokyo Axion Helioscope, uses a more powerful magnet
 323 and dynamic tracking of the Sun [81, 82, 83]. The CERN Axion Solar Telescope (CAST), a helioscope of

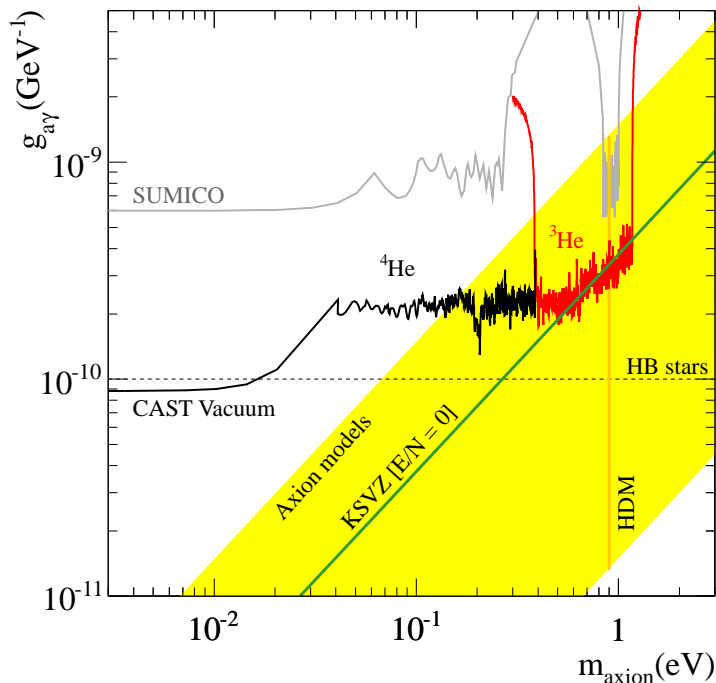


Figure 1-4. Exclusion regions in the $m_a - g_{a\gamma}$ plane achieved by CAST in the vacuum [86, 87], ^4He [88], and ^3He phase [89, 90]. We also show constraints from the Tokyo helioscope, horizontal branch (HB) stars [91], and the hot dark matter (HDM) bound [92]. The yellow band labeled "Axion models" represents typical theoretical models with $|E/N - 1.95| = 0.07 - 7$. The green solid line inside the band corresponds to $E/N = 0$ (KSVZ model).

324 the third generation and the most sensitive solar axion search to date, began data collection in 2003. It
 325 employs an LHC dipole test magnet of 10 m length and 10 T field strength [84] with an elaborate elevation
 326 and azimuth drive to track the Sun. CAST is the first solar axion search exploiting x-ray optics to improve
 327 the signal to background ratio (a factor of 150 in the case of CAST) [85]. For $m_a < 0.02$ eV, CAST has
 328 set an upper limit of $g_{a\gamma} < 8.8 \times 10^{-11}$ GeV $^{-1}$ and a slightly larger value of $g_{a\gamma}$ for higher axion masses
 329 [86, 87, 88, 89, 90]. The exclusion plots are shown in Fig. 1-4. CAST has also established the first helioscope
 330 limits for non-hadronic axion models [93].

331 So far each subsequent generation of axion helioscopes has resulted in an improvement in sensitivity to the
 332 axion-photon coupling constant $g_{a\gamma}$ of about a factor 6 over its predecessors. To date, all axion helioscopes
 333 have used "recycled" magnets built for other purposes. The IAXO collaboration has recently shown [94] that
 334 a further substantial step beyond the current state-of-the-art represented by CAST is possible with a new
 335 fourth-generation axion helioscope, dubbed the International AXion Observatory (IAXO). The concept relies
 336 on a purpose-built ATLAS-like magnet capable of tracking the sun for about 10 hours each day, focusing
 337 x-ray optics to minimize detector area, and low background x-ray detectors optimized for operation in the
 338 0.5 – 10 keV energy band. Pushing the current helioscope boundaries to explore the range in $g_{a\gamma}$ down
 339 to a few 10^{-12} GeV $^{-1}$ (see Fig. 1-5), with sensitivity to QCD axion models down to the meV scale and
 340 to ALPs at lower masses, is highly motivated as was shown in previous sections. Lowering x-ray detector
 341 thresholds to 0.1 keV would allow IAXO to test whether solar processes can create chameleons [95] and
 342 further constrain standard axion-electron models. More speculative, but of tremendous potential scientific
 343 gain, would be the operation of microwave cavities inside IAXO's magnet, to allow a simultaneous search for

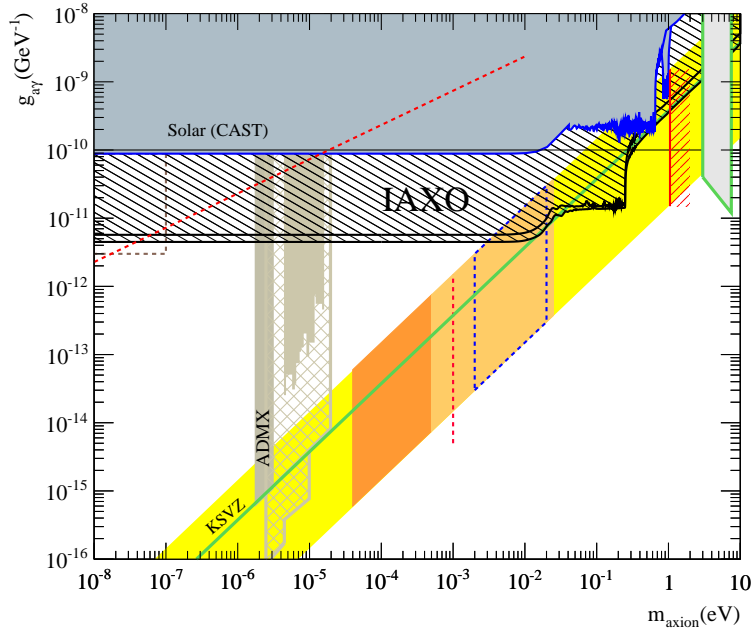


Figure 1-5. Expected sensitivity of IAXO compared with current bounds from CAST and ADMX. Also future prospects of ADMX are shown (dashed brown region).

344 solar and dark matter axions [*e.g.*, [96]]. Searches for solar axions and chameleons which exploit naturally
 345 occurring magnetic fields are described in [96, 97, 98] and reviewed in [99]. IAXO can carry out this task
 346 as one of the main experimental pathways in the next decade for the axion community. More generally, a
 347 detection with IAXO would have profound implications for particle physics, with clear evidence of physics
 348 beyond the SM.

349 1.2.3.4 Beam Dumps and Colliders

350 Axions and ALPs can also be searched for in beam dump and collider experiments. These types of
 351 experiments are described in greater detail in the search for dark photons and similar particles. Under
 352 the appropriate configuration, such experiments can also explore axion and ALP parameter space.

353 1.3 Dark Photons

354 1.3.1 Theory & Theory Motivation

355 This section describes the theory and motivation for new forces mediated by new abelian $U(1)$ gauge bosons
 356 A' — also called “U-bosons,” or “hidden-sector,” “heavy,” “dark,” “para-,” and “secluded” photons — that
 357 couple very weakly to electrically charged particles through “kinetic mixing” with the photon [100, 101].

358 Kinetic mixing produces an effective parity-conserving interaction $\epsilon e A'_\mu J_{EM}^\mu$ of the A' to the electromagnetic
 359 current J_{EM}^μ , suppressed relative to the electron charge e by the parameter ϵ , which can be naturally small

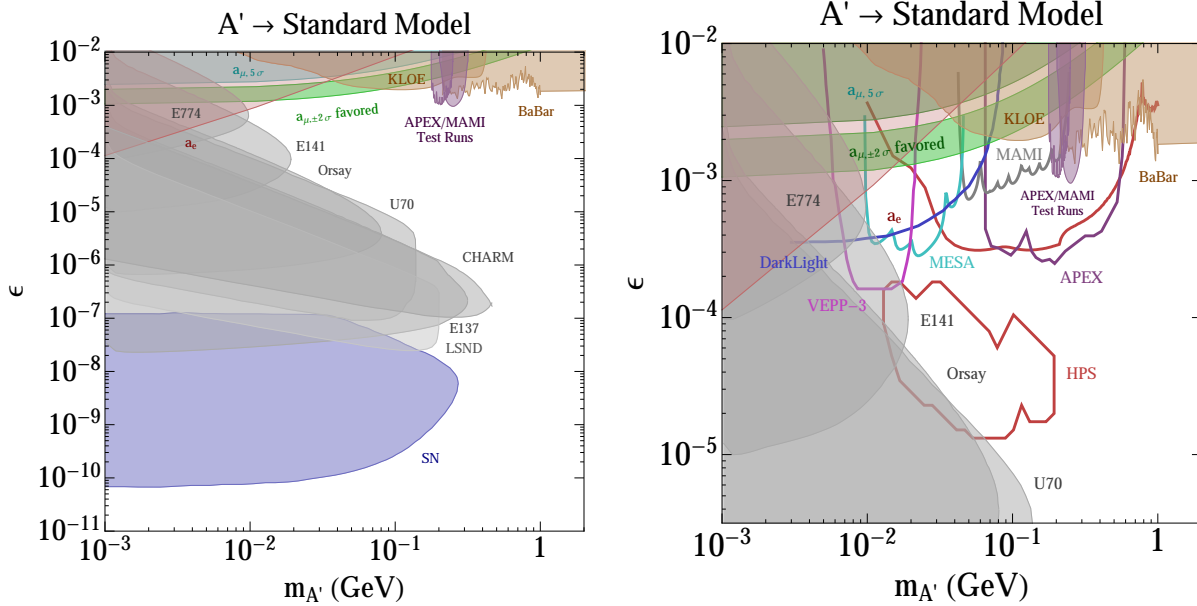


Figure 1-6. Parameter space for hidden-photons (A') with mass $m_{A'} > 1$ MeV (see Fig. 1-7 for $m_{A'} < 1$ MeV). Shown are existing 90% confidence level limits from the SLAC and Fermilab beam dump experiments E137, E141, and E774 [102, 103, 104, 105] the muon anomalous magnetic moment a_μ [106], KLOE [107], the test run results reported by APEX [108] and MAMI [109], an estimate using a BaBar result [105, 110, 111], and a constraint from supernova cooling [105] (see also [112]). In the green band, the A' can explain the observed discrepancy between the calculated and measured muon anomalous magnetic moment [106] at 90% confidence level. On the right, we show in more detail the parameter space for larger values of ϵ . This parameter space can be probed by several proposed experiments, including APEX [113], HPS [114], DarkLight [115], VEPP-3 [116, 117], MAMI, and MESA [118]. Existing and future e^+e^- colliders such as BABAR, BELLE, KLOE, SuperB, BELLE-2, and KLOE-2 can also probe large parts of the parameter space for $\epsilon > 10^{-4} - 10^{-3}$; their reach is also not explicitly shown.

360 (we often write the coupling strength as $\alpha' \equiv \epsilon^2 \alpha$ where $\alpha = e^2/4\pi \simeq 1/137$). In particular, if the value of ϵ at
 361 very high energies is zero, then ϵ can be generated by perturbative or non-perturbative effects. Perturbative
 362 contributions can include heavy messengers that carry both hypercharge and the new $U(1)$ charge, and
 363 quantum loops of various order can generate $\epsilon \sim 10^{-8} - 10^{-2}$ [119]. Non-perturbative and large-volume
 364 effects common in string theory constructions can generate much smaller ϵ . While there is no clear minimum
 365 for ϵ , values in the $10^{-12} - 10^{-3}$ range have been predicted in the literature [120, 121, 122].

366 A hidden-sector consisting of particles that do not couple to any of the known forces and containing an
 367 A' is generic in many new physics scenarios. Hidden-sectors can have a rich structure, consisting of, for
 368 example, fermions and many other gauge bosons. The photon coupling to the A' could provide the only
 369 non-gravitational window into their existence. Hidden-sectors are generic, for example, in string theory
 370 constructions [123, 124, 125, 126]. Several other “portals” (connections between a visible and hidden-sector)
 371 beyond the kinetic mixing portal are possible, many of which can be investigated at the intensity frontier.

372 Masses for the A' can arise via the Higgs mechanism and can take on a large range of values. A' masses in
 373 the MeV–GeV range arise in the models of [127, 128, 129, 130] (these models often involve supersymmetry).
 374 However, much smaller (sub-eV) masses are also possible. Masses can also be generated via the Stückelberg
 375 mechanism, which is especially relevant in the case of large volume string compactifications with branes. In
 376 this case, the mass and size of the kinetic mixing are typically linked through one scale, the string scale M_s ,
 377 and therefore related to each other. In Fig. 1-7, various theoretically motivated regions are shown [120, 121].

378 The A' mass can be as small as M_s^2/M_{Pl} , i.e. $m_{A'} \sim \text{meV}$ (GeV) for $M_s \sim \text{TeV}$ (10^{10} GeV). Note that
 379 particles charged under a *massive* A' do not have an electromagnetic millicharge, but a *massless* A' can lead
 380 to millicharged particles (see §1.4.1.3).

381 The previous discussion focused on kinetic mixing between the hypercharge $U(1)_Y$ and the dark $U(1)$ gauge
 382 bosons, parametrized by ϵ . This can be generalized by allowing for the possibility of mass matrix mixing,
 383 parametrized by ϵ_Z , between the dark photon and the heavy Z boson of the SM [131]. Because of its
 384 expanded properties, the dark $U(1)$ vector boson has been dubbed the “dark Z ” and labeled Z_d in such a
 385 picture, in order to emphasize its Z -like properties [131]. Overall, the Z_d couples to both the electromagnetic
 386 (J_μ^{EM}) and the weak neutral (J_μ^{NC}) currents of the SM, via [131]

$$\mathcal{L}_{\text{int}} = - \left(\epsilon e J_\mu^{\text{EM}} + \epsilon_Z \frac{g}{2 \cos \theta_W} J_\mu^{\text{NC}} \right) Z_d^\mu. \quad (1.8)$$

387 The additional interactions involving ϵ_Z violate parity and current conservation. Consequently, potential new
 388 phenomena such as “Dark Parity Violation” in atoms and polarized electron scattering can result [131, 132].
 389 Enhancements in rare “dark” decays of the Higgs as well as K and B mesons into Z_d particles can also
 390 occur, suggesting new experimental areas of discovery [131, 133, 134].

391 1.3.2 Phenomenological Motivation and Current Constraints

392 A natural dividing line is $m_{A'} \sim 2m_e \sim 1$ MeV. For $m_{A'} > 1$ MeV, an A' can decay to electrically charged
 393 particles (*e.g.*, e^+e^- , $\mu^+\mu^-$, or $\pi^+\pi^-$) or to light hidden-sector particles (if available), which can in turn decay
 394 to ordinary matter. Such an A' can be efficiently produced in electron or proton fixed-target experiments
 395 [105, 115, 113, 108, 114, 109, 135, 136, 116] and at e^+e^- and hadron colliders [119, 128, 137, 110, 138, 139, 140,
 396 141, 142, 143, 107, 144, 145]. Hidden-sector particles could be directly produced through an off-shell A' and
 397 decay to ordinary matter. An A' in this mass range is motivated by the theoretical considerations discussed
 398 above, by anomalies related to dark matter [146, 147], and by the discrepancy between the measured and
 399 calculated value of the anomalous magnetic moment of the muon [106].

400 Fig. 1-6 shows existing constraints for $m_{A'} > 1$ MeV [105] and the sensitivity of several planned experiments
 401 that will explore part of the remaining allowed parameter space. These include the future fixed-target exper-
 402 iments APEX [113, 108], HPS [114], DarkLight [115] at Jefferson Laboratory, experiments at MAMI [109]
 403 at the University of Mainz (whose reach are not shown, but which may probe similar parameter regions as
 404 other experiments), and another at VEPP-3 [116]. Existing and future e^+e^- colliders can also probe large
 405 parts of the parameter space for $\epsilon > 10^{-4} - 10^{-3}$, and include *BABAR*, *Belle*, *KLOE*, *SuperB*, *Belle II*, and
 406 *KLOE-2* (the figure only shows existing constraints, and no future sensitivity). Proton colliders such as the
 407 LHC and Tevatron can also see remarkable signatures for light hidden-sectors [137]. This rich experimental
 408 program is discussed in more detail in §1.3.3.

409 For $m_{A'} < 1$ MeV, the A' decay to e^+e^- is kinematically forbidden, and only a much slower decay to three
 410 photons is allowed. Fig. 1-7 shows the constraints, theoretically and phenomenologically motivated regions,
 411 and some soon-to-be-probed parameter space. At very low masses, the most prominent implication of kinetic
 412 mixing is that, similar to neutrino mixing, the propagation and the interaction eigenstates are misaligned,
 413 giving rise to the phenomenon of photon $\leftrightarrow A'$ oscillations [149].

414 As axions or ALPs, A' bosons can also be dark matter through the vacuum-misalignment mechanism [150].
 415 This intriguing possibility can be realized in a wide range of values for $m_{A'}$ and ϵ [16], see Fig. 1-7. It appears
 416 that experiments such as ADMX, looking for axion dark matter, can be very sensitive to A' bosons as well,

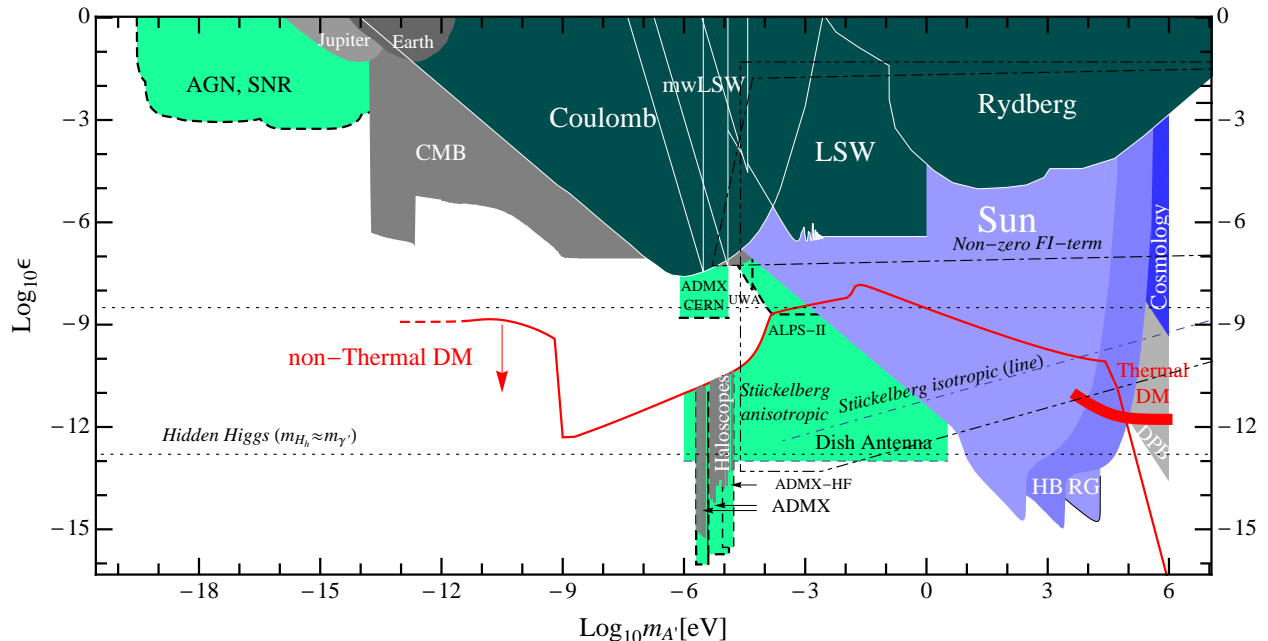


Figure 1-7. Parameter space for hidden-photons (A') with mass $m_{A'} < 1$ MeV (see Fig. 1-6 for $m_{A'} > 1$ MeV). Colored regions are: experimentally excluded regions (dark green), constraints from astronomical observations (gray) or from astrophysical or cosmological arguments (blue), and sensitivity of planned and suggested experiments (light green) [ADMX [30], ALPS-II [31], Dish antenna [34], AGN/SNR [148]]. Shown in red are boundaries where the A' would account for all the dark matter produced either thermally in the big bang or non-thermally by the misalignment mechanism (the corresponding line is an upper bound). The regions bounded by dotted lines show predictions from string theory corresponding to different possibilities for the nature of the A' mass: Hidden-Higgs, a Fayet-Iliopoulos term, or the Stückelberg mechanism. In general, predictions are uncertain by factors of order 1.

417 but in this case the use of magnetic fields to trigger the $A' \rightarrow$ photon conversion is not required. The same
 418 experimental apparatus can often look for several kinds of particles.

419 Other existing constraints, theoretically and phenomenologically motivated parameter regions, and future
 420 experimental searches for A' bosons with $m_{A'} < 1$ MeV are shown in Fig. 1-7. A few experimental searches
 421 are planned and discussed in §1.3.3.6, but a large parameter space still remains to be experimentally explored.

422 1.3.2.1 Hints for MeV-GeV mass Dark Photons from Dark Matter

423 Couplings between dark matter and dark photons at the MeV-GeV scale can drastically modify the phe-
 424 nomenology of dark matter. In direct detection experiments, the scattering cross section can be increased
 425 due to the light mediator, or alternatively the kinematics of the scattering can be altered if the mediator
 426 couples to nearly-degenerate states. In indirect searches, the self-annihilation and self-scattering rates for
 427 the dark matter can both be enhanced at low velocities; the former can lead to striking signals in cosmic
 428 rays, photons and neutrinos, while the latter can significantly modify the internal structure of dark matter
 429 halos. While the search for dark photons has strong motivations entirely independent from their possible
 430 link to dark matter phenomenology, their detection could potentially provide an entirely new window on the
 431 dark sector.

432 **Cosmic rays:**

433 In 2008 the PAMELA experiment reported an unexpected rise in the ratio of cosmic-ray (CR) positrons to
 434 CR electrons, beginning at ~ 10 GeV and extending to above 100 GeV [151]. This result was later confirmed
 435 by the Fermi Gamma-Ray Space Telescope [152] and most recently by AMS-02 [153]. The (largely model-
 436 independent) expectation from standard CR propagation models is that the positron fraction should fall with
 437 increasing energy¹. Complementary measurements of the total e^+e^- spectrum by the Fermi Gamma-Ray
 438 Space Telescope [157] are consistent with a new source of e^+e^- pairs in the 10-1000 GeV energy range.

439 The annihilation of weak-scale dark matter provides an attractive hypothesis for the origin of this signal,
 440 but there are several difficulties with the conventional WIMP interpretation (e.g. [158])². Dark matter
 441 annihilating to a dark photon which subsequently decays, however, naturally yields (i) an enhanced signal
 442 (by up to 2-3 orders of magnitude) and (ii) a sufficiently hard positron spectrum to match the observations,
 443 as well as forbidding the production of antiprotons, if the dark photon is lighter than twice the proton mass
 444 (an antiproton excess was searched for, and not observed) [146, 147]. Benchmark models of this type were
 445 computed for a range of dark photon masses ranging from 200-900 MeV in [161], and found to provide a
 446 good fit to the data.

447 The AMS-02 data, with their much smaller uncertainties, prefer a somewhat softer spectrum of positrons
 448 than PAMELA. In turn, this favors dark photon models where the dark photon is heavy enough to decay to
 449 muons and charged pions, or possibly multi-particle final states (e.g. via decays through the dark sector);
 450 the spectrum due to dark photon decay to an e^+e^- pair is (as the sole channel) somewhat harder than
 451 preferred by the data [162]. Direct leptophilic annihilation to SM particles no longer appears to provide
 452 a good explanation for the signal: the softer spectrum favors $\tau^+\tau^-$ final states, which are constrained by
 453 searches for gamma-rays from dwarf galaxies [163].

454 There are also gamma-ray bounds on $\mu^+\mu^-$, $\pi^+\pi^-$ and e^+e^- final states, but gamma-ray production in
 455 these decays is small, and so the bounds are generally much weaker (unless upscattering of ambient starlight
 456 by electrons is included, but this contribution also depends on the electron propagation). Constraints
 457 from the inner Galaxy are dependent on the slope of the dark matter density profile, which is not well-
 458 constrained by the data or theory; constraints from the outer halo and extragalactic gamma-ray background
 459 depend sensitively on the amount of small-scale substructure present, which is also poorly known. There is
 460 tension between gamma-ray observations and the predictions from models fitting the PAMELA signal (e.g.
 461 [164, 165, 166]), but stronger statements are limited by the astrophysical uncertainties.

462 A more robust constraint arises from measurements of the cosmic microwave background (CMB). Dark
 463 matter annihilation during the epoch of recombination can inject electrons and photons which modify the
 464 ionization history of the universe; this in turn modifies the scattering of CMB photons at late times and
 465 perturbs the observed anisotropy spectrum [167]. At present, the best constraints from this channel appear to
 466 be in tension with models explaining the AMS-02 signal at the factor-of-2 level [168]; the Planck experiment
 467 should improve this constraint by another factor of two when its polarization data is released (e.g. [169]).
 468 The current tension could be resolved by allowing the local dark matter density to be higher by a factor of
 469 $\sim \sqrt{2}$, or by permitting an $\mathcal{O}(1)$ contribution to the signal from local clumps of dark matter. This second
 470 option is particularly attractive for lighter dark photons ($m_{A'} \ll 1$ GeV), where the annihilation cross section
 471 continues to grow at velocities smaller than that of the main Milky Way halo, and so the constraints from
 472 the CMB (originating from an epoch when the dark matter was extremely slow-moving) grow even stronger;

¹While there are proposals for generating the positron excess by modifications to CR propagation, they require non-trivial changes to the usual propagation paradigm, e.g. that the positrons do not suffer significant radiative losses over kpc distances [154], or that the positron production by proton scattering occurs primarily within the original CR acceleration site [155, 156].

²Non-dark matter explanations involving a new e^+e^- source have also been advanced, with the most popular being a population of pulsars; see e.g. [159, 160].

473 this conclusion can be evaded if the excess observed by AMS-02 largely originates from dark matter clumps
 474 with small internal velocity dispersions [170].

475 These constraints do not apply if the signal originates from decaying dark matter (e.g. [171]). In this case
 476 the size of the signal is not a difficulty, but the lack of antiprotons and the hard spectrum still motivate
 477 scenarios with decay through dark photons.

478 **Light dark matter:**

479 There have been several experimental results that might hint at the presence of $\mathcal{O}(1 - 10)$ GeV dark matter.
 480 The CDMS experiment has recently reported three events in their signal region [172], with the best fit
 481 WIMP hypothesis being favored over the background-only hypothesis at 99.8% confidence. The best-fit
 482 WIMP mass is 8.6 GeV/cm², with a 68% confidence contour extending from 6.5 – 20 GeV. This region is
 483 in good agreement with earlier hints of a signal from CoGeNT [173]; it appears in tension with limits from
 484 XENON100, but the comparison does depend on the response of xenon to low-energy nuclear recoils and on
 485 the DM velocity distribution [174].

486 The preferred dark matter-nucleon scattering cross section for the CDMS events, $\sigma \approx 2 \times 10^{-41}$ cm², is quite
 487 large. The two Standard Model particles which might be expected to mediate such a scattering are the Z
 488 boson and the Higgs, both of which are constrained (for light dark matter) by bounds on the invisible decay
 489 width of the Z and the Higgs; the cross section preferred by CDMS seems clearly ruled out for Higgs portal
 490 dark matter [175], and barely consistent for scattering through the Z [176]. This observation motivates the
 491 existence of a new mediator particle, in the event that the signal is indeed due to dark matter. A dark
 492 photon mediator naturally enhances the cross section; if the mass of the dark photon is inherited from the
 493 weak scale, the relation $m_{A'} \sim \sqrt{\epsilon} m_Z$ naturally predicts a dark matter-nucleon cross section comparable to
 494 that mediated by the Z , but the constraints on invisible decays no longer apply.

495 There have also been hints of possible annihilation signals from ~ 10 GeV dark matter in the Galactic Center
 496 and inner Galaxy [177, 178, 179, 180]; these signals can be accommodated by light dark matter annihilation
 497 to dark photons which subsequently decay to Standard Model particles [181].

498 **Self-interacting dark matter:**

499 Any coupling between MeV-GeV dark photons and dark matter will also give rise to a long-range self-
 500 interaction for the dark matter. This in turn can modify dark matter structure formation, flattening the
 501 cusps at the centers of halos [182] and reducing the concentration of subhalos [183]. These are two areas in
 502 which there are marked disagreements between the predictions of collisionless cold dark matter simulations
 503 and observations of galaxies, and the effect of self-interaction is to bring the two into closer agreement.

504 Recent work on the cross section required to achieve agreement has pointed to a low-velocity cross section
 505 in the range of $\sigma/m_{\text{DM}} \sim 0.1 - 1$ cm²/g [184]. In dark-photon scenarios where the potential due to self-
 506 interaction can be approximated as a Yukawa potential, the maximum transfer cross section is given by
 507 $\sigma_T \approx 22.7/m_{A'}^2$ (e.g. [183]). Setting this value, divided by m_{DM} , to 1 cm²/g, we find the required mass scale
 508 to be $m_{A'} \approx 70$ MeV $\times \sqrt{\text{GeV}/m_{\text{DM}}}$, in agreement with similar estimates in [170]. It is remarkable that this
 509 entirely independent line of enquiry suggests a mass scale in the range accessible by dark photon searches.

510 **1.3.2.2 Hints for Ultra-light Dark Photons**

511 The photon $\leftrightarrow A'$ oscillation mechanism can generate the required A' energy density for them to account
 512 for all the dark matter for $m_{A'} \sim 100$ keV and $\epsilon \sim 10^{-12}$ [185]. This hypothesis can be tested in direct

513 dark matter detection experiments or indirectly through the A' decay into three photons, which could be
 514 observed above the astrophysical diffuse X-ray backgrounds [186].

515 1.3.3 Status and Plans for Terrestrial experiments

516 Our discussion here focuses on the case where the dark photon can only decay into Standard Model matter,
 517 with ϵ -suppressed decay width. Another possibility is that the dark photon has ϵ -unsuppressed couplings
 518 to some new species “ χ ” of fermions or bosons (dark-sector matter), which are neutral under the Standard
 519 Model gauge group, and in particular are electrically neutral. The latter will be discussed in detail in §1.4.

520 1.3.3.1 Electron Beam Dump Experiments

521 In electron beam dump experiments, a high-intensity electron beam dumped onto a fixed target provides
 522 the large luminosities needed to probe the weak couplings of dark photons. When the electrons from the
 523 beam scatter in the target, the dark photons can be emitted in a process similar to ordinary bremsstrahlung
 524 because of the kinetic mixing. The dark photons are highly boosted carrying most of the initial beam
 525 energy and get emitted at small angles in the forward direction. The detector is placed behind a sufficiently
 526 long shielding in order to suppress the Standard Model (SM) background. Dark photons can traverse this
 527 shielding due to their weak interactions with the SM and can then be detected through their decay into
 528 leptons (mostly e^+e^- for the mass range of interest). Therefore, a decay length of $\mathcal{O}(\text{cm} - \text{m})$ is needed in
 529 order for the dark photons to be observable by decaying behind the shield and before the detector. This is
 530 possible for dark photons with masses larger than $2m_e$ up to $\mathcal{O}(100)$ MeV and small values of the kinetic
 531 mixing ϵ (roughly $10^{-7} \lesssim \epsilon \lesssim 10^{-3}$). Electron beam dump experiments are thus well suited to probe this
 532 region of the parameter space.

533 Depending on the specific experimental set-up with respect to the decay length of the dark photon, the
 534 possible reach of an experiment is determined not only by the collected luminosity but also by the choice of
 535 the beam energy, the length of the shield and the distance to the detector. Large values of the kinetic mixing
 536 parameter ϵ for which the lifetime is very short are not accessible since the dark photon decays within the
 537 shield. At very small values of ϵ the sensitivity of these experiments is limited by statistics as there are too
 538 few dark photons which are produced and decay before the detector. The total number of expected events
 539 in an experiment from decays of dark photons has been determined in [105, 187].

540 Several electron beam dump experiments were operated in the last decades to search for light metastable pseu-
 541 doscalar or scalar particles (e.g. axion-like particles or Higgs-like particles). Examples are the experiments
 542 E141 [103] and E137 [102] at SLAC, the E774 [104] experiment at Fermilab, an experiment at KEK [188]
 543 and an experiment in Orsay [189]. The measurements performed by the experiments at SLAC and Fermilab
 544 have been reanalysed in [105] to derive constraints on the dark photon mass and coupling. Updated limits
 545 for all experiments were presented in [187], where the acceptances obtained with Monte Carlo simulations
 546 for each experimental set-up have been included. These limits are shown in Fig. 1-6 together with all current
 547 constraints. Electron beam dump experiments cover the lower left corner of the parameter space in which
 548 the lifetime of the dark photon is sufficiently large to be observed behind the shield. In order to extend
 549 these limits with future experiments to smaller values of ϵ large luminosities and/or a long distance to the
 550 detector are needed since the lower limit of an experiment’s reach scales only with the fourth root of those
 551 two parameters.

1.3.3.2 Fixed-Target Experiments

Fixed-target experiments using high-current electron beams are an excellent place to search for A' 's with masses $2m_e < m_{A'} < \text{GeV}$ and couplings down to $\epsilon^2 \equiv \alpha'/\alpha > 10^{-10}$. In these experiments, the A' is radiated off electrons that scatter on target nuclei. Radiative and Bethe-Heitler trident production give rise to large backgrounds. Generally speaking, three experimental approaches have been proposed: dual-arm spectrometers, forward vertexing spectrometers, and full final-state reconstruction. In most cases, the detectors are optimized to detect the e^+e^- daughters of the A' . The complementary approaches map out different regions in the mass-coupling parameter space. General strategies for A' searches with electron fixed-target experiments were laid out in [105]. The reach for recently proposed dark photon searches is shown in Fig. 1-6.

Existing dual-arm spectrometers at Hall A at Jefferson Lab (JLab) and MAMI at Mainz have been used to search for dark photons. These experiments use high-current beams ($\sim 100 \mu\text{A}$) on relatively thick targets (radiation length $X_0 \sim 1\text{-}10\%$) to overcome the low geometric acceptance of the detectors ($\sim 10^{-3}$). Beam energy and spectrometer angles are varied to cover overlapping regions of invariant mass. Searches for A' involve looking for a bump in the e^+e^- invariant mass distribution over the large trident background, which requires an excellent mass resolution.

Two groups, APEX at JLab and the A1 collaboration at Mainz, have performed short test runs (few days of data taking) and published search results with sensitivity down to $\alpha'/\alpha > 10^{-6}$ over narrow mass ranges [109, 108]. These results clearly demonstrate the high sensitivity which can be reached in fixed-target experiments. In the meantime the A1 collaboration has carried out two more data taking runs of approximately two weeks each. The analysis of data is ongoing. Preliminary results indicate that the A' mass range from 120 MeV down to 50 MeV could be covered with a sensitivity in α'/α similar to the test run published in 2011. Furthermore, A1 is developing a new experiment to search for dark photon decay vertices displaced from the target by approximately 10 millimeters. They hope to cover the A' mass range $40 < m_{A'} < 130 \text{ MeV}$ with a sensitivity in α'/α from 10^{-9} down to 10^{-11} .

The APEX test run in 2010 achieved sensitivity to $\alpha'/\alpha > 10^{-6}$ in a narrow mass range [108]. Using high-current beams ($\sim 100 \mu\text{A}$) at four different beam energies on relatively thick targets (1-10% of a radiation length), the proposed full APEX experiment will probe A' masses from 65 to 550 MeV for couplings $\alpha'/\alpha > 10^{-7}$ [113]. A full APEX run has been approved by the JLab PAC pending a radiation review by JLab management. They are tentatively scheduled for 2016.

The HPS collaboration [114] has proposed an experiment to take place in Hall B at JLAB using a Si-strip based vertex tracker inside a magnet to measure the invariant mass and decay point of e^+e^- pairs and a PbWO_4 crystal calorimeter to trigger. HPS uses lower beam currents and thinner targets than the dual arm spectrometers, but compensates with large forward acceptance. HPS has high rate data acquisition and triggering to handle significant beam backgrounds. Because it can discriminate A' decays displaced more than a few millimeters from the large, prompt, trident background, HPS has enhanced sensitivity to small couplings, roughly $10^{-7} > \alpha'/\alpha > 10^{-10}$ for masses $30 < m_{A'} < 500 \text{ MeV}$. Without requiring a displaced vertex, HPS will also explore couplings $\alpha'/\alpha > 10^{-7}$ over the same mass range. HPS has conducted a successful test run at JLab during the spring of 2012, which demonstrated technical feasibility and confirmed simulations of the background rates. The proposal for "full" HPS was reviewed by DOE in July, 2013. The Collaboration hopes for rapid approval and funding, and plans to build HPS during 2013-2014, install it at JLab in September, 2014, and commission and run it in late 2014 and 2015 at the upgraded CEBAF accelerator.

The DarkLight detector is a compact, magnetic spectrometer designed to search for decays to lepton pairs of a dark photon A' in the mass range $10 \text{ MeV} < m_{A'} < 90 \text{ MeV}$ at coupling strengths of $10^{-9} < \alpha' < 10^{-6}$.

597 The experiment will use the 100 MeV beam of the JLAB FEL incident on a hydrogen gas target at the
 598 center of a solenoidal detector, comprising silicon detectors (for proton recoil), a low mass tracker (for the
 599 leptons), and shower counters (for photon detection). By measuring all the final state particles, Darklight
 600 can provide full kinematic reconstruction. The available information also permits searching for invisible A'
 601 decays via a missing mass measurement. A series of beam tests in summer 2012 verified that sustained,
 602 high-power transmission of the FEL beam through millimeter-size apertures is feasible [193]. JLAB has
 603 approved Darklight. A full technical design is underway and funding is being sought. The goal is to begin
 604 data-taking in 2016.

605 The MESA accelerator [194], which recently has been approved for funding within the PRISMA cluster of
 606 excellence at the University of Mainz, hopes to cover a mass range comparable to that covered by Darklight.
 607 The MESA accelerator (155 MeV beam energy) will be operated in the energy recovering linac mode with one
 608 recirculating arc as well as a windowless gas jet target. The Mainz group is considering to use two compact
 609 high-resolution spectrometers rather than a high-acceptance tracking detector. The project is several years
 610 off.

611 1.3.3.3 Proton Beam Dump Experiments

612 Proton beam dump experiments can also probe dark photons decaying to visible channels. Several reinterpretations of past experimental analyses from LSND [135],[136],[195], ν -Cal I [196],[197],[198], NOMAD [199],[200], PS191 [199],[201], and CHARM [202],[203] have resulted in limits on dark photons that are complementary to those coming from electron beam dumps, precision QED, and B-factories. One can take advantage of the large sample of pseudoscalar mesons (*e.g.*, π^0 , η) produced in the proton-target collisions, which will decay to $\gamma A'$ with a branching ratio proportional to ϵ^2 if kinematically allowed [135]. These experiments probe of a similar region in A' mass and coupling parameter space as past electron beam dumps discussed in Section 1.3.3.1, but do have unique sensitivity in certain cases. It remains to be investigated whether future proton beam dump experiments can cover new regions of A' parameter space.

621 Proton beam dump experiments also have significant sensitivity to invisible decays of A' , particularly when the decay products are stable and can re-scatter in the detector, (*e.g.*, as in the case of A' decaying to dark matter), and looking forward there is a proposal to do a dedicated beam dump mode run at MiniBooNE to search for light dark matter [190]. This subject is discussed in more detail in Section 1.4.

625 1.3.3.4 Electron-positron Colliders

626 During the past fifteen years, high luminosity e^+e^- flavor factories have been producing an enormous amount of data at different center-of-mass energies. In Frascati (Italy), the KLOE experiment running at the DAΦNE collider, has acquired about 2.5 fb^{-1} of data at the $\phi(1020)$ peak. B-factories at PEP-II (USA) and KEK-B (Japan) have delivered an integrated luminosity of 0.5-1 ab^{-1} to BABAR and Belle, respectively. In China, the Beijing BEPC collider is currently running at various energies near the charm threshold and has already delivered several inverse femtobarns of data to the BESIII experiment.

632 These large datasets have been exploited to search for dark photon production in the following processes:

- 633 • The radiative production of a dark photon (A') followed by its decay into a charged lepton or photon pair, $e^+e^- \rightarrow \gamma A'$, $A' \rightarrow l^+l^-$, $\gamma\gamma$ ($l = e, \mu$) [127].
- 635 • The pair production of a dark photon with a new light scalar particle, generally dubbed as h' . The existence of the latter is postulated in models where the hidden symmetry is broken by some Higgs

mechanism [140]. Similarly to the SM Higgs, the mass of the h' is not predictable by first principles and could be at the GeV scale as well. The phenomenology is driven by the mass hierarchy. While scalar bosons heavier than two dark photons decay promptly, giving rise to events of the type $e^+e^- \rightarrow A'h' \rightarrow 3A', A' \rightarrow l^+l^-, \pi^+\pi^-$, their lifetime becomes large enough to escape undetected for $m_{h'} < m_{A'}$, resulting in $e^+e^- \rightarrow A'h' \rightarrow l^+l^- + \text{missing energy}$ events.

- Radiative meson decays, which could also produce a dark photon with a branching ratio suppressed by a factor ϵ^2 [110].

The search for a light CP-odd Higgs (A^0) in $\Upsilon(2S, 3S) \rightarrow \gamma A^0, A^0 \rightarrow \mu^+\mu^-$ conducted by *BABAR* [111] has been reinterpreted as constraints on dark photon production, as its signature is identical to that of $e^+e^- \rightarrow \gamma A', A' \rightarrow \mu^+\mu^-$. Limits on the coupling ϵ^2 at the level of 10^{-5} have been set. Future analyses based on the full *BABAR* and Belle datasets are expected to increase the sensitivity by an order of magnitude.

A search for dark photon and associated scalar boson has been performed at *BABAR* in the range $0.8 < m_{h'} < 10.0$ GeV and $0.25 < m_{A'} < 3.0$ GeV, with the constraint $m_{h'} > 2m_{A'}$ [144]. The signal is either fully reconstructed into three lepton or pion pairs, or partially reconstructed as two dileptonic resonances, assigning the remaining dark photon to the recoiling system. No significant signal is observed, and upper limits on the product $\alpha_D \epsilon^2$ are set at the level $10^{-10} - 10^{-8}$. These bounds are translated into constraints on the mixing strength in the range $10^{-4} - 10^{-3}$, assuming $\alpha_D = \alpha \simeq 1/137$. A similar search currently performed by Belle should improve these limits by a factor of two.

KLOE has searched for $\phi(1020) \rightarrow \eta A', A' \rightarrow e^+e^-$ decays, in which the η was tagged with either the $3\pi^0$ or the $\pi^+\pi^-\pi^0$ final states [204, 205]. The $A' \rightarrow \mu^+\mu^-, \pi^+\pi^-$ channels were not included due to a higher background level. After subtraction of the ϕ Dalitz decay background, no evident peak is observed, and the following limits are set at 90% CL: $\epsilon^2 < 1.5 \times 10^{-5}$ for $30 < m_{A'} < 420$ MeV, $\epsilon^2 < 5 \times 10^{-6}$ for $60 < m_{A'} < 190$ MeV.

The BESIII Collaboration has published a search for invisible decays of the η and η' mesons, motivated by the possible existence of light neutral dark matter particles [206]. Events are selected from $J/\psi \rightarrow \phi\eta(\eta')$ decays, where the ϕ is tagged by its charged kaon decay mode. No significant signal is observed, and 90% CL limits on the branching ratio $BR(\eta \rightarrow \text{invisible}) < 1.0 \times 10^{-4}$ and $BR(\eta' \rightarrow \text{invisible}) < 5.3 \times 10^{-4}$ are set. These bounds constrain the invisible dark photon decay through $\eta(\eta') \rightarrow A'A', A' \rightarrow \text{invisible}$.

Future perspectives

Further exploitation of the currently available datasets as well as the acquisition of larger samples at planned super-flavor factories should improve the aforementioned limits. The searches should proceed along two main directions: searches using current datasets and searches at future facilities.

Searches using current datasets

Current datasets have not been fully exploited to search for signatures of a dark sector. Current studies of the $e^+e^- \rightarrow \gamma A', A' \rightarrow l^+l^-, \pi^+\pi^-$ based on the full *BABAR* and Belle datasets are expected to probe values of the coupling ϵ^2 down to $\sim 10^{-6}$, and extend the coverage down to ~ 20 MeV, covering the full region favored by the $g-2$ discrepancy. KLOE is expected to probe values of ϵ^2 between $\sim 10^{-5}$ and $\sim 7 \times 10^{-7}$ in the range $500 < m_{A'} < 1000$ MeV using the $e^+e^- \rightarrow \mu^+\mu^-\gamma$ sample selected for the study of the hadronic contribution to the muon magnetic anomaly. Similarly, invisible dark photon decays could be studied in the $e^+e^- \rightarrow \gamma + \text{invisible}$ final state, using data collected at *BABAR* with a specific single-photon trigger. This search could probe dark photon masses $0 < m_{A'} < 5$ GeV, significantly extending the parameter space covered by proposed searches in neutrino experiments [190]. The calorimeter hercicity and energy resolution

679 plays a crucial role for this study, as well as the amount of accidental background produced by the machine.
680 Similar considerations apply to searches for purely neutral dark photon decays.

681 A search for a light h' , pair produced with a dark photon is being performed at KLOE using $e^+e^- \rightarrow A'h' \rightarrow$
682 $l^+l^- + \text{missing energy}$ events. This search fully complements the analysis performed by *BABAR* covering
683 a totally different parameter space. Extensions to non-Abelian model could easily be probed using current
684 datasets. The simplest scenario include four gauge bosons, one dark photon and three additional dark bosons,
685 generically denoted W' . A Search for di-boson production has been performed at *BABAR* in the four lepton
686 final state, $e^+e^- \rightarrow W'W', W' \rightarrow l^+l^-$ ($l = e, \mu$), assuming both bosons have similar masses [207]. More
687 generic setups could easily be investigated.

688 The existence of a dark scalar or pseudo-scalar particle can also be investigated in $B \rightarrow K^{(*)}l^+l^-$ decays.
689 The sensitivity of *BABAR* and Belle searches to the SM Higgs - dark scalar mixing angle and pseudo-scalar
690 couplings constants are projected to be at the level of $10^{-4} - 10^{-3}$ and 10^3 TeV, respectively [208].

691 1.3.3.5 Proton Colliders

692 Proton colliders have the ability to reach high center-of-mass energy, making it possible to produce Z bosons,
693 Higgs bosons, and perhaps other new, heavy particles (such as supersymmetric particles, W'/Z' states, or
694 hidden-sector particles) directly. As pointed out in many theoretical studies [129, 145, 209, 210], if new
695 states are produced, they could decay to A' bosons and other hidden-sector states with very large branching
696 ratios. For GeV-scale A' masses, the A' would be highly boosted when produced in such decays and its
697 decay products would form collimated jets, mostly composed of leptons (“lepton-jets” [129]).

698 The general-purpose proton collider experiments at the Tevatron and LHC have all presented first searches
699 for lepton-jets in heavy-particle decays [142, 143, 211, 212, 213]. The searches usually employ a specialized
700 lepton-jet identification algorithm to distinguish them from the large multi-jet background. Events with
701 additional large missing transverse energy (from other escaping hidden-sector particles) or a particular di-
702 lepton mass (corresponding to the A' mass) have also been searched for [214]. Results have often been
703 interpreted in supersymmetric scenarios; the updated ATLAS analysis using 7 TeV pp data from 2011
704 excludes di-squark production with a squark mass up to about 1000 GeV or a weakly-produced state with
705 mass up to about 400 GeV, decaying through cascades to two lepton-jets [215]. Current searches have mostly
706 focused on A' bosons heavy enough to decay to muon pairs, since this offers a cleaner signal than electron
707 pairs, but good sensitivity has also been seen down to ~ 50 MeV (limited by photon conversions to e^+e^-
708 pairs).

709 ATLAS has recently searched for decays of the Higgs boson to electron lepton-jets, excluding a branching
710 ratio of about 50% [216]. Searches have mostly focused so far on prompt decays of dark photons, but
711 ATLAS has now searched for decays of the Higgs boson to long-lived A' bosons decaying to muons in the
712 muon chambers, constraining the branching ratio to be less than 10% for a proper lifetime between 10 and
713 100 mm [217].

714 Large datasets expected at the LHC in the future (300 fb^{-1} at 14 TeV) will contain billions of Z and millions
715 of Higgs bosons, allowing branching ratios to lepton-jets as low as 10^{-7} (or $\epsilon \simeq 10^{-3}$) to be probed for Z
716 decays and 10^{-3} for Higgs decays. Electroweak (strongly-produced) SUSY particles with masses up to 1
717 (2.5) TeV could be discovered through cascade decays to lepton-jets.

1.3.3.6 Laser Experiments (ultra-light dark photons)

Light dark photons (\sim meV) may also be searched for through laser, cavity, and helioscope type experiments in much the same way as done for axions and ALPs. As those approaches have been described elsewhere, it is just mentioned that ordinary photons might be able to kinetically mix into the dark photon. Much of the parameter space for light shining through walls experiments has now been excluded although each configuration of a proposed experiment may still cover unexplored parameter space.

1.3.4 Opportunities for Future Experiments: New Ideas, Technologies, & Accelerators

The physics motivations for dark photons, as outlined in 1.3.1 above, easily motivate extending searches far beyond the present generation of experiments. Large parts of the mass-coupling parameter space, shown in Fig. ?, will remain uncovered after the experiments at JLAB and Mainz have run, and after data from the B and Phi factories will have been fully analyzed. If something is found in the present generation of experiments, it will of course have profound impact on high energy physics. In that fortuitous case, it will be incumbent on future experiments to confirm the findings, explore the detailed properties of the new particle, and to seek its cousins. That exercise will demand experiments with improved performance and reach. If nothing is found in the present searches, there remains a vast and viable region of parameter space to explore. Specific models for dark photons have been advanced which populate the virgin territory, and general considerations from theory and phenomenology do as well. So in this case too, extending searches for dark photons through the whole of the parameter space is a high priority.

Can new experiments be devised to explore the new territory? Of course! Future fixed target electron production experiments, new searches at future e+e- colliding beam facilities, and new searches at the LHC will all contribute to the hunt.

At fixed target machines, several generic improvements look possible which can expand the reach significantly. First, in HPS-like experiments, it should be possible to boost the integrated luminosity by one or more orders of magnitude. Accommodating 10 or more times the current will require tracking detectors that avoid the highest occupancy/radiation damage environments yet preserve most of the acceptance, or new pixellated and rad hard detectors that can tolerate the higher rates. Second, studies have shown that catching the recoil electron, in addition to the A decay products, will boost the mass resolution by a factor of two, and can reduce a primary physics background due to the Bethe Heitler process by as much as a factor 4. Both will greatly improve the significance, signal/sqrt(background), and extend the reach accordingly. Third, Triggering on pions and muons will boost the sensitivity for As for masses beyond the dimuon mass by large factors below 1 GeV, where the rho dominates the A decays, and help significantly at higher masses too. Fourth, using low Z nuclear targets and maximal beam energies improves the reach in this 300-1000MeV range too, since the radiative A cross section increases with higher beam energies, and since form factor effects will be mitigated by going to smaller, lower Z nuclei. CEBAF12 at JLAB will provide 12 GeV beams. Even higher energies will improve future experiments if further upgrades at JLAB are realized. Fifth, note that the sensitivity of the searches depend inversely with the square root of the invariant mass resolution, and directly with the square root of the acceptance; vertex searches of course depend critically on the vertex resolution. All these quantities can be improved rather directly with more ambitious experiments. It is not unreasonable to assume a factors of 2 improvement in the acceptance and 2-4 in the mass resolution. The vertex resolution can be improved in three direct ways: 1) thinner targets (with compensating higher currents); 2) shorter extrapolation distances from the first detector layer to the target; 3) thinner detectors, with correspondingly lower multiple coulomb scattering, and consequently better impact parameter resolution. Taken together,

761 future experiments may be able to discriminate A decays just a few mm from the target (vs 15 mm in the
 762 current version of HPS). The list goes on. Finally, optimized analysis procedures and multivariate analyses
 763 may buy factors of two improvement in sensitivity. An estimate of the reach of a future experiment which
 764 exploits these various factors is given in Fig. XX. Note that this exercise exploits just one of the current
 765 approaches for fixed target electroproduction; other existing approaches may offer other gains. Brand new
 766 approaches may be even more powerful. While detailed performance estimates for new experimental layouts
 767 are not yet available, several new ideas are being discussed which may further improve experimental reach.

768 1.3.4.1 Searches at future facilities

769 e^+e^- colliding beam machines have conducted sensitive searches for dark photons over a wide range of masses.
 770 These searches, using existing data sets, are continuing. Since future facilities are already approved, it is
 771 comparatively straight-forward to extrapolate their performance for future searches. The coupling accessible
 772 by current datasets from e^+e^- colliders are at the level $\epsilon^2 \sim 10^{-6} - 10^{-5}$ for dark photon masses below a few
 773 hundred MeV. This limitation comes essentially by the available statistics, i.e. the luminosity that can be
 774 delivered by the accelerators. The luminosity typically scales quadratically with their center of mass energy,
 775 basically compensating the inverse scaling of the relevant production cross-sections.

776 Current factories reach instantaneous luminosities of a few times 10^{32} (10^{34}) $\text{cm}^{-2}\text{s}^{-1}$ at 1 (10) GeV. Several
 777 next generation flavor factories have been proposed or are currently under construction. The upgraded KEK
 778 B-factory, SuperKEKB, is expected to start taking data in 2016 and should collect 50 ab^{-1} by 2022, about
 779 two orders of magnitude larger than the dataset collected by Belle. Several tau-charm factories operating
 780 between 2 – 5 GeV with instantaneous luminosities at the level of $10^{35} - 10^{36} \text{ cm}^{-2}\text{s}^{-1}$ have been proposed,
 781 but remain to be funded at the time of this writing. Their expected sensitivity would roughly be at the
 782 level SuperKEKB should reach. At Frascati, KLOE-2 will install a new inner tracker, a cylindrical GEM
 783 detector, to improve the momentum resolution of charged particles while keeping the amount of material
 784 at a minimum. This approach will hopefully reduce the background from photon conversions produced in
 785 $e^+e^- \rightarrow \gamma\gamma, \gamma \rightarrow e^+e^-$ events, allowing KLOE-2 to explore the very low mass region.

786 An alternative approach has been proposed by the authors of [117], colliding a *single* intense positron beam
 787 on an internal target. Specifically, the VEPP-3 collaboration has proposed to use a 500 MeV positron beam
 788 of VEPP-3 on a gas hydrogen internal target. The search method is based on the study of the missing mass
 789 spectrum in the reaction $e^+e^- \rightarrow A'\gamma$, which allows the observation of a dark photon independently of its
 790 decay modes and lifetime in the range $m_{A'} = 5 - 20 \text{ MeV}$.

791 In summary, next generation flavor factories could probe values of the coupling ϵ^2 down to a level comparable
 792 to fixed target experiments for prompt decays, while significantly extending their mass coverage. Should
 793 a signal be observed, e^+e^- colliders will be ideally suited to investigate in detail the structure of a hidden
 794 sector, complementing dedicated experiments.

795 1.4 Light Dark-Sector States (including Sub-GeV Dark Matter)

796 1.4.1 Theory & Theory Motivation

797 Dark matter and neutrino mass provide strong empirical evidence for physics beyond the Standard Model
 798 (SM). Arguably, rather than suggesting any specific mass scale for new physics, they point to a hidden (or
 799 dark) sector, weakly-coupled to the SM. Dark sectors containing light stable degrees of freedom, with mass

800 in the MeV-GeV range, are of particular interest as dark matter candidates as this regime is poorly explored
 801 in comparison to the weak scale. Experiments at the intensity frontier are ideally suited to explore this light
 802 dark-sector landscape, as discussed in this section.

803 Before going into details, it is useful to recall a general parametrization of the interactions between the SM
 804 and a dark sector. A natural assumption is that any light dark sector states are SM gauge singlets. This
 805 automatically ensures weak coupling to the visible (SM) sector, while the impact of heavier charged states is
 806 incorporated in an effective field theory expansion at or below the weak scale, $\mathcal{L} \sim \sum_n \frac{c_n}{\Lambda^n} \mathcal{O}_{\text{SM}}^{(k)} \mathcal{O}_{\text{hidden}}^{(l)}$, where
 807 k and l denote operator dimensions and $n = k + l - 4$. The generic production cross section for hidden sector
 808 particles then scales as $\sigma \sim E^{2n-2}/\Lambda^{2n}$. Thus lower dimension interactions, unsuppressed by the heavy scale
 809 Λ , are preferentially probed at lower energy. Such interactions are natural targets for the intensity frontier
 810 more generally. The set of lowest-dimension interactions, or *portals*, which generalizes the right-handed
 811 neutrino coupling, is quite compact. Up to dimension five ($n \leq 1$), assuming SM electroweak symmetry
 812 breaking, the list of portals includes: $-\frac{\kappa}{2} B_{\mu\nu} V^{\mu\nu}$ (dark photons kinetically mixed with hypercharge), $(AS +$
 813 $\lambda S^2) H^\dagger H$ (dark scalars coupled to the Higgs), $y_N LHN$ (sterile neutrinos coupled the lepton portal), and
 814 $\frac{\partial_\mu a}{f_a} \bar{\psi} \gamma^\mu \gamma^5 \psi$ (axion-like pseudoscalars coupled to an axial current). On general grounds, the couplings of
 815 these lowest dimension operators are minimally suppressed by any heavy scale, and new weakly-coupled
 816 physics would naturally manifest itself first via these portals in any generic top-down model. Thus portals
 817 play a primary role in mediating interactions of light dark sector states with the SM.

818 1.4.1.1 Light Dark Matter

819 Dark matter provides one of the strongest empirical motivations for new particle physics, with evidence
 820 coming from various disparate sources in astrophysics and cosmology. While most activity has focused on
 821 the possibility of weakly-interacting massive particles (WIMPs) with a weak-scale mass, this is certainly not
 822 the only possibility. The lack of evidence for non-SM physics at the weak scale from the LHC motivates a
 823 broader perspective on the physics of DM, and new experimental strategies to detect its non-gravitational
 824 interactions are called for. A wider theoretical view has also been motivated in recent years by anomalies
 825 in direct and indirect detection [151, 218, 219], possible inconsistencies of the Λ CDM picture of structure
 826 formation on galactic scales [220], and the advent of precision CMB tests of light degrees of freedom during
 827 recombination.

828 The mass range from the electron threshold ~ 0.5 MeV up to multi-TeV characterizes the favored range
 829 for dark matter candidates with non-negligible SM couplings (on the scale of terrestrial particle physics
 830 experiments). The simple thermal relic framework, with abundance fixed by freeze-out in the early universe,
 831 allows dark matter in the MeV-GeV mass range if there are light (dark force) mediators which control
 832 the annihilation rate [221]. Related scenarios, such as asymmetric dark matter, also require significant
 833 annihilation rates in the early universe, and thus light mediators are a rather robust prediction of models
 834 of MeV-GeV scale dark matter which achieve thermal equilibrium. Current direct detection experiments
 835 searching for nuclear recoils lose sensitivity rapidly once the mass drops below a few GeV, and experiments
 836 at the intensity frontier provide a natural alternative route to explore this light MeV-GeV scale dark matter
 837 regime. Crucially, the light mediators required for DM annihilation to the SM provide, by inversion, an
 838 accessible production channel for light dark matter that can be exploited in high luminosity experiments.

839 Models of sub-GeV dark matter are subject to a number of terrestrial and cosmological constraints, as
 840 discussed below. However, simple models interacting through one or more of the portal couplings are viable
 841 over a large parameter range; e.g. an MeV-GeV mass complex scalar charged under a massive dark photon
 842 can be thermal relic DM, with SM interactions mediated by the kinetic mixing portal.

843 1.4.1.2 Light Dark-Sector States

844 There is no compelling argument, beyond simplicity, for cold dark matter to be composed of a single species,
 845 or even a small number. Light stable thermal relics require the presence of additional light mediators as
 846 discussed above, and the dark sector may be quite complex. Indeed, the annihilation channels required for
 847 (thermalized) dark matter in the early universe could occur within the dark sector itself if there are additional
 848 light states, subject to constraints from cosmology on the number of relativistic degrees of freedom. Indeed,
 849 since SM neutrinos do contribute a (highly sub-dominant) fraction of hot dark matter, we already know
 850 that in the broadest sense dark matter must be comprised of multiple components. Thus care is required to
 851 assess the experimental sensitivity according to the underlying assumptions about the stability of the dark
 852 sector state in cosmological scales, and whether or not stable dark sector states under study comprise some
 853 or all of dark matter.

854 1.4.1.3 Millicharged Particles

855 Particles with small un-quantized electric charge, often called mini- or milli-charged particles (MCPs), also
 856 arise naturally in many extensions of the Standard Model. MCPs are a natural consequence of extra $U(1)$ s
 857 and the kinetic mixing discussed in §1.3.1 for massless A' fields. In this case any matter charged (solely)
 858 under the hidden $U(1)$ obtains a small electric charge. MCPs can also arise in extra-dimensional scenarios
 859 or as hidden magnetic monopoles receiving their mass from a magnetic mixing effect [222, 223, 224]. Milli-
 860 charged fermions are particularly attractive because chiral symmetry protects their mass against quantum
 861 corrections, making it more natural to have small or even vanishing masses. MCPs have also been suggested
 862 as dark matter candidates [225, 226, 227].

863 Terrestrial experiments as well as astrophysical and cosmological observations provide interesting bounds on
 864 MCPs. These limits in addition to comments on future prospects are summarized in Sec. 1.4.2.2.

865 1.4.2 Phenomenological Motivation and Current Constraints

866 1.4.2.1 Constraints on Light Dark Matter and Dark Sectors

867 A variety of terrestrial, astrophysical and cosmological constraints exist on light dark matter and dark sector
 868 states, which we now summarize. We focus on the scenario with dark sector states χ (including dark matter)
 869 interacting with the SM through a dark photon, emphasizing the assumptions going into each limit. These
 870 limits, along with prospects for various future experiments to be discussed below, are displayed in Fig. 1-8.

871 Constraints that rely only on the presence of a kinetically mixed dark photon come from precision QED
 872 measurements [106]. Precision tests of the fine-structure constant α (including the electron anomalous
 873 magnetic moment) constrain the kinetic mixing parameter $\epsilon \lesssim 10^{-4}(10^{-2})$ for a dark photon mass $m_{A'} \sim$
 874 $1 \text{ MeV}(100 \text{ MeV})$. The muon anomalous magnetic moment provides a stronger constraint for heavier dark
 875 photons, with $\epsilon \lesssim \text{few} \times 10^{-3}(10^{-2})$ as the dark photon mass increases from $m_{A'} \sim 50 \text{ MeV}(300 \text{ MeV})$.
 876 Furthermore, model independent constraints from the measurements of the Z boson mass, precision elec-
 877 troweak observables, and e^+e^- reactions at a variety of c.o.m energies constrain $\epsilon \lesssim 3 \times 10^{-2}$ independent
 878 of $m_{A'}$ [228].

879 The next class of constraints relevant to this scenario relies on the assumption that the dark photon decays
 880 invisibly (but not necessarily to stable states e.g., dark matter). Measurements of the $K^+ \rightarrow \pi^+ \nu \bar{\nu}$ branching

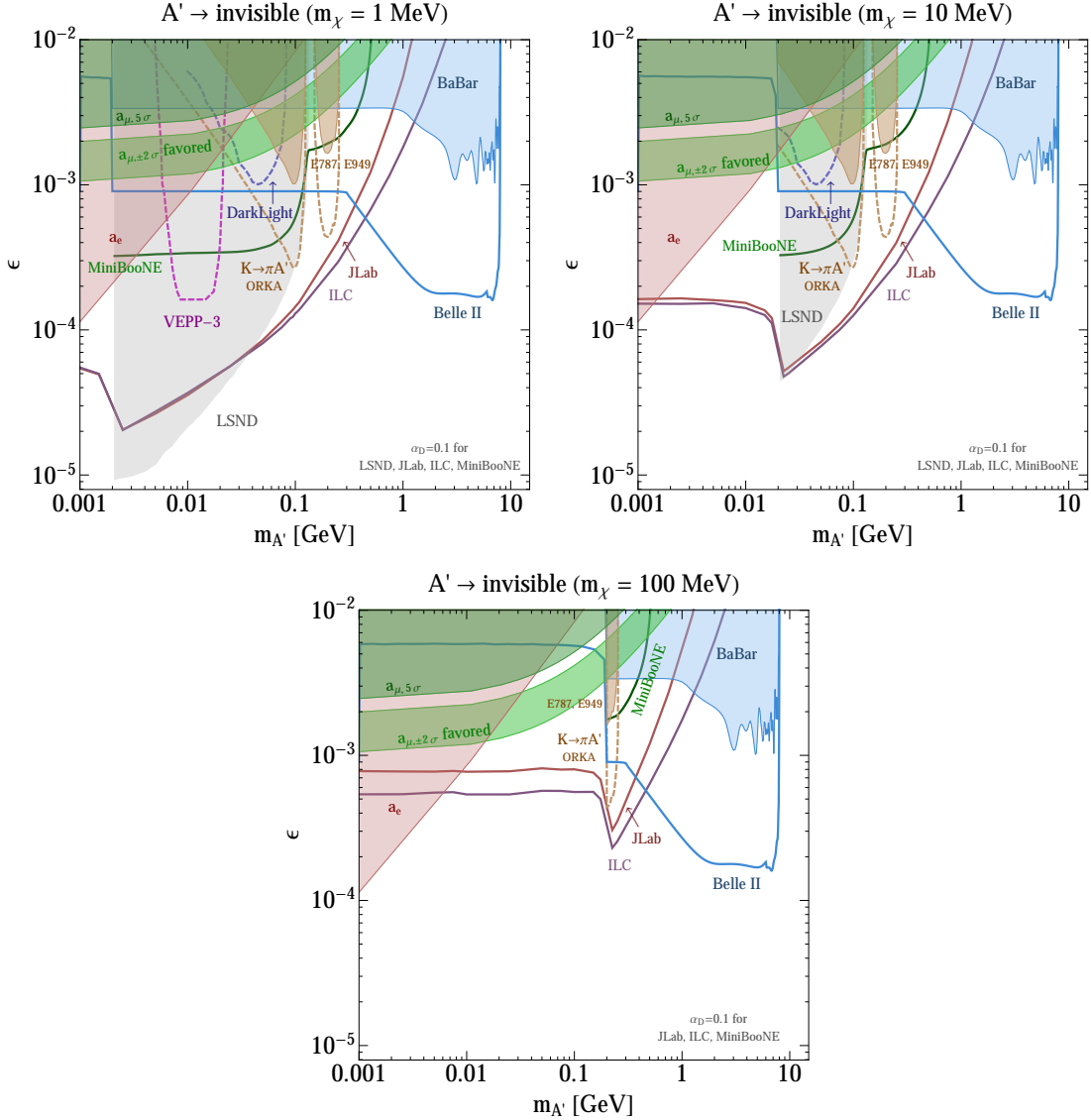


Figure 1-8. Parameter space for invisible A' 's. Precision QED tests of α (red) and the muon anomalous magnetic moment (dark green) constrain the low $m_{A'}$, large ϵ region. In the green band, the A' can explain the observed discrepancy between the calculated and measured muon anomalous magnetic moment [106]. Constraints from invisible A' decays arise from the measured $K^+ \rightarrow \pi^+ \nu \bar{\nu}$ branching ratio [230, 106, 190] (brown) from a mono-photon search at BABAR [231, 243, 192] (blue). LSND (gray) constrains A' 's decaying to dark matter for masses $m_{A'} < m_{\pi^0}$, $m_{\chi} < m_{A'}/2$ [233]. We also display projections from future searches/experiments, including the DarkLight experiment [229] (dark blue dashed), the MiniBooNE beam off target run [190], future electron beam dump experiments at JLAB (dark red) and the ILC (purple) [192], and BELLE II (blue).

ratio [230] place limits on ϵ in the range $10^{-2} - 10^{-3}$ if the decay $K^+ \rightarrow \pi^+ A'$ is kinematically allowed. Strong constraints on ϵ exist in a narrow region $m_{A'} \sim m_{J/\psi}$, in which case the the decay $J/\psi \rightarrow$ invisible is resonantly enhanced. Furthermore, a limit on the branching fraction $\Upsilon(3S) \rightarrow \gamma + A^0$, $A^0 \rightarrow$ invisible (with A^0 a scalar [231]) can be recast as a limit on the continuum process $e^+e^- \rightarrow \gamma A'$, $A' \rightarrow$ invisible, leading to $\epsilon \lesssim \text{few} \times 10^{-3}$ [192].

If the dark sector states χ are stable (e.g., if χ is the dark matter), or at least metastable with lifetimes of $O(100\text{m})$, then proton- and electron- beam fixed target experiments are sensitive to the scattering of χ with electrons or nuclei, which depend on α_D . The LSND measurement of the electron-neutrino elastic scattering cross section [232] places a limit in the range $\epsilon \lesssim 10^{-5} - 10^{-3}$ for $\alpha_D = 0.1$, $m'_A < m_{\pi^0}$, $m_\chi < m'_A/2$ [233]. Furthermore, the SLAC MQ search for milli-charged particles [234] is sensitive to A' 's heavier than π^0 , and constrains values of ϵ as low as 10^{-3} [191].

Direct detection experiments can probe light dark matter χ in the halo through its scattering with electrons [235]. An analysis of the XENON10 dataset has placed limits on the χ -electron scattering cross section $\sigma_e < 10^{-37} \text{cm}^2$ for χ masses in the range 20 MeV - 1 GeV.

Late time dark matter annihilation to electromagnetic particles can distort the CMB. Assuming χ saturates the observed relic density and annihilates to charged particles through an s -wave reaction, then the CMB essentially rules out this scenario [167, 168, 169]. These bounds are, however, model dependent and may be avoided in several ways: 1) χ may annihilate through a p -wave process, e.g. scalar DM annihilating through an s -channel dark photon to SM fermion pairs [233], 2) the dark sector may contain new light states, opening up new annihilation modes for χ which do not end with electromagnetic final states, 3) the dark matter may be matter-asymmetric [236], and 4) χ may comprise a sub-dominant component of the DM.

1.4.2.2 Additional constraints on Millicharged Particles

Several portions of the charge-mass parameter space for MCPs can be excluded based upon available experimental results. Some of these bounds, *e.g.* direct measurements, rely on relatively few assumptions, while others are dependent on the accuracy of astrophysical and cosmological models. Fig. 1-9 illustrates the parameter space for MCPs and a brief summary of the most stringent bounds follows.

Direct measurements cover a large portion of the parameter space of MCPs for $Q \sim e$. The ASP (Anomalous Single Photon) search at SLAC looked for $e^+e^- \rightarrow \gamma X$ final states, where X is any weakly interacting particle. It set a bound of $Q > 0.08e$ for $M_{\text{MCP}} \lesssim 10 \text{ GeV}$ [237, 238]. Data from a proton beam dump experiment, E613, at Fermilab excludes charges between $10^{-1}e$ and $10^{-2}e$ for $M_{\text{MCP}} < 200 \text{ MeV}$ [239]. The results of an electron beam dump experiment at SLAC that looked for trident production $e^- N \rightarrow e^- N Q^+ Q^-$ were reanalyzed and set a bound of $Q > 0.03e$ for $M_{\text{MCP}} < 1 \text{ GeV}$ [237]. Moreover, the SLAC MilliQ experiment set a bound of $5.8 \times 10^{-4}e$ for $M_{\text{MCP}} < 100 \text{ MeV}$ [234]. In addition to these accelerator-based experiments, the results of a search for orthopositronium decays into invisible particles can be recast into bounds on MCPs. This measurement gives a bound of $Q < 8.6 \times 10^{-5}e$ for $M_{\text{MCP}} < 500 \text{ KeV}$ [240]. Finally, the precise agreement between the measured and calculated values for the Lamb shift can be used to set a bound of $Q < (1/9)M_{\text{MCP}}e$ for $M \gtrsim 3 \text{ KeV}$ [241, 237].

Additional constraints can be placed on MCPs from indirect cosmology and astrophysics results (See [237] and references therein). Photons travelling in a plasma acquire an effective mass and can decay into MCPs. Therefore MCPs produced inside stars can contribute to their cooling. White Dwarfs and Red Giants provide laboratory settings which allow to place bounds on MCPs by requiring that the rate of energy going into MCP production not exceed the rate of nuclear energy production. The limits apply for $M_{\text{MCP}} \lesssim \text{KeV}$.

923 The constraints from cosmology are discussed in what follows. BBN bounds on the effective relativistic
 924 degrees of freedom can be used to set limits on the parameter space of MCPs. WMAP data of the CMB is
 925 also an indirect test ground for new invisible states that inject charged particles into the CMB. In addition,
 926 requiring that the MCPs relic density not over-close the universe excludes $M_{\text{MCP}} \sim \text{TeV}$ for $Q \sim e$ charges.

927 New electron and proton beam dump experiments, planned or proposed to search for light DM, could
 928 also cover new parameters space of MCPs, particularly the $M_{\text{MCP}} \sim \text{GeV}$ region. The primary modes of
 929 production are $pN \rightarrow pNQ^+Q^-$ or $pp \rightarrow Q^+Q^-$ at proton beam dump experiments, and $e^-N \rightarrow e^-NQ^+Q^-$
 930 at electron beam dump experiments. MCPs produced at the beam dump would then travel and scatter
 931 elastically off of nuclei at a detector situated downstream of the target and able to look for neutral current
 932 scattering events. The detection of MCPs relies on an experiment sensitive to low momentum recoil channels,
 such as electron recoils and/or coherent nuclear scattering, see Sec. 1.4.2.1.

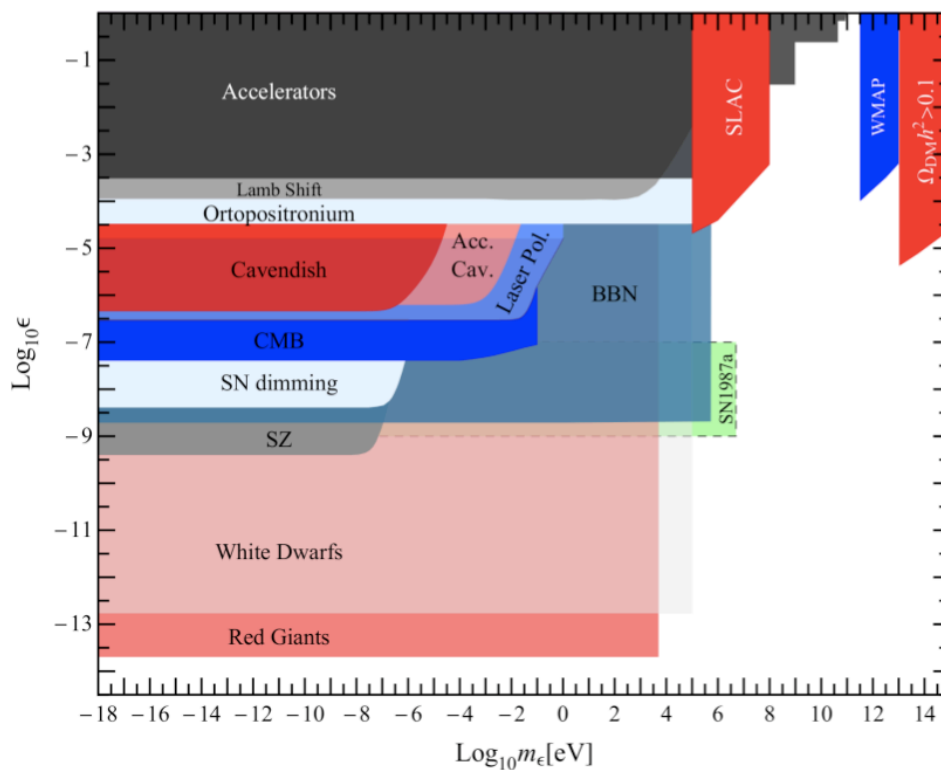


Figure 1-9. Bounds on the charge ϵ vs millicharged mass m_ϵ parameter space from various experiments.

933

934 1.4.3 Proposed and Future Searches

935 1.4.3.1 Proton-fixed Target

936 Proton beam-fixed target-detector setups have significant potential to search for light dark matter and other
 937 long-lived dark sector states. An intense source of dark sector states can be produced in the primary

938 proton-target collisions and detected through their scattering [135, 233, 242] or visible decays [135, 136]
 939 in a near detector. Of particular importance to this experimental program are the existing and future
 940 Fermilab neutrino factories such as MiniBooNE, MINOS, NO ν A, MicroBooNE, and LBNE, which have an
 941 unprecedented opportunity to search for light dark matter. The studies of Refs. [135, 233, 242] demonstrate
 942 the existence of a large dark matter signal in existing neutrino experiments for motivated regions of dark
 943 matter parameter space. However, numerous experimental challenges remain to maximize the sensitivity to
 944 the dark matter signal, foremost among them competing with the large neutrino neutral current background.

945 A proposal for a dedicated search for light dark matter at MiniBooNE is described in Ref. [190]. Dark
 946 matter particles χ , interacting with the SM through a kinetically mixed dark photon (here denoted as V ,
 947 with kinetic mixing parameter κ), can be produced through the decays of secondary pseudoscalar mesons,
 948 $\pi^0, \eta \rightarrow \gamma V$, $V \rightarrow \chi\chi^*$. Such dark matter particles can travel to the detector and scatter via V exchange,
 949 leaving the signature of a recoiling electron or nucleon. The MiniBooNE sensitivities to dark matter masses
 950 of 1, 10, 100 MeV are represented by the green contours in Figure. 1-8.

951 In order to mitigate the neutrino background Ref. [190] proposed to run in a beam-off target configuration,
 952 in which the protons are steered past the target and onto either 1) the permanent iron absorber located
 953 at the end of the 50 m decay volume, or 2) a deployed absorber positioned 25 m from the target. A one
 954 week test run in the 50 m absorber configuration measured a reduction of the neutrino flux by a factor
 955 of 42. Additional improvements in distinguishing χ signal from the neutrino background are possible by
 956 exploiting the fine ns-level timing resolution between the detector and proton spill, since heavy $O(100 \text{ MeV})$
 957 dark matter particles will scatter out of time.

958 The MiniBooNE sensitivity to light dark matter interacting via a dark photon mediator is represented in
 959 Figure. nlwcp:fig:invisible-A'. MiniBooNE can probe motivated regions of dark matter parameter space in
 960 which the relic density is saturated and the muon anomalous magnetic moment discrepancy is explained.
 961 The signal significance for several operational modes is can be found in [190].

962 The experimental approach to search for light dark matter employed by MiniBooNE is applicable to other
 963 neutrino experiments and intense proton sources, such as MINOS, NO ν A, MicroBooNE, LBNE and Project
 964 X. For instance, the MicroBooNE LAr detector can also perform a search with comparable sensitivity to
 965 that outlined for MiniBooNE with a long enough beam-off-target run. More generally, the dark matter mass
 966 range that can be covered is governed by the proton beam energy and the production mechanism, as well as
 967 the ability to overcome the neutrino neutral current background. For instance with the FNAL Booster (8.9
 968 GeV) and Main Injector (120 GeV) as well as a future Project X, the accessible DM mass range is from a
 969 few MeV up to a few GeV.

970 The search for light dark matter provides an additional physics motivation for intense proton beam facilities.
 971 Given the significant investment in existing and future infrastructure for neutrino experiments, it is critical
 972 to take advantage of the unique opportunity afforded by these experiments to probe the non-gravitational
 973 interactions of light dark matter and more generally explore the possibility of of a dark sector with new light
 974 weakly coupled states.

975 1.4.3.2 B-factories

976 B-factories like *BABAR* and *Belle* and future super-B factories like *Belle 2* are powerful probes of light dark
 977 matter with a light mediator. An existing mono-photon search by *BABAR* [231] already places important
 978 constraints on this class of models [243, 192] (see also [244, 127, 119]), and similar search at a future *B*-factory
 979 can probe significantly more parameter space [243]. Such searches are more powerful than searches at other
 980 collider or fixed-target facilities for mediator and hidden-sector particle masses between a few hundred MeV

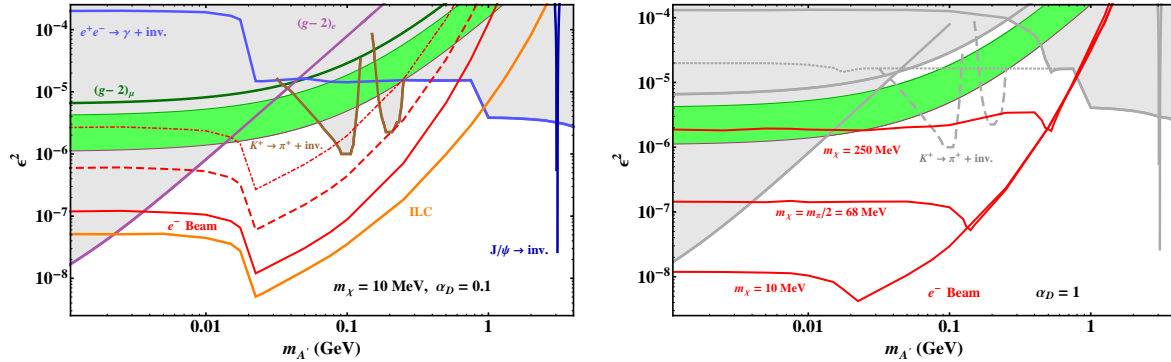


Figure 1-10. The ϵ^2 sensitivity of electron-beam fixed-target experiments for benchmark values of m_χ . Left: the solid, dashed, and dot-dashed red curves mark the parameter space for which the basic setup — a 12 GeV beam impinging on an aluminum beam dump, with a 1 m^3 mineral oil detector placed 20 m downstream of the dump — respectively yields 40, 10^3 , and $2 \cdot 10^4$ χ -nucleon quasi-elastic scattering events with $Q^2 > (140 \text{ MeV})^2$ per 10^{22} electrons on target. The orange curve shows the 10 event reach for a pulsed ILC style 125 GeV beam using the same detector. Comparable sensitivity can be achieved with much smaller fiducial volumes than we consider, especially for detectors with active muon and neutron shielding and/or veto capabilities. Right: the 40 event yield with a 12 GeV beam for different m_χ . For $2m_\chi > m_\pi$, this parameter space is inaccessible via pion decays to NLWCP at neutrino factories.

981 to 10 GeV. Mediators produced on-shell and decaying invisibly to hidden-sector particles such as dark matter
 982 can be probed particularly well. Sensitivity to light dark matter produced through an off-shell mediator is
 983 more limited, but may be improved with a better theoretical control of backgrounds, allowing background
 984 subtraction and a search for kinematic edges. The implementation of a mono-photon trigger at Belle II
 985 would be a necessary step towards providing this crucial window into such light hidden sectors.

986 1.4.3.3 Electron fixed target

987 Electron beam fixed target experiments enable powerful low-background searches for new light weakly-
 988 coupled particles and can operate parasitically at several existing facilities [192]. Electron-nucleus collisions
 989 feature a NLWCP production rate comparable to that of neutrino factories, but the production mechanism
 990 is analogous to QED bremsstrahlung. Importantly, beam related neutrino and neutron backgrounds are
 991 negligible. Electron beam production also features especially forward-peaked NLWCP kinematics, so for
 992 multi GeV beam energies, experimental baselines on a 10m scale, and meter-scale detectors, the signal
 993 acceptance is of order one for sub-GeV NLWCP masses. This approach is sensitive to any new physics that
 994 couples to leptonic currents and is limited only by cosmogenic backgrounds, which are both beatable and
 995 systematically reducible; even a test implementation with no cosmogenic neutron reduction (see Fig. 1-10
 996 red dot-dashed curve) offers sensitivity to well motivated regions of parameter space. Previous generations
 997 of electron beam experiments, such as the MilliQ experiment at SLAC have already demonstrated sensitivity
 998 to NLWCP [191].

999 The minimal setup requires on a cubic-meter fiducial volume (or smaller) detector sensitive to neutral current
 1000 scattering placed 10s of meters downstream of an existing electron beam dump. At low momentum transfers,
 1001 NLWCP scattering predominantly yields elastic electron and coherent nuclear recoils in the detector. At
 1002 higher momentum transfers, inelastic hadro-production and quasi-elastic nucleon ejection dominate the
 1003 signal yield. The approach can offer comparable sensitivity using either continuous wave (CW) or pulsed
 1004 electron beams, but CW sensitivity is limited by cosmogenic background so background reduction strategies

1005 are required to achieve optimal sensitivity; for pulsed beams timing cuts render cosmogenic backgrounds
 1006 negligible. This approach can be realized parasitically at several existing electron fixed target facilities
 1007 including SLAC, Jefferson Laboratory, and Mainz. It may also be possible to utilize pulsed beams at the
 1008 SuperKEK linac beam and (in the future) at the ILC.

1009 Fig. 1-10 (left) shows the sensitivity projections for a 1 m^3 detector placed 20 m downstream of an Aluminum
 1010 beam dump. The dot-dashed, dashed, and solid red curves show yields for $2 \cdot 10^4$, 10^3 , and 40 signal events
 1011 using a 12 GeV CW beam modeled after JLab's CEBAF-12 upgrade. These projections correspond 2σ ϵ
 1012 sensitivity assuming 0%, 95%, and 99.9% cosmogenic neutron reduction with 0%, 1% and 2.5% systematic
 1013 uncertainties respectively. The orange curve is the ϵ sensitivity for a pulsed ILC style beam operating at 125
 1014 GeV. For comparison with neutral current studies in the at neutrino factories [245], the red and orange curves
 1015 assume a mineral oil detector with sensitivity only to quasi-elastic nucleon scattering, however, a dedicated
 1016 study of various detector materials and scattering processes (e.g. electron, coherent-nuclear, and inelastic
 1017 scattering) can optimize this proof of concept to greatly enhance signal sensitivity and reduce cosmogenic
 1018 backgrounds.

1019 1.5 Chameleons

1020 1.5.1 Theory & Motivation

1021 Cosmological observations are able to pinpoint with great precision details of the universe on the largest
 1022 scales, while particle physics experiments probe the nature of matter on the very smallest scales with
 1023 equally astounding precision. However, these observations have left us with some of the greatest unsolved
 1024 problems of our time, most notably the remarkable realisation that the most dominant contribution to the
 1025 energy density of our universe is also the least well understood. Dark energy, credited with the observed
 1026 accelerated expansion of the universe, makes up around 70% of the total matter budget in the universe
 1027 however there is no single convincing explanation for this observation nor is there a clear pathway to
 1028 distinguishing between different models through cosmological observations. If this acceleration is not caused
 1029 by a cosmological constant then the most convincing explanations come in the form of scalar field models
 1030 that are phenomenological but with the hope of being effective field theories of ultra-violet physics. If a
 1031 scalar field is indeed responsible for this observed acceleration it would need to be very light $m \sim H_0$ and
 1032 evolving still today. These light fields should couple to all forms of matter with a coupling constant set by
 1033 G_N . A coupling of this kind would cause an as yet unobserved fifth force and should be observable in a
 1034 plethora of settings from the early universe through big bang nucleosynthesis, structure formation and in all
 1035 tests of gravity done today. Thus, we are left with a puzzle as to how a scalar field can both be observable
 1036 as dark energy and yet not be observed to date in all other contexts.

1037
 1038 A solution to this puzzle was presented in [246, 247, 248] with so-called chameleon fields. Chameleon fields
 1039 are a compelling dark energy candidate, as they couple to all Standard Model particles without violating any
 1040 known laws or experiments of physics. Importantly, these fields are testable in ways entirely complementary
 1041 to the standard observational cosmology techniques, and thus provide a new window into dark energy through
 1042 an array of possible laboratory and astrophysical tests and space tests of gravity. Such a coupling, if detected,
 1043 could reveal the nature of dark energy and may help lead the way to the development of a quantum theory
 1044 of gravity.

1045

A canonical scalar field is the simplest dynamical extension of the Standard Model that could explain dark energy. In the absence of a self interaction, this field’s couplings to matter — which we would expect to exist unless a forbidden by some symmetry — would lead to a new, fifth fundamental force whose effects have yet to be observed. However, scalar field dark energy models typically require a self interaction, resulting in a nonlinear equation of motion [249, 250]. Such a self interaction, in conjunction with a matter coupling, gives the scalar field a large effective mass in regions of high matter density [246, 247]. A scalar field that is massive locally mediates a short-range fifth force that is difficult to detect, earning it the name “chameleon field.” Furthermore, the massive chameleon field is sourced only by the thin shell of matter on the outer surface of a dense extended object. These nonlinear effects serve to screen fifth forces, making them more difficult to detect in certain environments.

Current best theories treat chameleon dark energy as an effective field theory [248, 251] describing new particles and forces that might be seen in upcoming experiments, and whose detection would point the way to a more fundamental theory. The ultraviolet (UV) behavior of such theories and their connection to fundamental physics are not yet understood, although progress is being made [252, 253, 254, 255].

A chameleon field couples to dark matter and all matter types, in principle with independent strengths. At the classical level, a chameleon field is not required to couple to photons, though such a coupling is not forbidden. However, when quantum corrections are included, a photon coupling about three orders of magnitude smaller than the matter coupling is typically generated [256]. The lowest order chameleon-photon interaction couples the chameleon field to the square of the photon field strength tensor, implying that in a background electromagnetic field, photons and chameleon particles can interconvert through oscillations. The mass of chameleon fields produced will depend on the environmental energy density as well as the electromagnetic field strength. This opens the vista to an array of different tests for these fields on Earth, in space, and through astrophysical observations. Several astrophysical puzzles could also be explained by chameleons, *e.g.*, [257]. Their coupling to photons, combined with their light masses in certain environments, allows chameleons to be produced with intense beams of photons, electrons, or protons and detected with sensitive equipment. This makes them, by definition, targets for the intensity frontier. In fact chameleon particles are a natural bridge between the cosmic frontier and the intensity frontier; not only do they hold the possibility of being a dark energy candidate but they are testable through astrophysical and laboratory means.

The chameleon dark energy parameter space is considerably more complicated than that of axions, but constraints can be provided under some assumptions. With the caveat that all matter couplings are the same but not equal to the photon coupling, and the assumption of a specific chameleon potential, $V(\phi) = M_\Lambda^4(1 + M_\Lambda^n/\phi^n)$ in which we set the scale $M_\Lambda = 2.4 \times 10^{-3}$ eV to the observed dark energy density and, for concreteness, $n = 1$, our constraints and forecasts are provided by Fig. 1-11. Current constraints (solid regions) and forecasts (curves) are discussed below.

1.5.2 Current laboratory constraints

Laboratory constraints on chameleon dark energy come from two different types of experiments: fifth force searches, and photon coupling experiments, both of which are shown as shaded regions in Figure 1-11. Gravitation-strength fifth forces can be measured directly between two macroscopic objects, such as the source and test masses in a torsion pendulum. Currently the shortest-range torsion pendulum constraints on gravitation-strength forces come from the Eöt-Wash experiment [258]. The source and test masses in

Experiment	Type	Couplings excluded
Eöt-Wash	torsion pendulum	$0.01 \lesssim \beta \lesssim 10$
Lamoreaux	Casimir	$\beta \gtrsim 10^5$ (ϕ^4)
Grenoble	bouncing neutron	$\beta \gtrsim 10^{11}$
GRANIT	bouncing neutron	forecast: $\beta \gtrsim 10^8$
NIST	neutron interferometry	forecast: $\beta \gtrsim 10^7$
CHASE	afterglow	$10^{11} \lesssim \beta_\gamma \lesssim 10^{16}$ subject to $10^4 \lesssim \beta_m \lesssim 10^{13}$,
ADMX	microwave cavity	$m_{\text{eff}} = 1.952 \mu\text{eV}$, $10^9 \lesssim \beta_\gamma \lesssim 10^{15}$
CAST	helioscope	forecast: $\beta_m \lesssim 10^9$, $\beta_\gamma > 10^{10}$

Table 1-1. *Laboratory tests of dark energy. Approximate constraints on chameleon models with potential $V(\phi) = M_\Lambda^4(1 + M_\Lambda/\phi)$ and $M_\Lambda = 2.4 \times 10^{-3}$ eV (unless otherwise noted).*

1089 Eöt-Wash are parallel metal disks a few centimeters in diameter with matched sets of surface features. As the
1090 lower disk is rotated, gravity and any fifth forces induce torques in the upper disk so as to align the surface
1091 features. The separation between the disks can be varied, and the torsional oscillations in the upper disk can
1092 be compared with predictions. Another type of fifth force experiment uses an ultracold gas of neutrons whose
1093 bouncing states in the gravitational field of the Earth are quantized, with energy splittings ~ 1 peV [259]. If
1094 the neutrons feel a fifth force from the experimental apparatus comparable to the gravitational force of the
1095 Earth, then the energy splittings will be altered. The Grenoble experiment measures these energy splittings
1096 at the $\sim 10\%$ level, excluding very strong matter couplings $\beta_m \gtrsim 10^{11}$.

1097 Dark energy may couple to the electroweak sector in addition to matter. Such a coupling would allow
1098 photons propagating through a magnetic field to oscillate into particles of dark energy, which can then
1099 be trapped inside a chamber if the dark energy effective mass becomes large in the chamber walls. An
1100 “afterglow experiment” produces dark energy particles through oscillation and then switches off the photon
1101 source, allowing the population of trapped dark energy particles to regenerate photons which may emerge
1102 from the chamber as an afterglow. Current afterglow constraints from the CHASE experiment exclude
1103 photon couplings $10^{11} \lesssim \beta_\gamma \lesssim 10^{16}$ for $\beta_m \gtrsim 10^4$, as shown in Fig. 1-11 for an inverse-power-law chameleon
1104 potential [260, 261, 262]. At yet higher photon couplings the trapped dark energy particles regenerate
1105 photons too quickly for CHASE to detect them. However, collider experiments can exclude such models, by
1106 constraining chameleon loop corrections to precision electroweak observables [263].

1107 1.5.3 Forecasts for Terrestrial experiments

1108 Proposed experiments promise to improve constraints on chameleon dark energy by orders of magnitude
1109 over the next several years. Fig. 1-11 summarizes forecasts and preliminary constraints, shown as solid lines.
1110 The next-generation Eöt-Wash experiment, currently under way, will have an increased force sensitivity and
1111 probe smaller distances. This will allow it to detect or exclude a large class of chameleon models with
1112 well-controlled quantum corrections [264, 265]. Improvements to fifth force measurements using neutrons
1113 should improve constraints on the chameleon-matter coupling considerably. Also proposed is a neutron
1114 interferometry experiment at NIST, which should be competitive with the bouncing neutron experiments.
1115 A neutron interferometer splits a neutron beam and sends the two through two different chambers, one
1116 containing a dense gas which suppresses chameleon field perturbations, and the other a vacuum chamber
1117 in which scalar field gradients are large. These gradients will retard the neutron beam passing through

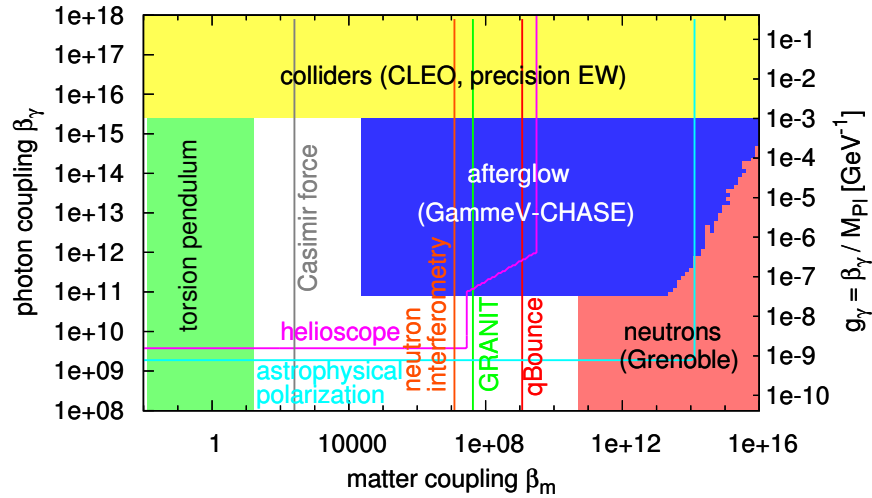


Figure 1-11. Constraints on the matter and photons couplings for a chameleon dark energy model with $V(\phi) = M_\Lambda^4(1 + M_\Lambda/\phi)$. Current constraints are shown as shaded regions, while forecasts are shown as solid lines.

1118 the vacuum chamber, resulting in a phase shift which varies nonlinearly with the gas pressure. Potentially
 1119 more powerful are the next-generation Casimir force experiments [266]. However, these currently suffer from
 1120 systematic uncertainties including the proper calculation of thermal corrections to the Casimir effect. The
 1121 forecasts shown require that the total uncertainty in the Casimir force be reduced below 1% at distances of
 1122 $5 - 10 \mu\text{m}$.

1123 Other planned experiments search for photon-coupled chameleons. Afterglow experiments have been pro-
 1124 posed at JLab and the Tore Supra tokamak, while a microwave cavity-based afterglow experiment is under
 1125 way at Yale. Since forecasts for these experiments are not available for the chameleon potential assumed in
 1126 Fig. 1-11, we are unable to include them in the figure. However, the JLab and Tore Supra experiments are
 1127 expected to fill in some of the gap between CHASE and torsion pendulum experiments, while the microwave
 1128 cavity search is a precision experiment capable of targeting a model with a specific mass in response to hints
 1129 from an afterglow experiment. Yet another type of experiment is the helioscope, which uses a high magnetic
 1130 field to regenerate photons from scalar particles produced in the Sun [267]. Since such particles do not need
 1131 to be trapped prior to detection, helioscope forecasts extend down to arbitrarily low matter couplings. One
 1132 proposed helioscope adds an X-ray mirror to the CAST axion helioscope at CERN in order to increase its
 1133 chameleon collecting area; forecasts for this experiment are shown.

1134 1.5.4 Tests of the Chameleon Mechanism by Astrophysical Observation

1135 Complimentary to detector based experiments, chameleons offer a rich phenomenology of unique astrophysi-
 1136 cal signatures. Combining data from astrophysical observations with laboratory experimental data will allow
 1137 us to constrain chameleon models. Below we review some of the more intriguing astrophysical signatures
 1138 predicted in chameleon models. One benefit of observational tests of chameleons is that these observations
 1139 may be performed complimentary with observations taken for reasons not related to chameleon gravity.
 1140 Ordinary matter interacting via a low mass particle ($m \sim H_0$) leading to a new fifth force typically requires

1141 a very small coupling. Bounds on any additional fifth force have been set by measuring the frequency shift
 1142 of photons passing near the Sun from the Cassini satellite on their way to Earth [268].

1143 The screening mechanism from chameleons has significant consequences for the formation of structure. These
 1144 modifications to structure formation include an earlier collapse of density perturbations compared to the
 1145 prediction from Λ CDM and clumpier dark matter halos [269]. Another effect on structure formation in
 1146 chameleon gravity is that the critical density required for collapse depends on the comoving size of the
 1147 inhomogeneity itself [270]. Also, galactic satellite orbits become modified based on the size of the satellite
 1148 itself due to a backreaction from the satellite causing a velocity difference of up to 10% near the thin shell
 1149 [271].

1150 Due to the existence of the two-photon vertex ($\mathcal{L}_{\phi\leftrightarrow\gamma} = F^{\mu\nu}F_{\mu\nu}\phi/4M$), chameleons mix with photons in
 1151 the presence of a background magnetic field. This mixing is the result of the propagation eigenstates being
 1152 different from the photon polarization-chameleon eigenstates. The result of this mixing is a non-conservation
 1153 of photons. In the case of type Ia supernovae, [272] demonstrated that photons convert to chameleons in the
 1154 interior of the supernova, pass through the surface of the supernova, and then convert back to photons in the
 1155 intergalactic magnetic field. The net result is an observed brightening of supernovae. This scenario provides
 1156 an explanation for the discrepancy between distance measurements of standard candles and standard rulers
 1157 beyond $z \sim 0.5$ [273].

1158 Another prediction of chameleon gravity is that in unscreened environments, (such as voids) stellar structure
 1159 is modified, most notably in the red giant branch of stars. The authors of [274] found that chameleons affect
 1160 the size and temperature of red giant stars where they tend to be smaller ($\sim 10\%$), and hotter (~ 100 s of
 1161 Kelvins). Also, observations of circularly polarized starlight in the wavelength range $1 - 10^3 \text{ \AA}$ could be a
 1162 strong indication of chameleon-photon mixing [275].

1163 Astrophysical tests of chameleons in $f(R)$ theories may be parameterized by how efficiently bodies self-
 1164 screen (χ) and the strength of the fifth force (α) [276]. For the case of chameleon $f(R)$ gravity, $\chi \equiv df/dR$ is
 1165 measured at present time. The additional force is parametrized by rescaling Newton's constant $G \rightarrow G(1+\alpha)$
 1166 for unscreened objects and $G(r) \rightarrow G[1+\alpha(1-M(r_s)/M(r))]$ for partially screened objects. Fifth forces are
 1167 screened at radii $r < r_s$, unscreened for radii $r_s < r$, and $M(r)$ is the mass contained within a shell at radius
 1168 r . For an object to be unscreened, $\Phi_N \ll \chi$ where Φ_N is the Newtonian potential. The Sun and Milky
 1169 Way (coincidentally) possess a similar gravitational potential: $\Phi_\odot \sim 2 \times 10^{-6}$ and $\Phi_{MW} \sim 10^{-6}$. Stars
 1170 in the tip of the red giant branch of the HR diagram and Cepheid variables have gravitational potentials
 1171 $\Phi_N \sim 10^{-7}$. These stars will have their outer layers unscreened provided they reside in smaller galaxies in a
 1172 shallow gravitational potential. For fifth forces of a strength described by $\alpha = 1/3$, values of χ greater than
 1173 5×10^{-7} may be ruled out at 95% confidence. This upper bound is moderately lower for fifth force strength
 1174 defined by $\alpha = 1$, where values of χ greater than 1×10^{-7} may be ruled out at a 95% confidence level [276]
 1175 (also see Fig.(5) of [276]). These constraints on χ and α from local universe observations are stronger than
 1176 current cosmological constraints on chameleon fifth forces [277]-[278] which typically give an upper limit not
 1177 less than $\chi \sim 10^{-6}$.

1178 1.5.5 Space tests of Gravity

1179 Remarkably, the original predictions of signatures in space for chameleon models would still be the most
 1180 striking [246, 247]. The proposed experiments discussed there have not yet taken place. However, the
 1181 MicroSCOPE [279] mission and STE-QUEST [280] are future satellite experiments that hold the promise of
 1182 testing these theories in a way complementary to the terrestrial and astrophysical methods discussed here.

1183 The expected signatures are large and for example an $\mathcal{O}(1)$ observed difference in Newton's constant for
1184 unscreened objects would be a smoking gun for these models.

1185 There is great potential for testing chameleon theories in the laboratory, the sky and through astrophysics ;
1186 both at the cosmic and the intensity frontiers. The possibilities for astrophysics are discussed further under
1187 the Novel Probes of Dark Energy and Gravity in the Cosmic Frontier.

1188 1.6 Conclusions

1189 Establishing the existence of Hidden Sectors, and the new light weakly-coupled particles they may contain,
1190 would revolutionize particle physics at the Copernican level: once again our simple conception of Nature
1191 would be fundamentally altered, and here we would realize that there is more than just the Standard Model
1192 sector. Searches for hidden sectors are strongly motivated and possible at presently accessible energies with
1193 existing technologies. New physics need not reside beyond the TeV scale, but could hide at the low-energy
1194 frontier. Axions, invented to solve the strong CP problem, are perfect dark matter candidate. Dark photons,
1195 and any hidden-sector particles that they couple to, can be equally compelling dark matter candidates,
1196 could resolve outstanding puzzles in particle and astro-particle physics, and may also explain dark matter
1197 interactions with the Standard Model. Other hidden sector particles could account for the Dark Energy.
1198 Discovery of any of these particles would redefine our worldview.

1199 Existing facilities and technologies, modest experiments, and experimental cleverness enable the exploration
1200 of hidden sectors. Searches for new light weakly-coupled particles depend on the tools and techniques of the
1201 intensity frontier, i.e. intense beams of photons and charged particles, on technological means of dealing with
1202 high intensities, and on extremely sensitive, needle-in-the-haystack detection techniques. A rich, diverse, and
1203 low-cost experimental program is already underway that has the potential for one or more game-changing
1204 discoveries. Current ideas for extending the searches to smaller couplings and higher masses increase this
1205 potential markedly. The US high-energy physics program needs to include such experimental searches,
1206 especially when the investment is so modest, the motives so clear, and the payoff could be so spectacular.
1207 At present, nearly all the experimental efforts world wide have strong US contributions or significant US
1208 leadership, a position that should be maintained.

1209 Axions, ALPS, dark photons, milli-charged particles, and light dark matter are all naturally connected by
1210 their hidden sector origins, and by the fact that all these particles couple to the photon, either directly,
1211 or through induced couplings generated by kinetic mixing. Microwave cavities and light-shining-through-
1212 walls experiments designed to search for axions and ALPs have been adapted to search for dark photons.
1213 So have helioscopes looking for solar axions. A series of beam dump experiments, originally motivated as
1214 axion searches, have set important limits on dark photon couplings and masses. More recently, a new series
1215 of electron and proton beam dump experiments, the latter capitalizing on existing neutrino detectors and
1216 eventually Project X beam intensities, will hunt for the interactions of light dark matter produced in the
1217 dump by dark photon decays.

1218 Searches for new, light weakly-coupled particles are, compared to typical contemporary particle physics
1219 experiments, small, accessible, hands-on, and personal in a way that is impossible with a 1000-person
1220 collaboration. This environment offers ideal educational opportunities for undergraduates, graduate students,
1221 and post docs, and revitalizes more experienced physicists too, who are all forced to deal with the full
1222 breadth of experimental activities: theory, design, proposal writing and defense, hardware construction and
1223 commissioning, software implementation, data taking, and analysis. These experiments have already joined
1224 theorists and experimentalists into close collaboration to their and to their field's benefit.

1225 A great deal remains to be done with existing tools and techniques, in searching for QCD axions that could
1226 account for the dark matter, in extending searches for dark photons throughout the favored parameter
1227 space, and in searching for new hidden-sector particles like light dark matter. Even more will be done
1228 with the addition of relatively modest investments in superconducting magnets, more sensitive microwave
1229 detection, resonant optical cavities, high rate, highly pixilated silicon detectors, and new higher energy
1230 electron accelerators, high intensity proton facilities, and upgraded e^+e^- and pp colliding beam facilities.
1231 Modest investments will pay great dividends. The hunt for the hidden sector is on in earnest, and prospects
1232 for its future look very bright indeed.

References

- 1233
- 1234 [1] R. D. Peccei and H. R. Quinn, “ CP Conservation in the Presence of Instantons,” *Phys. Rev. Lett.* **38**,
1235 1440 (1977).
- 1236 [2] S. Weinberg, “A New Light Boson?,” *Phys. Rev. Lett.* **40** (1978) 223.
- 1237 [3] F. Wilczek, “Problem of Strong p and t Invariance in the Presence of Instantons,” *Phys. Rev. Lett.* **40**,
1238 279 (1978).
- 1239 [4] K. Nakamura *et al.* [Particle Data Group], “Review of Particle Physics,” *J. Phys. G* **37** (2010) 075021.
- 1240 [5] E. Witten, “Some Properties of $O(32)$ Superstrings,” *Phys. Lett. B* **149**, 351 (1984).
- 1241 [6] J. Jaeckel and A. Ringwald, “The Low-Energy Frontier of Particle Physics,” *Ann. Rev. Nucl. Part. Sci.*
1242 **60**, 405 (2010) [arXiv:1002.0329 [hep-ph]].
- 1243 [7] J. P. Conlon, “The QCD axion and moduli stabilisation,” *JHEP* **0605**, 078 (2006) [hep-th/0602233].
- 1244 [8] P. Svrcek and E. Witten, “Axions In String Theory,” *JHEP* **0606**, 051 (2006) [hep-th/0605206].
- 1245 [9] A. Arvanitaki, S. Dimopoulos, S. Dubovsky, N. Kaloper and J. March-Russell, “String Axiverse,” *Phys.*
1246 *Rev. D* **81**, 123530 (2010) [arXiv:0905.4720 [hep-th]].
- 1247 [10] B. S. Acharya, K. Bobkov and P. Kumar, “An M Theory Solution to the Strong CP Problem and
1248 Constraints on the Axiverse,” *JHEP* **1011** (2010) 105 [arXiv:1004.5138 [hep-th]].
- 1249 [11] M. Cicoli, M. Goodsell, A. Ringwald, M. Goodsell and A. Ringwald, “The type IIB string axiverse and
1250 its low-energy phenomenology,” *JHEP* **1210**, 146 (2012) [arXiv:1206.0819 [hep-th]].
- 1251 [12] S. Hannestad, A. Mirizzi, G. G. Raffelt and Y. Y. Y. Wong, “Neutrino and axion hot dark matter
1252 bounds after WMAP-7,” *JCAP* **1008**, 001 (2010) [arXiv:1004.0695 [astro-ph.CO]].
- 1253 [13] P. Sikivie, “Axion Cosmology,” *Lect. Notes Phys.* **741** 19 (2008) [astro-ph/0610440].
- 1254 [14] T. Hiramatsu *et al.*, “Production of dark matter axions from collapse of string-wall systems,” *Phys.*
1255 *Rev. D* **85** 105020 (2012). [1202.5851 [hep-ph]].
- 1256 [15] O. Wantz and E. P. S. Shellard, “Axion Cosmology Revisited,” *Phys. Rev. D* **82** (2010) 123508
1257 [arXiv:0910.1066 [astro-ph.CO]].
- 1258 [16] P. Arias, D. Cadamuro, M. Goodsell, J. Jaeckel, J. Redondo and A. Ringwald, “Wispy Cold Dark
1259 Matter,” arXiv:1201.5902 [hep-ph].
- 1260 [17] O. Erken, P. Sikivie, H. Tam and Q. Yang, “Cosmic axion thermalization,” arXiv:1111.1157 [astro-
1261 ph.CO].
- 1262 [18] J. Isern, E. Garcia-Berro, S. Torres and S. Catalan, “Axions and the cooling of white dwarf stars,”
1263 *Astrophys. J.* **682**, L109 (2008) [arXiv:0806.2807 [astro-ph]].
- 1264 [19] J. Isern, S. Catalan, E. Garcia-Berro and S. Torres, “Axions and the white dwarf luminosity function,”
1265 *J. Phys. Conf. Ser.* **172**, 012005 (2009) [arXiv:0812.3043 [astro-ph]].
- 1266 [20] J. Isern, L. Althaus, S. Catalan, A. Corsico, E. Garcia-Berro, M. Salaris, S. Torres and L. Althaus *et*
1267 *al.*, “White dwarfs as physics laboratories: the case of axions,” arXiv:1204.3565 [astro-ph.SR].

- 1268 [21] A. H. Corsico, L. G. Althaus, M. M. M. Bertolami, A. D. Romero, E. Garcia-Berro, J. Isern
1269 and S. O. Kepler, “The rate of cooling of the pulsating white dwarf star G117–B15A: a new
1270 asteroseismological inference of the axion mass,” *Monthly Notices of the Royal Astronomical Society*,
1271 Volume 424, Issue 4, pp. 2792-2799. arXiv:1205.6180 [astro-ph.SR].
- 1272 [22] A. H. Corsico, L. G. Althaus, A. D. Romero, A. S. Mukadam, E. Garcia-Berro, J. Isern, S. O. Kepler
1273 and M. A. Corti, “An independent limit on the axion mass from the variable white dwarf star R548,”
1274 *JCAP* **1212**, 010 (2012) [arXiv:1211.3389 [astro-ph.SR]].
- 1275 [23] B. Melendez, M. M. Bertolami and L. Althaus, “Revisiting the Impact of Axions in the Cooling of
1276 White Dwarfs,” arXiv:1210.0263 [hep-ph].
- 1277 [24] D. Horns and M. Meyer, “Indications for a pair-production anomaly from the propagation of VHE
1278 gamma-rays,” arXiv:1201.4711 [astro-ph.CO].
- 1279 [25] A. De Angelis, O. Mansutti and M. Roncadelli, “Evidence for a new light spin-zero boson from
1280 cosmological gamma-ray propagation?,” *Phys. Rev. D* **76**, 121301 (2007) [arXiv:0707.4312 [astro-ph]].
- 1281 [26] M. Simet, D. Hooper and P. D. Serpico, “The Milky Way as a Kiloparsec-Scale Axionscope,” *Phys.*
1282 *Rev. D* **77**, 063001 (2008) [arXiv:0712.2825 [astro-ph]].
- 1283 [27] M. A. Sanchez-Conde, D. Paneque, E. Bloom, F. Prada and A. Dominguez, “Hints of the existence of
1284 Axion-Like-Particles from the gamma-ray spectra of cosmological sources,” *Phys. Rev. D* **79**, 123511
1285 (2009) [arXiv:0905.3270 [astro-ph.CO]].
- 1286 [28] A. De Angelis, G. Galanti and M. Roncadelli, “Relevance of axion-like particles for very-high-energy
1287 astrophysics,” *Phys. Rev. D* **84**, 105030 (2011) [arXiv:1106.1132 [astro-ph.HE]].
- 1288 [29] M. Meyer, D. Horns and M. Raue, “First lower limits on the photon-axion-like particle coupling from
1289 very high energy gamma-ray observation,” *Phys. Rev. D* **87**, 035027 (2013) [arXiv:1302.1208 [astro-
1290 ph.HE]].
- 1291 [30] S. J. Asztalos, R. Bradley, G. Carosi, J. Clarke, C. Hagmann, J. Hoskins, M. Hotz and D. Kinion *et al.*,
1292 “The axion dark-matter eXperiment: Results and plans,”
- 1293 [31] R. Bhre, B. Dbrich, J. Dreyling-Eschweiler, S. Ghazaryan, R. Hodajerdi, D. Horns, F. Januschek and
1294 E. -A. Knabbe *et al.*, “Any Light Particle Search II – Technical Design Report,” arXiv:1302.5647
1295 [physics.ins-det].
- 1296 [32] I. G. Irastorza, F. T. Avignone, S. Caspi, J. M. Carmona, T. Dafni, M. Davenport, A. Dudarev
1297 and G. Fanourakis *et al.*, “Towards a new generation axion helioscope,” *JCAP* **1106** (2011) 013
1298 [arXiv:1103.5334 [hep-ex]].
- 1299 [33] J. K. Vogel, F. T. Avignone, G. Cantatore, J. M. Carmona, S. Caspi, S. A. Cetin, F. E. Christensen
1300 and A. Dael *et al.*, “IAXO - The International Axion Observatory,” arXiv:1302.3273 [physics.ins-det].
- 1301 [34] D. Horns, J. Jaeckel, A. Lindner, A. Lobanov, J. Redondo and A. Ringwald, “Searching for WISPy
1302 Cold Dark Matter with a Dish Antenna,” *JCAP* **1304**, 016 (2013) [arXiv:1212.2970 [hep-ph]].
- 1303 [35] W. Hu, R. Barkana and A. Gruzinov, *Phys. Rev. Lett.* **85**, 1158 (2000) [astro-ph/0003365].
- 1304 [36] M. Boylan-Kolchin, J. S. Bullock and M. Kaplinghat, *Mon. Not. Roy. Astron. Soc.* **415**, L40 (2011)
1305 [arXiv:1103.0007 [astro-ph.CO]].
- 1306 [37] L. Amendola and R. Barbieri, *Phys. Lett. B* **642**, 192 (2006) [hep-ph/0509257].

- 1307 [38] D. J. E. Marsh, E. Macaulay, M. Trebitsch and P. G. Ferreira, Phys. Rev. D **85**, 103514 (2012)
1308 [arXiv:1110.0502 [astro-ph.CO]].
- 1309 [39] L. Amendola *et al.* [Euclid Theory Working Group Collaboration], arXiv:1206.1225 [astro-ph.CO].
- 1310 [40] D. J. E. Marsh, D. Grin, R. eHlozek and P. G. Ferreira, arXiv:1303.3008 [astro-ph.CO].
- 1311 [41] C. P. Burgess, M. Cicoli and F. Quevedo, arXiv:1306.3512 [hep-th].
- 1312 [42] A. V. Maccio, S. Paduroiu, D. Anderhalden, A. Schneider and B. Moore, arXiv:1202.1282 [astro-ph.CO].
- 1313 [43] K. van Bibber, N.R. Dagdeviren, S.E. Koonin, A.K. Kerman and H.N. Nelson, Phys. Rev. Lett. **59**, 759
1314 (1987).
- 1315 [44] F. Hoogeveen and T. Ziegenhagen Nucl. Phys. B **358**, 3 (1991).
- 1316 [45] P. Sikivie, D.B. Tanner, and Karl van Bibber, Phys. Rev. Lett. **98**, 172002 (2007).
- 1317 [46] G. Mueller, P. Sikivie, D.B. Tanner and K. van Bibber, Phys. Rev. D **80**, 072004 (2009).
- 1318 [47] G. Mueller, P. Sikivie, D.B. Tanner, and K. van Bibber, AIP Conf. Proc. **1274**, 150 (2010).
- 1319 [48] Robin Bähre, Babette Döbrich, Jan Dreyling-Eschweiler, Samvel Ghazaryan, Reza Hodajerd, Dieter
1320 Horns, Friederike Januschek, Ernst-Axel Knabbe, Axel Lindner, Dieter Notz, Andreas Ringwald, Jan
1321 Eike von Seggern, Richard Stromhagen, Dieter Trines, and Benno Willke, arXiv:1302.5647 [physics.ins-
1322 det].
- 1323 [49] B. Abbott *et al.* (LIGO Scientific Collaboration), Nucl. Instrum. Methods A **517**, 154–179 (2004); Rep.
1324 Prog. Phys. **72**, 076901/1–25 (2009).
- 1325 [50] R.J. Cruz, J.I. Thorpe, A. Preston, R. Delgado, M. Hartman, S. Mitryk, A. Worley, G. Boothe, S. R.
1326 Guntaka, S. Klimenko, D.B. Tanner and G. Mueller, Class. Quant. Grav. **23**, S751-S760 (2006).
- 1327 [51] P. Sikivie, Phys. Rev. Lett. **51**, 1415 (1983).
- 1328 [52] G. Raffelt and L. Stodolsky, Phys. Rev. D **37**, 1237 (1988).
- 1329 [53] G. Ruoso, R. Cameron, G. Cantatore, A. C. Melissinos, Y. Semertzidis, H. J. Halama, D. M. Lazarus,
1330 A. G. Prodel, F. Nezzrick, C. Rizzo and E. Zavattini, Z. Phys. C **56**, 505 (1992).
- 1331 [54] R. Cameron, G. Cantatore, A. C. Melissinos, G. Ruoso, and Y. Semertzidis, H. J. Halama, D. M.
1332 Lazarus, and A. G. Prodel, F. Nezzrick, C. Rizzo and E. Zavattini, Phys. Rev. D **47**, 3707 (1993).
- 1333 [55] C. Robilliard, R. Battesti, M. Fouché, J. Mauchain, A.-M. Sautivet, F. Amiranoff, and C. Rizzo, Phys.
1334 Rev. Lett. **99**, 190403 (2007).
- 1335 [56] A. S. Chou, W. Wester, A. Baumbaugh, H. R. Gustafson, Y. Irizarry-Valle, P. O. Mazur, J. H. Steffen,
1336 R. Tomlin, X. Yang, and J. Yoo, Phys. Rev. Lett. **100**, 080402 (2008).
- 1337 [57] A. Afanasev, O. K. Baker, K. B. Beard, G. Biallas, J. Boyce, M. Minarni, R. Ramdon, M. Shinn, and
1338 P. Slocum, Phys. Rev. Lett. **101**, 120401 (2008).
- 1339 [58] Pierre Pugnât, Lionel Duvillaret, Remy Jost, Guy Vitrant, Daniele Romanini, Andrzej Siemko, Rafik
1340 Ballou, Bernard Barbara, Michael Finger, Miroslav Finger, Jan Hošek, Miroslav Král, Krzysztof A.
1341 Meissner, Miroslav Šulc, and Josef Zicha, Phys. Rev. D **78**, 092003 (2008).

- 1342 [59] Klaus Ehret, Maik Frede, Samvel Ghazaryan, Matthias Hildebrandt, Ernst-Axel Knabbe, Dietmar
1343 Kracht, Axel Lindner, Jenny List, Tobias Meier, Niels Meyer, Dieter Notz, Javier Redondo, Andreas
1344 Ringwald, Günter Wiedemann, and Benno Willke, arXiv:0905.4159v1.
- 1345 [60] A.E. Siegman, *Lasers* (University Science Books, Sausalito, 1984).
- 1346 [61] For example, see <http://lma.in2p3.fr/Activites/loss.htm>
- 1347 [62] R.W.P. Drever, J.L. Hall, F.V. Kowalski, J. Hough, G.M. Ford, A.J. Munley, and H. Ward, *Appl. Phys.*
1348 *B* **31**, 97 (1983); Eric D. Black, *Am. J. Phys.* **69**, 79 (2001).
- 1349 [63] K. Goda, D. Ottaway, B. Connelly, R. Adhikari, N. Mavalvala, and A. Gretarsson, “Frequency-resolving
1350 spatiotemporal wave-front sensor,” *Optics Letters* **29**, 1452–1454 (2004).
- 1351 [64] K. Zioutas *et al.* (CAST collaboration), *Phys. Rev. Lett.* **94**, 121301 (2005); E. Arik *et al.* (CAST
1352 collaboration) *J. Cosmo. Astropart. Phys.* **02**, 008 (2009).
- 1353 [65] G.G. Raffelt, *Stars as Laboratories for Fundamental Physics* (University of Chicago Press, Chicago,
1354 1996).
- 1355 [66] M. Ahlers, H. Gies, J. Jaeckel, J. Redondo, and A. Ringwald, *Phys. Rev. D* **77**, 095001 (2008).
- 1356 [67] S.A. Abel, M.D. Goodsell, J. Jaeckel, V.V. Khoze, and A. Ringwald, *JHEP* **07**, 124 (2008).
- 1357 [68] A. Afanasev, O.K. Baker, K.B. Beard, G. Biallas, J. Boyce, M. Minarni, R. Ramdon, M. Shinn, and P.
1358 Slocum, *Phys. Lett. B* **679**, 317–320 (2009).
- 1359 [69] Joerg Jaeckel, Javier Redondo, and Andreas Ringwald, *Phys. Rev. Lett.* **101**, 131801 (2008).
- 1360 [70] P. Sikivie, “Experimental tests of the ‘invisible’ axion,” *Phys. Rev. Lett.* **51**, 1415 (1983) [Erratum-*ibid.*
1361 **52**, 695 (1984)].
- 1362 [71] S. De Panfilis, *et al.*, “Limits on the abundance and coupling of cosmic axions at $4.5 \mu\text{eV} < m(a) < 5.0$
1363 μeV ,” *Phys. Rev. Lett.* **59**, 839 (1987).
- 1364 [72] C. Hagmann, P. Sikivie, N.S. Sullivan, D.B. Tanner, “Results for a search for cosmic axions,” *Phys.*
1365 *Rev. D* **42**, 1297 (1990).
- 1366 [73] S.J. Asztalos, *et al.*, “An improved RF cavity search for halo axion,” *Phys. Rev. D* **69**, 011101 (2004)
1367 [astro-ph/0310042].
- 1368 [74] E.I. Gates, G. Gyuk, M.S. Turner, “The local halo density,” *Astrophys. J.* **449**, L123 (1995) [astro-
1369 ph/9505039].
- 1370 [75] S.J. Asztalos *et al.*, “SQUID-Based Microwave Cavity Search for Dark-Matter Axions,” *Phys. Rev. Lett.*
1371 **104**, 041301 (2010).
- 1372 [76] H. Primakoff, “Photo-Production of Neutral Mesons in Nuclear Electric Fields and the Mean Life of
1373 the Neutral Meson,” *Phys. Rev.* **81**, 899 (1951).
- 1374 [77] P. Sikivie, “Experimental Tests of the ‘Invisible’ Axion,” *Phys. Rev. Lett.* **51**, 1415 (1983).
- 1375 [78] P. Sikivie, “Detection rates for ‘invisible’-axion searches,” *Phys. Rev. D* **32**, 2988 (1985).
- 1376 [79] K. van Bibber, P. M. McIntyre, D. E. Morris, and G. G. Raffelt, “Design for a practical laboratory
1377 detector for solar axions,” *Phys. Rev. D* **39**, 2089 (1989).

- 1378 [80] D. M. Lazarus *et al.*, "Search for solar axions," Phys. Rev. Lett. **69**, 2333 (1992).
- 1379 [81] S. Moriyama *et al.*, "Direct search for solar axions by using strong magnetic field and X-ray detectors,"
1380 Phys. Lett. B **434**, 147 (1998).
- 1381 [82] Y. Inoue *et al.*, "Search for sub-electronvolt solar axions using coherent conversion of axions into photons
1382 in magnetic field and gas helium," Phys. Lett. B **536**, 18 (2002).
- 1383 [83] Y. Inoue *et al.*, "Search for solar axions with mass around 1 eV using coherent conversion of axions into
1384 photons," Phys. Lett. B **668**, 93 (2008).
- 1385 [84] K. Zioutas *et al.*, "A decommissioned LHC model magnet as an axion telescope," NIM A **425**, 480
1386 (1999).
- 1387 [85] M. Kuster *et al.*, "The x-ray telescope of CAST," New Journal of Physics **9**, 169 (2007).
- 1388 [86] CAST Collaboration, K. Zioutas *et al.*, "First Results from the CERN Axion Solar Telescope," Phys.
1389 Rev. Lett. **94**, 121301 (2005).
- 1390 [87] S. Andriamonje *et al.*, "An improved limit on the axionphoton coupling from the CAST experiment,"
1391 Journal of Cosmology and Astroparticle Physics **2007**, 010 (2007).
- 1392 [88] E. Arik *et al.*, "Probing eV-scale axions with CAST," Journal of Cosmology and Astroparticle Physics
1393 **2009**, 008 (2009).
- 1394 [89] CAST Collaboration, M. Arik *et al.*, "Search for Sub-eV Mass Solar Axions by the CERN Axion Solar
1395 Telescope with ^3He Buffer Gas," Phys. Rev. Lett. **107**, 261302 (2011) [arXiv:1106.3919].
- 1396 [90] CAST Collaboration, M. Arik *et al.*, "CAST solar axion search with ^3He buffer gas: Closing the hot
1397 dark matter gap," publication in preparation for Phys. Rev. Lett. (2013), [arxiv:1307.1985].
- 1398 [91] G. G. Raffelt, "Astrophysical axion bounds," Lect. Notes Phys. **741**, 51 (2008).
- 1399 [92] S. Hannestad, A. Mirizzi, G. G. Raffelt, Y. Y. Y. Wong, "Neutrino and axion hot dark matter bounds
1400 after WMAP-7," JCAP **08** 001 (2010).
- 1401 [93] K. Barth *et al.*, "CAST constraints on the axion-electron coupling," JCAP **1305**, 010 (2013).
- 1402 [94] I. Irastorza *et al.*, "Towards a new generation axion helioscope," Journal of Cosmology and Astroparticle
1403 Physics **2011**, 013 (2011).
- 1404 [95] P. Brax and K. Zioutas, "Solar chameleons," Phys. Rev. D **82**, 043007 (2010).
- 1405 [96] O.K. Baker, M. Betz, F. Caspers, J. Jaeckel, A. Lindner, A. Ringwald, Y. Semertzidis, P. Sikivie,
1406 K. Zioutas, "Prospects for searching axionlike particle dark matter with dipole, toroidal, and wiggler
1407 magnets," Phys. Rev. D **85**, 035018 (2012).
- 1408 [97] P. Brax, A. Lindner, K. Zioutas, "Detection prospects for solar and terrestrial chameleons," Phys. Rev.
1409 D **85**, 043014 (2012).
- 1410 [98] K. Zioutas, M. Tsagri, Y. Semertzidis, T. Papaevangelou, T. Dafni, V Anastassopoulos, "Axion searches
1411 with helioscopes and astrophysical signatures for axion(-like) particles," New J. Phys. **11**, 105020 (2009).
- 1412 [99] The Annual Patras Workshops on Axions, WIMPs & WISPs, <http://axion-wimp.desy.de/>
- 1413 [100] B. Holdom, "Two $U(1)$'s and Epsilon Charge Shifts," Phys. Lett. B **166** (1986) 196.

- 1414 [101] P. Galison and A. Manohar, “Two Z ’s Or Not Two Z ’s?,” Phys. Lett. B **136** (1984) 279.
- 1415 [102] J. D. Bjorken *et al.*, “Search for Neutral Metastable Penetrating Particles Produced in the SLAC Beam
1416 Dump,” Phys. Rev. D **38** (1988) 3375.
- 1417 [103] E. M. Riordan *et al.*, “A Search for Short Lived Axions in an Electron Beam Dump Experiment,”
1418 Phys. Rev. Lett. **59** (1987) 755.
- 1419 [104] A. Bross, M. Crisler, S. H. Pordes, J. Volk, S. Errede and J. Wrbanek, “A Search for Shortlived
1420 Particles Produced in an Electron Beam Dump,” Phys. Rev. Lett. **67** (1991) 2942.
- 1421 [105] J. D. Bjorken, R. Essig, P. Schuster and N. Toro, “New Fixed-Target Experiments to Search for Dark
1422 Gauge Forces,” Phys. Rev. D **80**, 075018 (2009) [arXiv:0906.0580 [hep-ph]].
- 1423 [106] M. Pospelov, “Secluded $U(1)$ Below the Weak Scale,” Phys. Rev. D **80** (2009) 095002 [arXiv:0811.1030
1424 [hep-ph]].
- 1425 [107] KLOE-2 Collaboration, “Search for a Vector Gauge Boson in Phi Meson Decays with the KLOE
1426 Detector,” Phys. Lett. B **706** (2012) 251 [arXiv:1110.0411 [hep-ex]].
- 1427 [108] S. Abrahamyan *et al.* [APEX Collaboration], “Search for a New Gauge Boson in Electron-
1428 Nucleus Fixed-Target Scattering by the APEX Experiment,” Phys. Rev. Lett. **107**, 191804 (2011)
1429 [arXiv:1108.2750 [hep-ex]].
- 1430 [109] H. Merkel *et al.* [A1 Collaboration], “Search for Light Gauge Bosons of the Dark Sector at the Mainz
1431 Microtron,” Phys. Rev. Lett. **106**, 251802 (2011) [arXiv:1101.4091 [nucl-ex]].
- 1432 [110] M. Reece and L. T. Wang, “Searching for the Light Dark Gauge Boson in GeV-Scale Experiments,”
1433 JHEP **0907** (2009) 051 [arXiv:0904.1743 [hep-ph]].
- 1434 [111] B. Aubert *et al.* [BABAR Collaboration], Phys. Rev. Lett. **103**, 081803 (2009) [arXiv:0905.4539 [hep-
1435 ex]].
- 1436 [112] J. B. Dent, F. Ferrer and L. M. Krauss, “Constraints on Light Hidden-Sector Gauge Bosons from
1437 Supernova Cooling,” arXiv:1201.2683 [astro-ph.CO].
- 1438 [113] R. Essig, P. Schuster, N. Toro and B. Wojtsekhowski, “An Electron Fixed Target Experiment to Search
1439 for a New Vector Boson A' Decaying to e^+e^- ,” JHEP **1102**, 009 (2011) [arXiv:1001.2557 [hep-ph]].
- 1440 [114] The Heavy Photon Search Collaboration (HPS), <https://confluence.slac.stanford.edu/display/hpsg/>
- 1441 [115] M. Freytsis, G. Ovanessian and J. Thaler, “Dark Force Detection in Low Energy ep Collisions,” JHEP
1442 **1001** (2010) 111 [arXiv:0909.2862 [hep-ph]].
- 1443 [116] B. Wojtsekhowski, “Searching for a U-Boson with a Positron Beam,” AIP Conf. Proc. **1160** (2009)
1444 149 [arXiv:0906.5265 [hep-ex]].
- 1445 [117] B. Wojtsekhowski, D. Nikolenko and I. Rachek, “Searching for a New Force at Vepp-3,” arXiv:1207.5089
1446 [hep-ex].
- 1447 [118] T. Beranek, H. Merkel and M. Vanderhaeghen, “Theoretical Framework to Analyze Searches for Hidden
1448 Light Gauge Bosons in Electron Scattering Fixed Target Experiments,” arXiv:1303.2540 [hep-ph].
- 1449 [119] R. Essig, P. Schuster and N. Toro, “Probing Dark Forces and Light Hidden-Sectors at Low-Energy
1450 e^+e^- Colliders,” Phys. Rev. D **80** (2009) 015003 [arXiv:0903.3941 [hep-ph]].

- 1451 [120] M. Goodsell, J. Jaeckel, J. Redondo and A. Ringwald, “Naturally Light Hidden-Photons in Large
1452 Volume String Compactifications,” JHEP **0911**, 027 (2009) [arXiv:0909.0515 [hep-ph]].
- 1453 [121] M. Cicoli, M. Goodsell, J. Jaeckel and A. Ringwald, “Testing String Vacua in the Lab: From a Hidden
1454 CMB to Dark Forces in Flux Compactifications,” JHEP **1107**, 114 (2011) [arXiv:1103.3705 [hep-th]].
- 1455 [122] M. Goodsell, S. Ramos-Sanchez and A. Ringwald, “Kinetic Mixing of $U(1)$ s in Heterotic Orbifolds,”
1456 JHEP **1201**, 021 (2012) [arXiv:1110.6901 [hep-th]].
- 1457 [123] M. Goodsell and A. Ringwald, “Light hidden-sector $U(1)$ s in string compactifications,” Fortsch. Phys.
1458 **58**, 716 (2010) [arXiv:1002.1840 [hep-th]].
- 1459 [124] P. Candelas, G. T. Horowitz, A. Strominger and E. Witten, “Vacuum Configurations for Superstrings,”
1460 Nucl. Phys. B **258**, 46 (1985).
- 1461 [125] E. Witten, “New Issues in Manifolds of $SU(3)$ Holonomy,” Nucl. Phys. B **268**, 79 (1986).
- 1462 [126] S. Andreas, M. D. Goodsell and A. Ringwald, “Dark matter and Dark Forces from a Supersymmetric
1463 Hidden-Sector,” arXiv:1109.2869 [hep-ph].
- 1464 [127] P. Fayet, “ U -Boson Production in e^+e^- Annihilations, Psi and Upsilon Decays, and Light Dark
1465 Matter,” Phys. Rev. D **75** (2007) 115017 [arXiv:hep-ph/0702176].
- 1466 [128] C. Cheung, J. T. Ruderman, L. T. Wang and I. Yavin, “Kinetic Mixing as the Origin of Light Dark
1467 Scales,” Phys. Rev. D **80** (2009) 035008 [arXiv:0902.3246 [hep-ph]].
- 1468 [129] N. Arkani-Hamed and N. Weiner, JHEP **0812**, 104 (2008) [arXiv:0810.0714 [hep-ph]].
- 1469 [130] D. E. Morrissey, D. Poland and K. M. Zurek, “Abelian Hidden-Sectors at a GeV,” JHEP **0907** (2009)
1470 050 [arXiv:0904.2567 [hep-ph]].
- 1471 [131] H. Davoudiasl, H.-S. Lee and W. J. Marciano, “‘Dark’ Z implications for Parity Violation, Rare Meson
1472 Decays, and Higgs Physics,” Phys. Rev. D **85**, 115019 (2012) [arXiv:1203.2947 [hep-ph]].
- 1473 [132] H. Davoudiasl, H.-S. Lee and W. J. Marciano, “Muon Anomaly and Dark Parity Violation,” Phys.
1474 Rev. Lett. **109**, 031802 (2012) [arXiv:1205.2709 [hep-ph]].
- 1475 [133] H. Davoudiasl, H.-S. Lee and W. J. Marciano, “Dark Side of Higgs Diphoton Decays and Muon $g-2$,”
1476 Phys. Rev. D **86**, 095009 (2012) [arXiv:1208.2973 [hep-ph]].
- 1477 [134] H. Davoudiasl, H.-S. Lee, I. Lewis and W. J. Marciano, “Higgs Decays as a Window into the Dark
1478 Sector,” Phys. Rev. D **88**, 015022 (2013) [arXiv:1304.4935 [hep-ph]].
- 1479 [135] B. Batell, M. Pospelov and A. Ritz, “Exploring Portals to a Hidden-Sector Through Fixed Targets,”
1480 Phys. Rev. D **80**, 095024 (2009) [arXiv:0906.5614 [hep-ph]].
- 1481 [136] R. Essig, R. Harnik, J. Kaplan and N. Toro, “Discovering New Light States at Neutrino Experiments,”
1482 Phys. Rev. D **82**, 113008 (2010) [arXiv:1008.0636 [hep-ph]].
- 1483 [137] M. J. Strassler and K. M. Zurek, “Echoes of a Hidden Valley at Hadron Colliders,” Phys. Lett. B **651**
1484 (2007) 374 [arXiv:hep-ph/0604261].
- 1485 [138] G. Amelino-Camelia *et al.*, “Physics with the KLOE-2 Experiment at the Upgraded DaΦNe,” Eur.
1486 Phys. J. C **68** (2010) 619 [arXiv:1003.3868 [hep-ex]].
- 1487 [139] B. Aubert *et al.* [BaBar Collaboration], “Search for Dimuon Decays of a Light Scalar in Radiative
1488 Transitions $Y(3S) \rightarrow \text{Gamma} A0$,” arXiv:0902.2176 [hep-ex].

- 1489 [140] B. Batell, M. Pospelov and A. Ritz, “Probing a Secluded $U(1)$ at B -Factories,” *Phys. Rev. D* **79** (2009)
1490 115008 [arXiv:0903.0363 [hep-ph]].
- 1491 [141] B. Aubert *et al.* [BaBar Collaboration], “Search for a Narrow Resonance in e^+e^- to Four Lepton Final
1492 States,” arXiv:0908.2821 [hep-ex].
- 1493 [142] V. M. Abazov *et al.* [D0 Collaboration], “Search for dark photons from supersymmetric hidden valleys,”
1494 *Phys. Rev. Lett.* **103**, 081802 (2009) [arXiv:0905.1478 [hep-ex]].
- 1495 [143] V. M. Abazov *et al.* [D0 Collaboration], “Search for events with leptonic jets and missing transverse
1496 energy in $p\bar{p}$ collisions at $\sqrt{s} = 1.96$ TeV,” *Phys. Rev. Lett.* **105**, 211802 (2010) [arXiv:1008.3356
1497 [hep-ex]].
- 1498 [144] J. P. Lees and others [The BABAR Collaboration], “A Search for Dark Higgs Bosons,” arXiv:1202.1313
1499 [hep-ex].
- 1500 [145] M. Baumgart, C. Cheung, J. T. Ruderman, L. T. Wang and I. Yavin, “Non-Abelian Dark Sectors and
1501 Their Collider Signatures,” *JHEP* **0904**, 014 (2009) [arXiv:0901.0283 [hep-ph]].
- 1502 [146] N. Arkani-Hamed, D. P. Finkbeiner, T. R. Slatyer and N. Weiner, “A Theory of Dark Matter,” *Phys.*
1503 *Rev. D* **79** (2009) 015014 [arXiv:0810.0713 [hep-ph]].
- 1504 [147] M. Pospelov and A. Ritz, “Astrophysical Signatures of Secluded Dark Matter,” *Phys. Lett. B* **671**
1505 (2009) 391 [arXiv:0810.1502 [hep-ph]].
- 1506 [148] A. P. Lobanov, H. -S. Zechlin and D. Horns, “Astrophysical searches for a hidden-photon signal in the
1507 radio regime,” *Phys. Rev. D* **87**, Issue 6, id. 065004, arXiv:1211.6268 [astro-ph.CO].
- 1508 [149] L. B. Okun, “Limits Of Electrodynamics: Paraphotons?,” *Sov. Phys. JETP* **56**, 502 (1982) [*Zh. Eksp.*
1509 *Teor. Fiz.* **83**, 892 (1982)].
- 1510 [150] A. E. Nelson and J. Scholtz, “Dark Light, Dark Matter and the Misalignment Mechanism,” *Phys. Rev.*
1511 *D* **84**, 103501 (2011) [arXiv:1105.2812 [hep-ph]].
- 1512 [151] O. Adriani *et al.* [PAMELA Collaboration], “An anomalous positron abundance in cosmic rays with
1513 energies 1.5-100 GeV,” *Nature* **458**, 607 (2009) [arXiv:0810.4995 [astro-ph]].
- 1514 [152] M. Ackermann *et al.* [Fermi LAT Collaboration], “Measurement of separate cosmic-ray electron
1515 and positron spectra with the Fermi Large Area Telescope,” *Phys. Rev. Lett.* **108**, 011103 (2012)
1516 [arXiv:1109.0521 [astro-ph.HE]].
- 1517 [153] M. Aguilar *et al.* [AMS Collaboration], “First Result from the Alpha Magnetic Spectrometer on the
1518 International Space Station: Precision Measurement of the Positron Fraction in Primary Cosmic Rays
1519 of 0.5350 GeV,” *Phys. Rev. Lett.* **110**, no. 14, 141102 (2013).
- 1520 [154] K. Blum, B. Katz and E. Waxman, “AMS02 results support the secondary origin of cosmic ray
1521 positrons,” arXiv:1305.1324 [astro-ph.HE].
- 1522 [155] P. Blasi, “The origin of the positron excess in cosmic rays,” *Phys. Rev. Lett.* **103**, 051104 (2009)
1523 [arXiv:0903.2794 [astro-ph.HE]].
- 1524 [156] R. Cowsik and B. Burch, “On the Positron Fraction and the Spectrum of the Electronic Component
1525 in Cosmic Rays,” arXiv:0905.2136 [astro-ph.CO].

- 1526 [157] A. A. Abdo *et al.* [Fermi LAT Collaboration], “Measurement of the Cosmic Ray e+ plus e- spectrum
1527 from 20 GeV to 1 TeV with the Fermi Large Area Telescope,” *Phys. Rev. Lett.* **102**, 181101 (2009)
1528 [arXiv:0905.0025 [astro-ph.HE]].
- 1529 [158] I. Cholis, L. Goodenough, D. Hooper, M. Simet and N. Weiner, “High Energy Positrons From
1530 Annihilating Dark Matter,” *Phys. Rev. D* **80**, 123511 (2009) [arXiv:0809.1683 [hep-ph]].
- 1531 [159] P. -F. Yin, Z. -H. Yu, Q. Yuan and X. -J. Bi, “Pulsar interpretation for the AMS-02 result,”
1532 arXiv:1304.4128 [astro-ph.HE].
- 1533 [160] T. Linden and S. Profumo, “Probing the Pulsar Origin of the Anomalous Positron Fraction with
1534 AMS-02 and Atmospheric Cherenkov Telescopes,” arXiv:1304.1791 [astro-ph.HE].
- 1535 [161] D. P. Finkbeiner, L. Goodenough, T. R. Slatyer, M. Vogelsberger and N. Weiner, “Consistent Scenarios
1536 for Cosmic-Ray Excesses from Sommerfeld-Enhanced Dark Matter Annihilation,” *JCAP* **1105**, 002
1537 (2011) [arXiv:1011.3082 [hep-ph]].
- 1538 [162] I. Cholis and D. Hooper, “Dark Matter and Pulsar Origins of the Rising Cosmic Ray Positron Fraction
1539 in Light of New Data From AMS,” arXiv:1304.1840 [astro-ph.HE].
- 1540 [163] Q. Yuan, X. -J. Bi, G. -M. Chen, Y. -Q. Guo, S. -J. Lin and X. Zhang, “Implications of the AMS-02
1541 positron fraction in cosmic rays,” arXiv:1304.1482 [astro-ph.HE].
- 1542 [164] M. Ackermann *et al.* [LAT Collaboration], “Constraints on the Galactic Halo Dark Matter from Fermi-
1543 LAT Diffuse Measurements,” *Astrophys. J.* **761** (2012) 91 [arXiv:1205.6474 [astro-ph.CO]].
- 1544 [165] J. Zavala, M. Vogelsberger, T. R. Slatyer, A. Loeb and V. Springel, “The cosmic X-ray and gamma-ray
1545 background from dark matter annihilation,” *Phys. Rev. D* **83** (2011) 123513 [arXiv:1103.0776 [astro-
1546 ph.CO]].
- 1547 [166] K. N. Abazajian and J. P. Harding, “Constraints on WIMP and Sommerfeld-Enhanced Dark Matter
1548 Annihilation from HESS Observations of the Galactic Center,” *JCAP* **1201**, 041 (2012) [arXiv:1110.6151
1549 [hep-ph]].
- 1550 [167] N. Padmanabhan and D. P. Finkbeiner, “Detecting dark matter annihilation with CMB polarization:
1551 Signatures and experimental prospects,” *Phys. Rev. D* **72**, 023508 (2005) [astro-ph/0503486].
- 1552 [168] L. Lopez-Honorez, O. Mena, S. Palomares-Ruiz and A. C. Vincent, “Constraints on dark matter
1553 annihilation from CMB observations before Planck,” arXiv:1303.5094 [astro-ph.CO].
- 1554 [169] S. Galli, T. R. Slatyer, M. Valdes and F. Iocco, “Systematic Uncertainties In Constraining Dark Matter
1555 Annihilation From The Cosmic Microwave Background,” arXiv:1306.0563 [astro-ph.CO].
- 1556 [170] T. R. Slatyer, N. Toro and N. Weiner, “Sommerfeld-enhanced annihilation in dark matter substructure:
1557 Consequences for constraints on cosmic-ray excesses,” *Phys. Rev. D* **86**, 083534 (2012) [arXiv:1107.3546
1558 [hep-ph]].
- 1559 [171] M. Ibe, S. Matsumoto, S. Shirai and T. T. Yanagida, “AMS-02 Positrons from Decaying Wino in the
1560 Pure Gravity Mediation Model,” arXiv:1305.0084 [hep-ph].
- 1561 [172] R. Agnese *et al.* [CDMS Collaboration], “Dark Matter Search Results Using the Silicon Detectors of
1562 CDMS II,” Submitted to: *Phys.Rev.Lett.* [arXiv:1304.4279 [hep-ex]].
- 1563 [173] C. E. Aalseth *et al.* [CoGeNT Collaboration], “CoGeNT: A Search for Low-Mass Dark Matter using
1564 p-type Point Contact Germanium Detectors,” arXiv:1208.5737 [astro-ph.CO].

- 1565 [174] D. Hooper, “Revisiting XENON100’s Constraints (and Signals?) For Low-Mass Dark Matter,”
1566 arXiv:1306.1790 [hep-ph].
- 1567 [175] A. Djouadi, A. Falkowski, Y. Mambrini and J. Quevillon, “Direct Detection of Higgs-Portal Dark
1568 Matter at the LHC,” arXiv:1205.3169 [hep-ph].
- 1569 [176] K. -Y. Choi and O. Seto, “Light Dirac right-handed sneutrino dark matter,” arXiv:1305.4322 [hep-ph].
- 1570 [177] D. Hooper and T. Linden, “On The Origin Of The Gamma Rays From The Galactic Center,” Phys.
1571 Rev. D **84**, 123005 (2011) [arXiv:1110.0006 [astro-ph.HE]].
- 1572 [178] T. Linden, D. Hooper and F. Yusef-Zadeh, “Dark Matter and Synchrotron Emission from Galactic
1573 Center Radio Filaments,” Astrophys. J. **741**, 95 (2011) [arXiv:1106.5493 [astro-ph.HE]].
- 1574 [179] K. N. Abazajian and M. Kaplinghat, “Detection of a Gamma-Ray Source in the Galactic Center
1575 Consistent with Extended Emission from Dark Matter Annihilation and Concentrated Astrophysical
1576 Emission,” Phys. Rev. D **86**, 083511 (2012) [arXiv:1207.6047 [astro-ph.HE]].
- 1577 [180] D. Hooper and T. R. Slatyer, “Two Emission Mechanisms in the Fermi Bubbles: A Possible Signal of
1578 Annihilating Dark Matter,” arXiv:1302.6589 [astro-ph.HE].
- 1579 [181] D. Hooper, N. Weiner and W. Xue, “Dark Forces and Light Dark Matter,” Phys. Rev. D **86**, 056009
1580 (2012) [arXiv:1206.2929 [hep-ph]].
- 1581 [182] D. N. Spergel and P. J. Steinhardt, “Observational evidence for selfinteracting cold dark matter,” Phys.
1582 Rev. Lett. **84**, 3760 (2000) [astro-ph/9909386].
- 1583 [183] M. Vogelsberger, J. Zavala and A. Loeb, “Subhaloes in Self-Interacting Galactic Dark Matter Haloes,”
1584 Mon. Not. Roy. Astron. Soc. **423**, 3740 (2012) [arXiv:1201.5892 [astro-ph.CO]].
- 1585 [184] J. Zavala, M. Vogelsberger and M. G. Walker, “Constraining Self-Interacting Dark Matter with the
1586 Milky Way’s dwarf spheroidals,” arXiv:1211.6426 [astro-ph.CO].
- 1587 [185] J. Redondo and M. Postma, “Massive Hidden-Photons as Lukewarm Dark Matter,” JCAP **0902**, 005
1588 (2009) [arXiv:0811.0326 [hep-ph]].
- 1589 [186] M. Pospelov, A. Ritz and M. B. Voloshin, “Bosonic super-WIMPs as keV-scale dark matter,” Phys.
1590 Rev. D **78**, 115012 (2008) [arXiv:0807.3279 [hep-ph]].
- 1591 [187] S. Andreas, C. Niebuhr and A. Ringwald, “New Limits on Hidden Photons from Past Electron Beam
1592 Dumps,” Phys. Rev. D **86**, 095019 (2012) [arXiv:1209.6083 [hep-ph]].
- 1593 [188] A. Konaka, K. Imai, H. Kobayashi, A. Msaikhe, K. Miyake, T. Nakamura, N. Nagamine and N. Sasao
1594 *et al.*, “Search For Neutral Particles In Electron Beam Dump Experiment,” Phys. Rev. Lett. **57**, 659
1595 (1986).
- 1596 [189] M. Davier and H. Nguyen Ngoc, “An Unambiguous Search For A Light Higgs Boson,” Phys. Lett. B
1597 **229**, 150 (1989).
- 1598 [190] R. Dharmapalan *et al.* [MiniBooNE Collaboration], “Low Mass WIMP Searches with a Neutrino
1599 Experiment: A Proposal for Further MiniBooNE Running,” arXiv:1211.2258 [hep-ex].
- 1600 [191] M. D. Diamond and P. Schuster, “Searching for Light Dark Matter with the Slac Millicharge
1601 Experiment,” arXiv:1307.6861 [hep-ph].

- 1602 [192] E. Izaguirre, G. Krnjaic, P. Schuster and N. Toro, “New Electron Beam-Dump Experiments to Search
1603 for MeV to Few-GeV Dark Matter,” arXiv:1307.6554 [hep-ph].
- 1604 [193] J. Balewski, J. Bernauer, W. Bertozzi, J. Bessuille, B. Buck, R. Cowan, K. Dow and C. Epstein *et*
1605 *al.*, “DarkLight: A Search for Dark Forces at the Jefferson Laboratory Free-Electron Laser Facility,”
1606 arXiv:1307.4432 [physics.ins-det].
- 1607 [194] K. Aulenbacher, M. Dehn, H. -J. Kreidel, R. Heine and R. Eichhorn, “Status of the Mainz ERL-facility
1608 MESA,” ICFA Beam Dyn. Newslett. **58**, 145 (2012).
- 1609 [195] C. Athanassopoulos *et al.* [LSND Collaboration], “Evidence for muon-neutrino \rightarrow electron-neutrino
1610 oscillations from pion decay in flight neutrinos,” Phys. Rev. C **58**, 2489 (1998) [nucl-ex/9706006].
- 1611 [196] J. Blumlein and J. Brunner, “New Exclusion Limits for Dark Gauge Forces from Beam-Dump Data,”
1612 Phys. Lett. B **701**, 155 (2011) [arXiv:1104.2747 [hep-ex]].
- 1613 [197] J. Blumlein, J. Brunner, H. J. Grabosch, P. Lanius, S. Nowak, C. Rethfeldt, H. E. Ryseck and M. Walter
1614 *et al.*, “Limits on neutral light scalar and pseudoscalar particles in a proton beam dump experiment,”
1615 Z. Phys. C **51**, 341 (1991).
- 1616 [198] J. Blumlein, J. Brunner, H. J. Grabosch, P. Lanius, S. Nowak, C. Rethfeldt, H. E. Ryseck and M. Walter
1617 *et al.*, “Limits on the mass of light (pseudo)scalar particles from Bethe-Heitler e^+e^- and $\mu^+\mu^-$ pair
1618 production in a proton - iron beam dump experiment,” Int. J. Mod. Phys. A **7**, 3835 (1992).
- 1619 [199] S. N. Gninenko, “Stringent limits on the $\pi^0 \rightarrow \gamma X$, $X \rightarrow e^+e^-$ decay from neutrino experiments and
1620 constraints on new light gauge bosons,” Phys. Rev. D **85**, 055027 (2012) [arXiv:1112.5438 [hep-ph]].
- 1621 [200] P. Astier *et al.* [NOMAD Collaboration], “Search for heavy neutrinos mixing with tau neutrinos,”
1622 Phys. Lett. B **506**, 27 (2001) [hep-ex/0101041].
- 1623 [201] G. Bernardi, G. Carugno, J. Chauveau, F. Dicarolo, M. Dris, J. Dumarchez, M. Ferro-Luzzi and
1624 J. M. Levy *et al.*, “Search For Neutrino Decay,” Phys. Lett. B **166**, 479 (1986).
- 1625 [202] S. N. Gninenko, “Constraints on sub-GeV hidden sector gauge bosons from a search for heavy neutrino
1626 decays,” Phys. Lett. B **713**, 244 (2012) [arXiv:1204.3583 [hep-ph]].
- 1627 [203] F. Bergsma *et al.* [CHARM Collaboration], “A Search For Decays Of Heavy Neutrinos In The Mass
1628 Range 0.5-gev To 2.8-gev,” Phys. Lett. B **166**, 473 (1986).
- 1629 [204] F. Archilli, D. Babusci, D. Badoni, I. Balwierz, G. Bencivenni, C. Bini, C. Bloise and V. Bocci *et al.*,
1630 “Search for a vector gauge boson in phi meson decays with the KLOE detector,” Phys. Lett. B **706**,
1631 251 (2012) [arXiv:1110.0411 [hep-ex]].
- 1632 [205] D. Babusci *et al.* [KLOE-2 Collaboration], “Limit on the production of a light vector gauge boson in
1633 phi meson decays with the KLOE detector,” Phys. Lett. B **720**, 111 (2013) [arXiv:1210.3927 [hep-ex]].
- 1634 [206] M. Ablikim *et al.* [BESIII Collaboration], “Search for η and η' Invisible Decays in $J/\psi \rightarrow \phi\eta$ and $\phi\eta'$,”
1635 Phys. Rev. D **87**, 012009 (2013) [arXiv:1209.2469 [hep-ex]].
- 1636 [207] B. Aubert *et al.* [BABAR Collaboration], arXiv:0908.2821 [hep-ex].
- 1637 [208] B. Batell, M. Pospelov and A. Ritz, Phys. Rev. D **83**, 054005 (2011)
- 1638 [209] J. T. Ruderman and T. Volansky, “Decaying into the Hidden-Sector,” JHEP **1002**, 024 (2010)
1639 [arXiv:0908.1570 [hep-ph]].

- 1640 [210] C. Cheung, J. T. Ruderman, L. -T. Wang and I. Yavin, “Lepton Jets in (Supersymmetric) Electroweak
1641 Processes,” JHEP **1004**, 116 (2010) [arXiv:0909.0290 [hep-ph]].
- 1642 [211] [CDF Collaboration], “Search for Anomalous Production of Events with a W or Z Boson and
1643 Additional Leptons,” CDF/ANAL/EXOTIC/PUBLIC/10526.
- 1644 [212] [ATLAS Collaboration], “A Search for Lepton-Jets with Muons at ATLAS,” ATLAS-CONF-2011-076.
- 1645 [213] S. Chatrchyan *et al.* [CMS Collaboration], “Search for Light Resonances Decaying into Pairs of Muons
1646 as a Signal of New Physics,” JHEP **1107**, 098 (2011) [arXiv:1106.2375 [hep-ex]].
- 1647 [214] S. Chatrchyan *et al.* [CMS Collaboration], “Search for a non-standard-model Higgs boson decaying to
1648 a pair of new light bosons in four-muon final states,” arXiv:1210.7619 [hep-ex].
- 1649 [215] G. Aad *et al.* [ATLAS Collaboration], “A search for prompt lepton-jets in pp collisions at $\sqrt{s} = 7$ TeV
1650 with the ATLAS detector,” Phys. Lett. B **719**, 299 (2013) [arXiv:1212.5409].
- 1651 [216] G. Aad *et al.* [ATLAS Collaboration], “Search for WH production with a light Higgs boson decaying
1652 to prompt electron-jets in proton-proton collisions at $\sqrt{s}=7$ TeV with the ATLAS detector,” New J.
1653 Phys. **15**, 043009 (2013) [arXiv:1302.4403 [hep-ex]].
- 1654 [217] G. Aad *et al.* [ATLAS Collaboration], “Search for displaced muonic lepton jets from light Higgs boson
1655 decay in proton-proton collisions at $\sqrt{s} = 7$ TeV with the ATLAS detector,” Phys. Lett. B **721**, 32
1656 (2013) [arXiv:1210.0435 [hep-ex]].
- 1657 [218] R. Bernabei *et al.* [DAMA Collaboration], “First results from DAMA/LIBRA and the combined results
1658 with DAMA/NaI,” Eur. Phys. J. C **56**, 333 (2008) [arXiv:0804.2741 [astro-ph]].
- 1659 [219] C. E. Aalseth *et al.* [CoGeNT Collaboration], “Results from a Search for Light-Mass Dark Matter with
1660 a P-type Point Contact Germanium Detector,” Phys. Rev. Lett. **106**, 131301 (2011) [arXiv:1002.4703
1661 [astro-ph.CO]].
- 1662 [220] See e.g. D. H. Weinberg, J. S. Bullock, F. Governato, R. K. de Naray and A. H. G. Peter, “Cold dark
1663 matter: controversies on small scales,” arXiv:1306.0913 [astro-ph.CO].
- 1664 [221] C. Boehm and P. Fayet, “Scalar dark matter candidates,” Nucl. Phys. B **683**, 219 (2004) [hep-
1665 ph/0305261].
- 1666 [222] B. Batell and T. Gherghetta, “Localized $U(1)$ gauge fields, millicharged particles, and holography,”
1667 Phys. Rev. D **73** (2006) 045016 [hep-ph/0512356].
- 1668 [223] F. Brummer and J. Jaeckel, “Minicharges and Magnetic Monopoles,” Phys. Lett. B **675** (2009) 360
1669 [arXiv:0902.3615 [hep-ph]].
- 1670 [224] F. Brummer, J. Jaeckel and V. V. Khoze, “Magnetic Mixing: Electric Minicharges from Magnetic
1671 Monopoles,” JHEP **0906** (2009) 037 [arXiv:0905.0633 [hep-ph]].
- 1672 [225] H. Goldberg and L. J. Hall, “A New Candidate For Dark Matter,” Phys. Lett. B **174** (1986) 151.
- 1673 [226] K. Cheung and T. -C. Yuan, “Hidden-Fermion as Milli-Charged Dark Matter in Stückelberg Z' Model,”
1674 JHEP **0703** (2007) 120 [hep-ph/0701107].
- 1675 [227] D. Feldman, Z. Liu and P. Nath, “The Stückelberg Z-prime Extension with Kinetic Mixing and Milli-
1676 Charged Dark Matter From the Hidden-Sector,” Phys. Rev. D **75** (2007) 115001 [hep-ph/0702123
1677 [HEP-PH]].

- 1678 [228] A. Hook, E. Izaguirre and J. G. Wacker, “Model Independent Bounds on Kinetic Mixing,” *Adv. High*
1679 *Energy Phys.* **2011**, 859762 (2011) [arXiv:1006.0973 [hep-ph]].
- 1680 [229] Y. Kahn and J. Thaler, “Searching for an invisible A' vector boson with DarkLight,” *Phys. Rev. D*
1681 **86**, 115012 (2012) [arXiv:1209.0777 [hep-ph]].
- 1682 [230] A. V. Artamonov *et al.* [BNL-E949 Collaboration], “Study of the decay $K^+ \rightarrow \mu^+ \pi^+ \nu$ anti- ν in the
1683 momentum region $140 < P(\pi) < 199$ -MeV/c,” *Phys. Rev. D* **79**, 092004 (2009) [arXiv:0903.0030 [hep-ex]].
- 1684 [231] B. Aubert *et al.* [BaBar Collaboration], “Search for Invisible Decays of a Light Scalar in Radiative
1685 Transitions $\nu_{3S} \rightarrow \gamma A_0$,” arXiv:0808.0017 [hep-ex].
- 1686 [232] L. B. Auerbach *et al.* [LSND Collaboration], “Measurement of electron - neutrino - electron elastic
1687 scattering,” *Phys. Rev. D* **63**, 112001 (2001) [hep-ex/0101039].
- 1688 [233] P. deNiverville, M. Pospelov and A. Ritz, “Observing a light dark matter beam with neutrino
1689 experiments,” *Phys. Rev. D* **84**, 075020 (2011) [arXiv:1107.4580 [hep-ph]].
- 1690 [234] A. A. Prinz, R. Baggs, J. Ballam, S. Ecklund, C. Fertig, J. A. Jaros, K. Kase and A. Kulikov *et al.*,
1691 “Search for millicharged particles at SLAC,” *Phys. Rev. Lett.* **81**, 1175 (1998) [hep-ex/9804008].
- 1692 [235] R. Essig, J. Mardon and T. Volansky, “Direct Detection of Sub-GeV Dark Matter,” *Phys. Rev. D* **85**,
1693 076007 (2012) [arXiv:1108.5383 [hep-ph]].
- 1694 [236] T. Lin, H. -B. Yu and K. M. Zurek, “On Symmetric and Asymmetric Light Dark Matter,” *Phys. Rev.*
1695 *D* **85**, 063503 (2012) [arXiv:1111.0293 [hep-ph]].
- 1696 [237] S. Davidson, S. Hannestad and G. Raffelt, “Updated bounds on millicharged particles,” *JHEP* **0005**,
1697 003 (2000) [hep-ph/0001179].
- 1698 [238] S. Davidson and M. E. Peskin, “Astrophysical bounds on millicharged particles in models with a
1699 paraphoton,” *Phys. Rev. D* **49**, 2114 (1994) [hep-ph/9310288].
- 1700 [239] E. Golowich and R. W. Robinett, “Limits On Millicharged Matter From Beam Dump Experiments,”
1701 *Phys. Rev. D* **35**, 391 (1987).
- 1702 [240] T. Mitsui, R. Fujimoto, Y. Ishisaki, Y. Ueda, Y. Yamazaki, S. Asai and S. Orito, “Search for invisible
1703 decay of orthopositronium,” *Phys. Rev. Lett.* **70**, 2265 (1993).
- 1704 [241] M. I. Dobroliubov and A. Y. Ignatiev, “Millicharged Particles,” *Phys. Rev. Lett.* **65**, 679 (1990).
- 1705 [242] P. deNiverville, D. McKeen and A. Ritz, “Signatures of sub-GeV dark matter beams at neutrino
1706 experiments,” *Phys. Rev. D* **86**, 035022 (2012) [arXiv:1205.3499 [hep-ph]].
- 1707 [243] R. Essig, J. Mardon, M. Papucci, T. Volansky, Y. Zhong, “Constraining Light Dark Matter with
1708 Low-Energy e^+e^- Colliders”, to appear.
- 1709 [244] N. Borodatchenkova, D. Choudhury and M. Drees, “Probing MeV Dark Matter at Low-Energy E+E-
1710 Colliders,” *Phys. Rev. Lett.* **96** (2006) 141802 [hep-ph/0510147].
- 1711 [245] A. A. Aguilar-Arevalo *et al.* [MiniBooNE Collaboration], “Measurement of the Neutrino Neutral-
1712 Current Elastic Differential Cross Section on Mineral Oil at $E_\nu \sim 1$ GeV,” *Phys. Rev. D* **82**, 092005
1713 (2010) [arXiv:1007.4730 [hep-ex]].
- 1714 [246] J. Houry and A. Weltman. *Phys. Rev. Lett.*, 93, 2004. 171104.

- 1715 [247] J. Khoury and A. Weltman. *Phys. Rev. D*, 69, 2004. 044026.
- 1716 [248] P. Brax, C. van de Bruck, A. C. Davis, J. Khoury, A. Weltman, Aug 2004. 31pp. Published in
1717 *Phys.Rev.D*70:123518,2004. e-Print: astro-ph/0408415
- 1718 [249] P. J. E. Peebles and B. Ratra. *Ap. J. Lett.*, 325:17, 1988.
- 1719 [250] B. Ratra and P. J. E. Peebles. *Phys. Rev. D*, 37(12):3406, 1988.
- 1720 [251] L. Hui and A. Nicolis. *Phys. Rev. Lett.*, 105, 2010. 231101.
- 1721 [252] K. Hinterbichler, J. Khoury, and H. Nastase. *JHEP*, 1103(61), 2011.
- 1722 [253] K. Hinterbichler, J. Khoury, H. Nastase and R. Rosenfeld [arXiv:1301:6756 [hep-th]].
- 1723 [254] H. Nastase and A. Weltman [arXiv:1301:7120[hep-th]].
- 1724 [255] H. Nastase and A. Weltman [arXiv:1302:1748 [hep-th]].
- 1725 [256] P. Brax, C. Burrage, A.-C. Davis, D. Seery, and A. Weltman. *Phys. Rev. D*, 81:103524, 2010. e-Print
1726 arXiv:0911.1267.
- 1727 [257] L. Hui, A. Nicolis and C. Stubbs, “Equivalence Principle Implications of Modified Gravity Models,”
1728 *Phys. Rev. D* **80** (2009) 104002 [arXiv:0905.2966 [astro-ph.CO]].
- 1729 [258] D. Kapner et al. *Phys. Rev. Lett.*, 98:021101, 2007. e-Print arXiv:hep-ph/0611184.
- 1730 [259] P. Brax and G. Pignol. *Phys. Rev. Lett.*, 107:111301, 2011.
- 1731 [260] J. H. Steffen et al. *Phys. Rev. Lett.*, 105:261803, 2010. ePrint: arXiv:1010.0988.
- 1732 [261] A. Upadhye, J. H. Steffen, and A. Weltman. *Phys. Rev. D*, 81:015013, 2010.
- 1733 [262] A. Upadhye, J. H. Steffen, and A. S. Chou. *Phys. Rev. D*, 86:035006, 2012.
- 1734 [263] P. Brax, C. Burrage, A.-C. Davis, D. Seery, and A. Weltman. *JHEP*, 0909:128, 2009. e-print
1735 arXiv:0904.3002.
- 1736 [264] A. Upadhye, W. Hu, and J. Khoury. *Phys. Rev. Lett*, 109:041301, 2012.
- 1737 [265] A. Upadhye. *Phys. Rev. D*, 86:102003, 2012. e-Print: arXiv:1209.0211.
- 1738 [266] P. Brax, C. van de Bruck, A. C. Davis, D. F. Mota, and D. J. Shaw. *Phys. Rev. D*, 76:124034, 2007.
1739 e-Print arXiv:0709.2075.
- 1740 [267] P. Brax, A. Lindner and K. Zioutas, “Detection prospects for solar and terrestrial chameleons,” *Phys.*
1741 *Rev. D* **85** (2012) 043014 [arXiv:1110.2583 [hep-ph]].
- 1742 [268] B. Bertotti, L. Iess and P. Tortora, “A test of general relativity using radio links with the Cassini
1743 spacecraft,” *Nature* **425** (2003) 374.
- 1744 [269] P. Brax, C. van de Bruck, A. -C. Davis and A. M. Green, “Small scale structure formation in chameleon
1745 cosmology,” *Phys. Lett. B* **633** (2006) 441 [astro-ph/0509878].
- 1746 [270] P. .Brax, R. Rosenfeld and D. A. Steer, “Spherical Collapse in Chameleon Models,” *JCAP* **1008** (2010)
1747 033 [arXiv:1005.2051 [astro-ph.CO]].

- 1748 [271] R. Pourhasan, N. Afshordi, R. B. Mann and A. C. Davis, “Chameleon Gravity, Electrostatics, and
1749 Kinematics in the Outer Galaxy,” JCAP **1112** (2011) 005 [arXiv:1109.0538 [astro-ph.CO]].
- 1750 [272] C. Burrage, “Supernova Brightening from Chameleon-Photon Mixing,” Phys. Rev. D **77** (2008) 043009
1751 [arXiv:0711.2966 [astro-ph]].
- 1752 [273] B. A. Bassett and M. Kunz, “Cosmic distance-duality as a probe of exotic physics and acceleration,”
1753 Phys. Rev. D **69** (2004) 101305 [astro-ph/0312443].
1754 [267]
- 1755 [274] P. Chang and L. Hui, “Stellar Structure and Tests of Modified Gravity,” Astrophys. J. **732** (2011) 25
1756 [arXiv:1011.4107 [astro-ph.CO]].
- 1757 [275] C. Burrage, A. -C. Davis and D. J. Shaw, “Detecting Chameleons: The Astronomical Polarization
1758 Produced by Chameleon-like Scalar Fields,” Phys. Rev. D **79** (2009) 044028 [arXiv:0809.1763 [astro-
1759 ph]].
- 1760 [276] B. Jain, V. Vikram and J. Sakstein, “Astrophysical Tests of Modified Gravity: Constraints from
1761 Distance Indicators in the Nearby Universe,” arXiv:1204.6044 [astro-ph.CO].
- 1762 [277] F. Schmidt, A. Vikhlinin and W. Hu, “Cluster Constraints on f(R) Gravity,” Phys. Rev. D **80** (2009)
1763 083505 [arXiv:0908.2457 [astro-ph.CO]].
- 1764 [278] L. Lombriser, K. Koyama, G. -B. Zhao and B. Li, “Chameleon f(R) gravity in the virialized cluster,”
1765 Phys. Rev. D **85** (2012) 124054 [arXiv:1203.5125 [astro-ph.CO]].
- 1766 [279] <http://microscope.onera.fr/>
- 1767 [280] <http://sci.esa.int/science-e/www/area/index/cfm?fareaid=127>
- 1768 [281] **THE REMAINING CITATIONS ARE NEVER REFERED TO.**
- 1769 [282] A. Loeb and M. Zaldarriaga, “The Small-scale power spectrum of cold dark matter,” Phys. Rev. D
1770 **71**, 103520 (2005).
- 1771 [283] J. Dunkley, R. Hlozek, J. Sievers, V. Acquaviva, P. A. R. Ade, P. Aguirre, M. Amiri and J. W. Appel
1772 *et al.*, “The Atacama Cosmology Telescope: Cosmological Parameters from the 2008 Power Spectra,”
1773 Astrophys. J. **739**, 52 (2011) [arXiv:1009.0866 [astro-ph.CO]].
- 1774 [284] V. Spevak, N. Auerbach, V. V. Flambaum, “Enhanced T odd P odd electromagnetic moments in
1775 reflection asymmetric nuclei,” Phys. Rev. **C56**, 1357-1369 (1997). [nucl-th/9612044].
- 1776 [285] J. Albert, S. Bettarini, M. Biagini, G. Bonneaud, Y. Cai, G. Calderini, M. Ciuchini and G. P. Dubois-
1777 Felsmann *et al.*, “SuperB: A Linear high-luminosity B factory,” physics/0512235.
- 1778 [286] C. W. Leemann, D. R. Douglas and G. A. Krafft, “The Continuous Electron Beam Accelerator Facility:
1779 CEBAF at the Jefferson Laboratory,” Ann. Rev. Nucl. Part. Sci. **51**, 413 (2001).
- 1780 [287] P. Brax, A. Lindner, and K. Zioutas. 2011. ePrint arXiv:1110.2583.
- 1781 [288] C. Athanassopoulos *et al.* [LSND Collaboration], “The Liquid scintillator neutrino detector and
1782 LAMPF neutrino source,” Nucl. Instrum. Meth. A **388**, 149 (1997) [nucl-ex/9605002].
- 1783 [289] F. Bergsma *et al.* [CHARM Collaboration], “Search for Axion-like Particle Production in 400 GeV
1784 Proton-Copper Interactions,” Phys. Lett. B **157**, 458 (1985).

- 1785 [290] R. Cameron, G. Cantatore, A. C. Melissinos, G. Ruoso, Y. Semertzidis, H. J. Halama, D. M. Lazarus
1786 and A. G. Prodell *et al.*, “Search for nearly massless, weakly coupled particles by optical techniques,”
1787 *Phys. Rev. D* **47**, 3707 (1993).
- 1788 [291] M. Ablikim *et al.* [BES Collaboration], “Search for the invisible decay of J/ψ in $\psi(2S) \rightarrow \pi^+ \pi^-$
1789 J/ψ ,” *Phys. Rev. Lett.* **100**, 192001 (2008) [arXiv:0710.0039 [hep-ex]].
- 1790 [292] M. Kaplinghat, A. Peter and K. Sigurdson, to appear.
- 1791 [293] M. Davier, A. Hoecker, B. Malaescu and Z. Zhang, *Eur. Phys. J. C* **71**, 1515 (2011) [arXiv:1010.4180
1792 [hep-ph]].
- 1793 [294] B. Osmanov [on behalf of MINERvA Collaboration], “MINERvA Detector: Description and
1794 Performance,” arXiv:1109.2855 [physics.ins-det].
- 1795 [295] D. G. E. Walker, D. Finkbeiner, L. Moustakas and K. Sigurdson, to appear.
- 1796 [296] R. Balest *et al.* *Phys. Rev. D*, 51:2053, 1995.
- 1797 [297] E. Komatsu *et al.* [WMAP Collaboration], “Seven-Year Wilkinson Microwave Anisotropy Probe
1798 (WMAP) Observations: Cosmological Interpretation,” *Astrophys. J. Suppl.* **192**, 18 (2011)
1799 [arXiv:1001.4538 [astro-ph.CO]].
- 1800 [298] S. V. Benson, D. Douglas, G. R. Neil and M. D. Shinn, “The Jefferson Lab Free Electron Laser
1801 Program,” *J. Phys. Conf. Ser.* **299**, 012014 (2011).
- 1802 [299] V. V. Nesvizhevsky *et al.* *Nature*, 415:297, 2002.
- 1803 [300] I. Ambats *et al.* [MINOS Collaboration], “The MINOS Detectors Technical Design Report,” NUMI-L-
1804 337.
- 1805 [301] M. Kleban and R. Rabadan. 2005. ePrint arXiv:hep-ph/0510183.
- 1806 [302] A. S. Chou, W. C. Wester, A. Baumbaugh, H. R. Gustafson, Y. Irizarry-Valle, P. O. Mazur, J. H.
1807 Steffen, R. Tomlin, A. Upadhye, A. Weltman, X. Yang, and J. Yoo. *Phys. Rev. Lett.*, 102, 2009. 030402.
- 1808 [303] G. Venanzoni, “Dafne upgrade,” *Nucl. Phys. Proc. Suppl.* **162**, 339 (2006).
- 1809 [304] E. Zavattini *et al.* [PVLAS Collaboration], “Experimental observation of optical rotation generated in
1810 vacuum by a magnetic field,” *Phys. Rev. Lett.* **96**, 110406 (2006) [arXiv:hep-ex/0507107]; “New PVLAS
1811 results and limits on magnetically induced optical rotation and ellipticity in vacuum,” *Phys. Rev. D* **77**,
1812 032006 (2008) [arXiv:0706.3419 [hep-ex]].
- 1813 [305] A. S. Chou and others [GammeV (T-969) Collaboration]. *Phys. Rev. Lett.*, 100, 2008. 080402
1814 [arXiv:0710.3783 [hep-ex]].
- 1815 [306] G. Mueller, P. Sikivie, D. B. Tanner and K. van Bibber, “Detailed Design of a Resonantly-Enhanced
1816 Axion-Photon Regeneration Experiment,” *Phys. Rev. D* **80**, 072004 (2009) [arXiv:0907.5387 [hep-ph]].
1817 P. Arias, J. Jaeckel, J. Redondo and A. Ringwald, “Optimizing Light-Shining-through-a-Wall Experi-
1818 ments for Axion and other WISP Searches,” *Phys. Rev. D* **82**, 115018 (2010) [arXiv:1009.4875 [hep-ph]].
1819 P. Arias and A. Ringwald, “Illuminating WISPs with Photons,” arXiv:1110.2126 [hep-ph].
- 1820 [307] J. Redondo and A. Ringwald, “Light shining through walls,” *Contemp. Phys.* **52**, 211 (2011)
1821 [arXiv:1011.3741 [hep-ph]].

- 1822 [308] A. A. Anselm, “Arion-Photon oscillations in a steady magnetic field,” (in Russian) *Yad. Fiz.* **42**, 1480
1823 (1985).
- 1824 [309] M. Kreuz et al. 2009. ePrint arXiv:0902.0156.
- 1825 [310] P. Brax and K. Zioutas. *Phys. Rev. D*, 82:043007, 2010.
- 1826 [311] P. W. Graham and S. Rajendran, “Axion Dark Matter Detection with Cold Molecules,” *Phys. Rev. D*
1827 **84**, 055013 (2011) [arXiv:1101.2691 [hep-ph]].
- 1828 [312] A. Afanasev et al. *AIP Conf. Proc.*, 1274:163, 2010.
- 1829 [313] K. Abe *et al.* [T2K Collaboration], “The T2K Experiment,” *Nucl. Instrum. Meth. A* **659**, 106 (2011)
1830 [arXiv:1106.1238 [Unknown]].
- 1831 [314] C. Burrage, A.-C. Davis, and D. J. Shaw. *Phys. Rev. D*, 79:044028, 2009.
- 1832 [315] L. Lombriser, A. Slosar, U. Seljak and W. Hu, “Constraints on $f(R)$ gravity from probing the large-scale
1833 structure,” *Phys. Rev. D* **85** (2012) 124038 [arXiv:1003.3009 [astro-ph.CO]].
- 1834 [316] A. E. Nelson and J. Walsh, “Short Baseline Neutrino Oscillations and a New Light Gauge Boson,”
1835 *Phys. Rev. D* **77**, 033001 (2008) [arXiv:0711.1363 [hep-ph]].
- 1836 [317] N. Auerbach, V. V. Flambaum, V. Spevak, “Collective T and P odd electromagnetic moments in nuclei
1837 with octupole deformations,” *Phys. Rev. Lett.* **76**, 4316-4319 (1996). [nucl-th/9601046].
- 1838 [318] K. Hinterbichler, J. Khoury, and H. Nastase. *JHEP*, 1103(61), 2011.
- 1839 [319] E. Bertschinger, “The Effects of Cold Dark Matter Decoupling and Pair Annihilation on Cosmological
1840 Perturbations,” *Phys. Rev. D* **74**, 063509 (2006).
- 1841 [320] T. Kageyama, “The SuperKEKB project,” *AIP Conf. Proc.* **842**, 1064 (2006).
- 1842 [321] P. Brax and C. Burrage. *Phys. Rev. D*, 83:035020, 2011.
- 1843 [322] C. Burrage, A.-C. Davis, and D. J. Shaw. *Phys. Rev. Lett.*, 102:201101, 2009.
- 1844 [323] M. Fouche *et al.* [BMV Collaboration], “Search for photon oscillations into massive particles,” *Phys.*
1845 *Rev. D* **78**, 032013 (2008) [arXiv:0808.2800 [hep-ex]].
- 1846 A. S. Chou *et al.* [GammeV Collaboration], “Search for axion-like particles using a variable baseline
1847 photon regeneration technique,” *Phys. Rev. Lett.* **100**, 080402 (2008) [arXiv:0710.3783 [hep-ex]].
- 1848 A. Afanasev *et al.* [LIPSS Collaboration], “New Experimental limit on Optical Photon Coupling to
1849 Neutral, Scalar Bosons,” *Phys. Rev. Lett.* **101**, 120401 (2008) [arXiv:0806.2631 [hep-ex]].
- 1850 P. Pugnati *et al.* [OSQAR Collaboration], “First results from the OSQAR photon regeneration
1851 experiment: No light shining through a wall,” *Phys. Rev. D* **78**, 092003 (2008) [arXiv:0712.3362 [hep-
1852 ex]].
- 1853 K. Ehret *et al.* [ALPS Collaboration], “New ALPS results on hidden-sector lightweights,” *Phys. Lett.*
1854 *B* **689**, 149 (2010).
- 1855 [324] N. D. Scielzo, I. Ahmad, K. Bailey *et al.*, “Progress towards laser trapping of Ra-225 for an electric
1856 dipole moment measurement,” *AIP Conf. Proc.* **842**, 787-789 (2006).
- 1857 [325] L. D. Carr, D. DeMille *et al.*, [arXiv:0904.3175 [quant-ph]].

- 1858 [326] A. A. Aguilar-Arevalo *et al.* [MiniBooNE Collaboration], “The Neutrino Flux prediction at Mini-
1859 BooNE,” *Phys. Rev. D* **79**, 072002 (2009) [arXiv:0806.1449 [hep-ex]].
- 1860 [327] R. Essig, A. Manalaysay, J. Mardon, P. Sorensen and T. Volansky, “First Direct Detection Limits
1861 on sub-GeV Dark Matter from XENON10,” *Phys. Rev. Lett.* **109**, 021301 (2012) [arXiv:1206.2644
1862 [astro-ph.CO]].
- 1863 [328] K. Van Bibber, N. R. Dagdeviren, S. E. Koonin, A. Kerman and H. N. Nelson, “Proposed experiment
1864 to produce and detect light pseudoscalars,” *Phys. Rev. Lett.* **59**, 759 (1987).
- 1865 [329] R. Keisler, C. L. Reichardt, K. A. Aird, B. A. Benson, L. E. Bleem, J. E. Carlstrom, C. L. Chang
1866 and H. M. Cho *et al.*, “A Measurement of the Damping Tail of the Cosmic Microwave Background
1867 Power Spectrum with the South Pole Telescope,” *Astrophys. J.* **743**, 28 (2011) [arXiv:1105.3182 [astro-
1868 ph.CO]].
- 1869 [330] L. AMoustakas, A. J. Bolton, J. T. Booth, J. SBullock, E. Cheng, D. Coe, C. D. Fassnacht and
1870 V. Gorjian *et al.*, “The Observatory for Multi-Epoch Gravitational Lens Astrophysics (OMEGA),”
1871 arXiv:0806.1884 [astro-ph].
- 1872 [331] R. Poltis and A. Weltman “Chameleon Lensing and Time Delay”
- 1873 [332] S. D. Holmes [Project X Collaboration], “Project X: A Multi-MW Proton Source at Fermilab,” *Conf.*
1874 *Proc. C* **100523**, TUYRA01 (2010).
- 1875 [333] E. G. Adelberger *et al.* *Phys. Rev. Lett.*, 98:131104, 2007. e-Print arXiv:hep-ph/0611223.
- 1876 [334] M. Ahlers, H. Gies, J. Jaeckel, J. Redondo and A. Ringwald, “Laser Experiments Explore the Hidden-
1877 Sector,” *Phys. Rev. D* **77**, 095001 (2008) [arXiv:0711.4991 [hep-ph]].
- 1878 [335] J. Hamann, S. Hannestad, G. G. Raffelt and Y. Y. Y. Wong, “Isocurvature forecast in the anthropic
1879 axion window,” *JCAP* **0906** (2009) 022 [arXiv:0904.0647 [hep-ph]].
- 1880 [336] M. Dehn, K. Aulenbacher, R. Heine, H. J. Kreidel, U. Ludwig-Mertin and A. Jankowiak, “The MAMI
1881 C accelerator: The beauty of normal conducting multi-turn recirculators,” *Eur. Phys. J. ST* **198**, 19
1882 (2011).